

National Library
of Canada

Canadian Theses Service

Ottawa, Canada
K1A 0N4

Bibliothèque nationale
du Canada

Servic s des th ses canadiennes

CANADIAN THESES

TH SES CANADIENNES

NOTICE

The quality of this microfiche is heavily dependent upon the quality of the original thesis submitted for microfilmimg. Every effort has been made to ensure the highest quality of reproduction possible.

If pages are missing, contact the university which granted the degree.

Some pages may have indistinct print especially if the original pages were typed with a poor typewriter ribbon or if the university sent us an inferior photocopy.

Previously copyrighted materials (journal articles, published tests, etc.) are not filmed.

Reproduction in full or in part of this film is governed by the Canadian Copyright Act, R.S.C. 1970, c. C-30.

AVIS

La qualit  de cette microfiche d pend grandement de la qualit  de la th se soumise au microfilmage. Nous avons tout fait pour assurer une qualit  sup rieure de reproduction.

S'il manque des pages, veuillez communiquer avec l'universit  qui a conf r  le grade.

La qualit  d'impression de certaines pages peut laisser  d閞irer, surtout si les pages originales ont t  dactylographies  l'aide d'un ruban us  ou si l'universit  nous a fait parvenir une photocopie de qualit  inf rieure.

Les documents qui font dj  l'objet d'un droit d'auteur (articles de revue, examens publis, etc.) ne sont pas microfilms.

La reproduction, m me partielle, de ce microfilm est soumise  la Loi canadienne sur le droit d'auteur, SRC 1970, c. C-30.

THIS DISSERTATION
HAS BEEN MICROFILMED
EXACTLY AS RECEIVED

LA TH SE A T 
MICROFILM E TELLE QUE
NOUS L'AVONS RE UE

**Fourier Transform and Diode Laser IR Spectra
of Formaldehyde and its Application to Air
Pollution Monitoring**

Shachar Nadler

A Thesis

**The Department
of
Chemistry**

**Presented in Partial Fulfillment of the Requirements
for the Degree of Doctor of Philosophy at
Concordia University
Montréal, Québec, Canada**

January 1986

© Shachar Nadler, 1986

Permission has been granted
to the National Library of
Canada to microfilm this
thesis and to lend or sell
copies of the film.

The author (copyright owner)
has reserved other
publication rights, and
neither the thesis nor
extensive extracts from it
may be printed or otherwise
reproduced without his/her
written permission.

L'autorisation a été accordée
à la Bibliothèque nationale
du Canada de microfilmer
cette thèse et de prêter ou
de vendre des exemplaires du
film.

L'auteur (titulaire du droit
d'auteur) se réserve les
autres droits de publication;
ni la thèse ni de longs
extraits de celle-ci ne
doivent être imprimés ou
autrement reproduits sans son
autorisation écrite..

ISBN 0-315-30599-1

ABSTRACT

Fourier Transform and Diode Laser IR Spectra of Formaldehyde and its Application to Air Pollution Monitoring.

Shachar, Nadler, Ph.D.
Concordia University, 1986

High resolution FT-IR spectra have been recorded with a Bomem interferometer ($\Delta\nu \sim 0.004 \text{ cm}^{-1}$) and covered the region from 890 to 1580 cm^{-1} . Over 3200 transitions in the ν_4 , ν_6 , and ν_3 bands of H_2CO have been assigned. Line positions have been analyzed using a least-squares-fit to a Watson reduced Hamiltonian. Since the 3 bands have been fitted simultaneously, the analysis included the extensive Coriolis coupling effects between the upper states. The fit yielded improved molecular constants including, for the first time, all the sixth order coefficients and a third order Coriolis coupling constant for the interaction between ν_6 and ν_3 .

A tunable diode laser (TDL) has been used to determine absolute line strengths for 28 transitions in the ν_4 and ν_6 bands. These line strengths have been used to determine the dipole moment derivatives and consequently facilitated the prediction of the ν_4 and ν_6 band strengths.

The TDL system has also been used to study the effects of pressure broadening due to collision with foreign gases. Pressure broadening coefficients for air, H₂, O₂ and N₂ have been determined. These are very similar to theoretical literature values in the cases of air, N₂ and O₂. The H₂-H₂CO values are in good agreement with earlier experimental millimeter-wave results.

A method for the measurement of small amounts of H₂CO in air has been developed for use in domestic air pollution monitoring. Conventional reduced pressure techniques have been found unsuitable due to the adsorptive nature of formaldehyde. Our suggested technique employs the TDL spectrometer coupled with a multipass White cell (4-100 meter) and a cold trap (liq. N₂) installed between the sample cell and the analytical White cell. The cold trap allows the reduction of pressure within the White cell (to <10 torr) without loss of sample since the H₂CO is frozen out in the trap. The H₂CO sample is sublimated by heating and then analyzed. This method may employ relatively shorter absorption pathlengths since most of the original H₂CO sample (mass) is available for the analysis. Based on the mass of H₂CO present in 5 liter air samples in a 100 m optical pathlength this technique has demonstrated a limit of detection of 6×10^{-3} absorption units and a sensitivity of $4.4 \times 10^{-5} \text{ m}^{-1}$. For the strongest line in Q₃ of ν₁ (C-H stretch) this limits the detection to ~7 ppbv. The limit of

detection can be easily reduced to < 5 ppb by simply increasing the sample volume to 10 or 15 liters.

The standard 5 liter grab bags used for air sampling have been proven to be unsuitable for work with H₂CO. It has been demonstrated that due to adsorption and possibly polymerization these bags show a decreased H₂CO content with time. Consequently the construction of a mobile "super sniffer" has been suggested since samples of H₂CO could not be collected in the field and analyzed in the laboratory. The design and operational parameters of a super sniffer have been outlined. This unit may be easily modified (in the field) to allow for the analysis of other air pollutants.

ACKNOWLEDGEMENTS

First I would like to express my sincere gratitude to my supervisor Dr. S. J. Daunt. His expertise, resources, and his excellent private library of pertinent texts were invaluable to this work.

Appreciation is extended to the staff of the Laboratory of Extraterrestrial Physics at NASA/Goddard Space Flight Center for making their laboratories and computer facilities available. Perhaps the greatest debt I owe to Dr. D. C. Reuter of the Goddard Laboratory for Atmospheric Sciences, without whose extensive contributions in the area of data analysis and interpretation this dissertation would not have been possible.

Dr. J. W. C. Johns of the Herzberg Institute of Astrophysics, NRC Ottawa, is thanked for supplying the FT-IR spectra and the original fitting programs.

Thanks are also due to Dr. C. H. Langford for constructive contributions to the analytical aspects of this project, and to Drs. W. E. Blass and G. W. Halsey of the University of Tennessee for their assistance with the deconvolution programs.

Finally, I must thank three people without whose friendship and care this work would have never been finished: Michael Bozarth, Ann English and Helen Wicki.

The financial support of Concordia University and NSERC Program for Research in Aid of Industry (PRAI) grant P-8206 is gratefully acknowledged.

To Daphnée

TABLE OF CONTENTS

	Page
ABSTRACT	111
ACKNOWLEDGEMENTS	vi
LIST OF FIGURES	xii
LIST OF TABLES	xiv

CHAPTER 1

INTRODUCTION

1.1 Introductory Remarks	1
1.2 Experimental Objectives	1
1.2.1 Part A: The Molecular Constants for the ν_3 , ν_4 and ν_6 Bands of H_2CO	2
1.2.2 Part B: Absolute Line Strength Determination for Indi- vidual Rovibrational Lines in the ν_4 and ν_6 Bands of H_2CO	2
1.2.3 Part C: Foreign Gas Broadening Parameters	3
1.2.4 Part D: Trace Analysis of H_2CO in Ambient Air	3

CHAPTER 2

THEORY OF ASYMMETRIC TOP MOLECULAR SPECTRA

2.1 Introductory Remarks	5
2.2 The Rigid Rotor - Harmonic Oscillator Hamiltonian	6
2.3 The Rotational Hamiltonian	14

2.4	The Reduced Hamiltonian	20
2.5	Asymmetric Rotor Notation and Selection Rules	22
2.6	Line Intensities	33
2.7	Coriolis Perturbations	38

CHAPTER 3

INSTRUMENTATION AND DATA ACQUISITION

3.1	Introduction	48
3.2	FT-IR Survey Spectra	48
3.3	TDL Experimental Apparatus	49
3.4	Data Acquisition	54

CHAPTER 4

EXPERIMENTAL RESULTS - H₂CO LINE ASSIGNMENTS, AND DETERMINATION OF LINE STRENGTHS AND BROADENING COEFFICIENTS

4.1	Introduction	59
4.2	Frequency Assignments	59
4.3	Line Strength Determinations	62
4.4	Pressure Broadening by Foreign Gases	67

CHAPTER 5

ROTATIONAL ANALYSIS OF ν₃, ν₄ AND ν₆ BANDS OF FORMALDEHYDE

5.1	Introduction	73
5.2	Least-Square Fitting to the Model Hamiltonian	75

5.3	Input to the Fitting Program	80
5.4	Wavenumbers Fit; Results and Discussion	82
5.5	Intensity Fitting	91
5.6	Intensity Fitting; Results and Discussion	93

CHAPTER 6.

TRACE ANALYSIS OF FORMALDEHYDE IN AMBIENT AIR

6.1	Introduction	99
6.2	Preliminary Analysis	100
6.3	Experimental	103
6.4	The Mobile TDL "Super Sniffer" System	111

CHAPTER 7.

GENERAL CONCLUSIONS AND SUGGESTIONS FOR FUTURE

RESEARCH

7.1	Conclusions	118
7.1.1	The Molecular Constants of Formaldehyde	118
7.1.2	Line Strengths and Foreign-Gas Pressure Broadening	119
7.1.3	Analytical	119
7.2	Suggestions for Future Research	120

REFERENCES	122
------------	-----

APPENDIX A

A-1	Least-Squares-Fitting: Results for Fit A	128
-----	--	-----

LIST OF FIGURES

	Page
Figure 2-1 Correlation Diagram for the Asymmetric Rotor Energy Levels	28
Figure 2-2 The ν_3 , ν_4 and ν_6 Vibrations and Their relation to $\Delta\mu$.	31
Figure 3-1 Two Typical Examples of FT-IR Spectra	50
Figure 3-2 Schematic Diagram of the TDL Spectrometer	53
Figure 3-3 Measurable Parameters From TDL Spectra	55
Figure 3-4 Survey Spectra of Selected Regions in the ν_4 band of H_2CO Recorded with a TDL	57
Figure 3-5 TDL Survey Spectra: Identification of Transitions in ν_4 Using Ge Etalon Fringes for Relative Calibration and N_2O for Absolute Calibration.	58
Figure 4-1 A Schematic Diagram of the Ground-State-Combination-Difference Technique	61
Figure 4-2 Beer's Law Plot of Absorbance vs. Optical Density For the $18_{2,17} \leftarrow 18_{1,17}$ Transition at $1172.38603 \text{ cm}^{-1}$ in the ν_4 band of H_2CO	64
Figure 4-3 TDL Spectra from Hydrogen Pressure Broadening Experiments on the $3_{0,3} \leftarrow 3_{1,3}$ transition at $1159.47176 \text{ cm}^{-1}$ of the ν_4 band of H_2CO	69
Figure 4-4 Plots of Foreign Gas Broadening Collision Widths (FWHM) of $\text{X}-\text{H}_2\text{CO}$ ($\text{X}=\text{air, N}_2$ or O_2) as a Function of Pressure	70

Figure 5-1 Block Diagram of Computer Program Used for the Determination of Asymmetric Top Molecular Constants by Least-Squares Fitting	74
Figure 5-2 Stick Diagram Comparing Observed and Calculated Wave-numbers and Line Strengths for P_0 , of ν_4	90
Figure 6-1 Formaldehyde Sampling Apparatus for Trapping H_2CO from a Fixed Volume of Air	101
Figure 6-2 First Efforts at Determining Concentrations of H_2CO in Air Using the Cold Trap	102
Figure 6-3 Survey Scans of Portions of the ν_1 Band of H_2CO in the 3 μm Region. The Strong Q_0 , Branch Lines were Selected for Monitoring	104
Figure 6-4 Analytical Detection Curve (Beer's plot) for the Transition $3_{3,1} \rightarrow 3_{3,0}$ of ν_1 Using Standard Solutions . . .	108
Figure 6-5 Same as Figure 6-4 but For Lower Concentrations of 10-100 ppb	109
Figure 6-6 Detection of H_2CO in Laboratory Air by the TDL System Using the Cold Trap and a 100.17 meter Optical Path . . .	112
Figure 6-7 Top View of the Proposed Mobile TDL System; The "Super Sniffer"	115
Figure 6-8 Side Views of the Mobile TDL System	116
Figure 6-9 Schematic of the System Electronic Connections	117

LIST OF TABLES

	Page
Table 2-1 Definitions of Commonly used Symbols	9
Table 2-2 Axis Representation	23
Table 2-3 Character Table for the Group $\nu_{(a,b,c)}$	26
Table 2-4 Asymmetric Top Selection Rules	31
Table 2-5 Direction of the Dipole Moment Permitting Transitions Between Rotational States	32
Table 2-6 The C_{2v} Point Group Table in the I' Representation ..	43
Table 4-1 Observed Line Strengths in the ν_4 and ν_6 Bands of H_2CO At $24+1^{\circ}C$	65
Table 4-2 Foreign Gas Pressure Broadening Coefficients For H_2CO ..	72
Table 5-1 Ground State, and Initial Upper State Rotational Con- stants	81
Table 5-2 Molecular Constants for the ν_4 , ν_6 and ν_3 bands of H_2CO ..	84
Table 5-3 Correlation Matrix from Least-Squares-Fit: Results From Fit A	87
Table 5-4 Results From Least-Squares Fitting of Line Strengths ..	94
Table 5-5 Calculated Dipole Moment Derivatives and Band Strengths ..	96

CHAPTER 1

INTRODUCTION

1.1 Introductory Remarks

Formaldehyde (H_2CO) is an important atmospheric pollutant both indoors and outdoors [1-3] and is also a molecule of considerable astrophysical interest [4-7]. Knowledge of line frequencies, absolute intensities and line shapes is necessary for quantitative analysis for both atmospheric and laboratory experiments since pressure and temperature changes can lead to frequency shifts and line shape variations.

The $3 \mu\text{m}$ C-H stretching vibration-rotation bands of H_2CO have been well studied at high resolution by several groups [8-11]. Recently the C=O stretching band has been studied using diode lasers [12]. The three low lying bands of H_2CO , ν_3 , ν_4 and ν_6 have been studied at low resolution ($\Delta\nu \sim 0.25 \text{ cm}^{-1}$) by Nakagawa and Morino [13] and at moderate resolution ($\Delta\nu \sim 0.05 \text{ cm}^{-1}$) by Allegrini et al. [14]. These three bands are the focal point of this experimental work.

1.2 Experimental Objectives

This project has four experimental objectives:

Part A: To obtain more accurate molecular constants for the ν_3 , ν_4 and ν_6 bands.

Part B: To determine absolute line strengths for individual ro-vibrational lines.

Part C: To determine broadening parameters induced by collision with foreign gases.

Part D: To develop an analytical technique for the detection of H₂CO in ambient air at low ppb levels.

1.2.1 Part A: The Molecular Constants for the ν_3 , ν_4 and ν_6 Bands of H₂CO.

High resolution FT-IR spectra have been recorded with a Bomem interferometer ($\Delta\nu \sim 0.004 \text{ cm}^{-1}$) covering the region from 890 to 1580 cm^{-1} . Using the ground-state-combination-difference technique IR transitions in the ν_3 , ν_4 and ν_6 bands will be assigned. The assigned transitions will then be analyzed by means of least-squares to a sixth order Hamiltonian. The transitions for the three bands will be fit simultaneously. This will permit the analysis of the extensive Coriolis interaction between the bands. The fit will yield the rotational and Coriolis interaction constants from which all transitions in the region may be predicted.

1.2.2 Part B: Absolute Line Strength Determination for Individual Ro-Vibrational Lines in the ν_4 and ν_6 bands of H₂CO.

Using tunable diode lasers (TDLs) the absolute line strengths of several transitions will be determined. Since

the TDL spectrometer allows for Doppler limited resolution, the line strengths will be evaluated using the direct method [15]. This technique allows the determination of line strengths from the absorption profiles of individual transitions since for Doppler limited transitions, $\ln(I/I_0)$ is directly proportional to the line strength S. At present only band strengths are available in the literature [16,17].

The line strengths will be used to evaluate the dipole moment derivatives of their respective bands. These derivatives may in turn be used to predict the entire spectrum from the eigenvalues and eigenvectors of the Hamiltonian (obtained in Part A).

1.2.3 Part C: Foreign Gas Broadening Parameters

The TDL spectrometer will also be used for the evaluation of pressure broadening parameters induced by collision with foreign gases. The effects of air, H_2 , O_2 and N_2 on several transitions in the ν_4 and ν_6 bands of H_2CO will be determined. The broadening parameters will be evaluated from plots of the absorption widths of individual transitions as a function of foreign gas pressure.

1.2.4 Part D: Trace Analysis of H_2CO in Ambient Air

In recent years TDLs have been used extensively to monitor trace gases. The literature covers a wide range of

analytical applications including the detection of NO_2 at <1 ppb levels, the measurement of pollutants (CO) at atmospheric pressures, and the detection of several gases simultaneously [18-25].

The aim of this work is to develop an analytical method for trace detection of H_2CO in ambient air. Hence, known analytical techniques will be modified to suit the detection of the "difficult to handle" H_2CO molecules [16]. These molecules adsorb easily to surfaces, have a tendency to polymerize, and are water soluble.

The experimental phase will evaluate and/or develop the following:

1. Transitions in the ν_4 , ν_6 and ν_1 bands suitable for trace analysis. Transitions in the ν_1 band are several orders of magnitude stronger than those in ν_4 and ν_6 and therefore may be used with relatively shorter optical pathlengths or for detection of lower concentrations.
2. The detection of samples at reduced pressures in a long optical path cell technique.
3. The feasibility of using 5 liter standard grab bags for field work (sample collection).
4. The lower limit of detection.
5. Preparation of calibration curves suitable for routine analysis
6. The design of mobile TDL system capable of on-site analysis.

CHAPTER 2

THEORY OF ASYMMETRIC TOP MOLECULAR SPECTRA

2.1 Introductory Remarks

The theoretical basis for both infrared (IR) and microwave (MW) spectroscopy is essentially the same. Using a Hamiltonian which represents the system under study and a proper set of wavefunctions one solves the Schrodinger equation $H\Psi = E\Psi$ for the eigenvalues and eigenvectors. These in turn yield, respectively, the energy levels and the intensities of the spectral lines.

The degree of difficulty in solving the Schrodinger equation, however, varies with the particular system and is a function of molecular size and symmetry. For asymmetric molecules the solution cannot be written in closed form, even in the rigid-rotor approximation. Rather, to obtain the energy levels, the Hamiltonian matrix is computed in some basis set and is then numerically diagonalized to yield the eigenvalues. It follows then that the accuracy of a predicted spectrum is governed by the quality of the equation of molecular motion used to generate the Hamiltonian operator.

The equation of motion is usually based on the rigid rotor-harmonic oscillator model. However, for meaningful results across a broad range of energy levels, it is

necessary to include terms accounting for "non-rigid" and anharmonic behaviour. Consideration must also be given to centrifugal distortion, and, when applicable, to Coriolis and Fermi interactions.

2.2 The Rigid Rotor - Harmonic Oscillator Hamiltonian

The quantum mechanical Hamiltonian operator for a polyatomic molecule can be expressed as

$$\hat{H} = T_E + T_N + V_{EN} + V_{NN} + V_{EE} \quad (2-1)$$

where T_E and T_N represent, respectively, the kinetic energy of all the electrons and all the nuclei in terms of momentum. The potential energy terms V_{EN} , V_{NN} and V_{EE} arise from the electrostatic attraction and repulsion between electrons and nuclei. Consequently, the total energy of a molecule can be written as

$$\begin{aligned} E_{\text{total}} = & E_{\text{translation}} + E_{\text{rotation}} + E_{\text{vibration}} + E_{\text{electronic}} \\ & + E_{\text{trans-rot}} + E_{\text{trans-vib}} + E_{\text{rot-vib}} \end{aligned} \quad (2-2)$$

The system can be greatly simplified by using the Born-Oppenheimer approximation [26]. This approximation assumes that the nuclei, owing to their much greater masses, move much more slowly than the electrons. Therefore, at any given time the motion of the electrons is the same as if the nuclei were fixed at their present instantaneous positions. This facilitates the separation of Schrodinger's equation

into an electronic part and a "mechanical" rotation vibration part. Each part may then be solved independently.

Further simplification may be achieved by describing the position of the nuclei in a molecule using a molecule-fixed coordinate system [27]. This axis system has its origin at the molecule's center of mass, and is rotating with the molecule. The orientation of the rotating system with respect to the space fixed axis may be described by a set of Euler angles. The molecule-fixed axis system eliminates the translation-coupled terms and allows the separation of the translational energy from the total energy equation. Hence, we are left with only the rotation-vibration energy

$$E_{\text{rov}} = E_{\text{rot}} + E_{\text{vib}} + E_{\text{rot-vib}} \quad (2-3)$$

This is represented in the Hamiltonian in terms of kinetic and potential energies

$$H_{\text{rov}} = T_{\text{rov}} + V_{\text{rov}} \quad (2-4)$$

The rotation-vibration Hamiltonian may now be solved, treating the molecule as a set of point masses representing the nuclei lying in some potential field. Here, the electronic energy as a function of nuclear positions, becomes the potential energy term.

The rotational kinetic energy is expressed in terms of angular momentum, while the vibrational energy may be stated

in harmonic oscillator form. Wilson and Howard [28], transformed the kinetic energy in the space-fixed frame to the molecule-fixed axis system. By doing so they obtained the following classical expression for the molecular kinetic energy,

$$T = \sum_{\alpha\beta} 1/2 (J_\alpha - p_\alpha) \mu_{\alpha\beta} (J_\beta - p_\beta) + \sum_i^{3N-6} p_i^2 \quad (2-5)$$

where the terms are defined in Table 2-1. Molecular vibrations are described relative to the molecular axes with the $3N-6$ normal vibrational coordinates Q_i where N is the number of atoms. Hence, $p_i = \partial T / \partial Q_i$ is the vibrational momentum conjugate to the normal coordinates, Q_i . It is assumed here that the potential energy is a function only of the normal coordinates.

Starting with this classical expression (Equation 2-5) the quantum-mechanical Hamiltonian operator has been derived by Wilson and Howard [28], and later by Darling and Dennison [29]. More recently, Watson [30] has simplified the rather complicated original expressions to give a more general Hamiltonian for non-linear polyatomic molecules

$$\hat{H} = 1/2 \sum_{\alpha\beta} (\hat{J}_\alpha - \hat{p}_\alpha) \mu_{\alpha\beta} (\hat{J}_\beta - \hat{p}_\beta) + 1/2 \sum_i \hat{p}_i^2 + \hat{V}(Q_i) + U \quad (2-6)$$

The last term, $U = -1/8h^2 \sum_{\alpha} \mu_{\alpha\beta}$ is a function only of the vibrational coordinates and therefore can be incorporated into the potential energy term. For practical purposes this Hamiltonian is usually simplified by expanding V and $\mu_{\alpha\beta}$

Table 2-1
Definition of Commonly Used Symbols

$\hat{\quad}$ circumflex denotes operator

\hat{H} Hamiltonian operator

\hat{J} quantum number defining eigenvalues of the total angular momentum J

\hat{J}_α component of total angular momentum, $\alpha = x, y, \text{ or } z$

\hat{P}_α component of vibrational angular momentum, $\alpha = x, y, z$

\hat{P}_i linear momentum conjugate to the i^{th} normal coordinates

\hat{Q}_i i^{th} normal coordinate

d_i degeneracy of \hat{Q}_i

v_i quantum number of vibration of \hat{Q}_i

I_α^v effective moment of inertia about $\alpha = x, y, \text{ or } z$ in vibrational state v

$\mu_{\alpha\beta}$ inverse of moment of inertia matrix, or $\beta = x, y, z$

about equilibrium values as a Taylor series in the normal coordinates. This series, however, converges relatively slowly for light asymmetric molecules such as H₂O and H₂CO. A perturbation calculation can be made using a unitary transformation on the Hamiltonian making it diagonal in vibrational quantum numbers [31]. The Hamiltonian may then be rewritten as

$$\hat{H} = \hat{H}_{\text{rot}} + \hat{H}_{\text{vib}} \quad (2-7)$$

where the rotational parameters are a function of the particular vibration under consideration. The zero order vibrational Hamiltonian is given by

$$\hat{H}_{\text{vib}} = 1/2 \sum_i (\hat{p}_i^2 + \hat{q}_i^2) \quad (2-8)$$

This gives rise to the harmonic oscillator vibrational energy levels defined by

$$E_{\text{vib}} = (v + d/2) \text{ (cm}^{-1}) \quad (2-9)$$

Hence the total vibrational energy of a given molecule is

$$G(v_1, v_2, \dots) = \sum_i \omega_i (v_i + d_i/2) \quad (2-10)$$

where i runs over the 3N-6 normal vibrational modes. Providing that no resonances exist between the various vibrational states the rotational Hamiltonians may now be diagonalized to yield the rotational energies for the individual vibrational bands. The discussion will now focus

on the rotational Hamiltonian, specifically for the case of the asymmetric rotor which is characterized by three unequal moments of inertia.

If the molecular axes are fixed so that they coincide with the principal axes of inertia [32], then the lowest-order approximation for the rotational Hamiltonian may be stated in terms of the rigid rotor as

$$\hat{H}_{\text{rot}} = \hat{H}_{\text{rigid}} = \hat{B}_x^{\prime} \hat{J}_x^2 + \hat{B}_y^{\prime} \hat{J}_y^2 + \hat{B}_z^{\prime} \hat{J}_z^2 \quad (2-11)$$

where the rotational constants $B_{\alpha}' = 1/2I_{\alpha} \text{ cm}^{-1}$ ($\alpha=x, y$ or z) and I_x, I_y, I_z are the principal moments of inertia of the molecule. The angular momentum components J_{α} are measured in units of \hbar , and obey commutation relations of the type

$$[\hat{J}_{\alpha}, \hat{J}_{\beta}] = \hat{J}_{\alpha}\hat{J}_{\beta} - \hat{J}_{\beta}\hat{J}_{\alpha} = -i\hat{J}_{\gamma} \quad (2-12)$$

where the subscripts cyclically represent the molecule-fixed axes x, y and z .

By introducing centrifugal distortion, Wilson and Howard [28] derived the next higher order of approximation to H_{rot} , giving

$$\hat{H}_{\text{rot}} = \hat{H}_{\text{rigid}} + 1/4 \sum T_{\alpha\beta\gamma\delta} \hat{J}_{\alpha}\hat{J}_{\beta}\hat{J}_{\gamma}\hat{J}_{\delta} \quad (2-13)$$

where the $T_{\alpha\beta\gamma\delta}$ coefficient in the quartic terms is given to a good approximation by [33]

$$T = -1/2 \sum_{ij} \mu_{\alpha\beta}^i (F^{-1}) \mu_{\alpha\beta}^j \quad (2-14)$$

where i and j run over the $3N-6$ internal displacement coordinates, which are used to evaluate both the inverse force field (F^{-1}) and the moment-of-inertia matrices. The general asymmetric rotor has 21 non-zero distortion coefficients, of which nine take on distinct values while the rest vanish due to symmetry. The nine distinct values are

$$T_{\alpha\alpha\alpha\alpha}, T_{\alpha\alpha\beta\beta} = T_{\beta\beta\alpha\alpha}$$

$$T_{\alpha\beta\alpha\beta} = T_{\alpha\beta\beta\alpha} = T_{\beta\alpha\alpha\beta} = T_{\beta\alpha\beta\alpha}$$

where $\alpha, \beta = x, y$ or z

By applying the commutation relations shown in equation (2-12) Kivelson and Wilson [9] have demonstrated that there are really only six independent distortion coefficients, and equation (2-13) can be written in a simpler form as

$$\hat{H}_{\text{rot}} = B_x \hat{J}_x^2 + B_y \hat{J}_y^2 + B_z \hat{J}_z^2 + 1/4 T'_{\alpha\beta\gamma\delta} \hat{J}_\alpha^2 \hat{J}_\beta^2 \quad (2-15)$$

where $T'_{xxxx} = T_{xxxx}$

$$T'_{yyyy} = T_{yyyy}$$

$$T'_{zzzz} = T_{zzzz}$$

$$T'_{xxyy} = T_{xxyy} + 2T_{xyxy}$$

$$T'_{yyzz} = T_{yyzz} + 2T_{yzyz}$$

$$T'_{xxzz} = T_{xxzz} + 2T_{xzxz}$$

$$B_x = B_x + 1/4(3T_{xyxy} - 2T_{xzxz} - 2T_{yzyz})$$

$$B_y = B_y + 1/4(3T_{yzyz} - 2T_{xyxy} - 2T_{xzxz})$$

$$B_z = B_z + 1/4(3T_{xzxz} - 2T_{xyxy} - 2T_{yzyz})$$

Note, however, that the new rotational constants $B_{x,y,z}$ are now also corrected for distortion.

It was later shown by Dowling [35] that for planar asymmetric top molecules such as H_2CO , the six independent T constants reduce to four independent coefficients. These H_{rot} models are however, only valid for a harmonic-oscillator approximation to the force field and for the equilibrium coefficients, not the vibrationally averaged ones that are observed in practice. If the energy levels of a molecule are known to high accuracy then this H_{rot} will yield a poor fit because of these two approximations. Watson [36] has demonstrated that the poor data fits obtained from the Kivelson and Wilson model are due to the fact that the matrix elements of the six $T_{\alpha\beta\gamma\delta}$ are linearly dependent on each other. Consequently, Watson developed a more general Hamiltonian which may be expanded to high orders in angular momentum operators that insures independence of the matrix elements of the effective operators. In this thesis, the rotational constants and distortion coefficients for formaldehyde were determined from a least-squares-fit to a sixth order Watson Hamiltonian. A detailed summary of the development of this Hamiltonian will now follow.

2.3 The Rotational Hamiltonian

The general rotational Hamiltonian for a particular vibrational band may be written as a power series in the angular momentum components \hat{J}_x , \hat{J}_y and \hat{J}_z . By means of commutation relations this representation is reduced to the so-called standard form [36,37] given as

$$\hat{H}_{\text{rot}} = \sum_{pqr} h_{pqr} (\hat{J}_x^p \hat{J}_y^q \hat{J}_z^r + \hat{J}_z^r \hat{J}_y^q \hat{J}_x^p) \quad (2-16)$$

where the coefficients h_{pqr} can be either real or complex and p , q and r are integers. However, molecular model Hamiltonians must be invariant to both time reversal [38] and to Hermitian conjugation denoted by the symbol * [32], so that

$$\hat{H}_{\text{rot}} = L \hat{H}_{\text{rot}} L^{-1} = \hat{H}_{\text{rot}}^* = (L \hat{H}_{\text{rot}} L^{-1})^* \quad (2-17)$$

Consequently, the standard expression is constrained by the fact that \hat{H}_{rot} must be Hermitian, h_{pqr} has to be real and not complex, and the sum $p+q+r$ is restricted to even integers. For orthorhombic molecules p, q and r are all even integers and some of the h_{pqr} coefficients can be shown to equal zero. By the use of unitary transformations the general non-orthorhombic asymmetric top Hamiltonian may be transformed to the orthorhombic form. The standard form Hamiltonian up to terms of sixth degree in J_α can be written [39] as

$$\hat{H}_{\text{rot}} = \hat{H}_2 + \hat{H}_4 + \hat{H}_6 \quad (2-18)$$

where

$$\begin{aligned}\hat{H}_2 &= \sum_{\alpha} B_{\alpha} \hat{J}_{\alpha}^2 \\ &= B_x \hat{J}_x^2 + B_y \hat{J}_y^2 + B_z \hat{J}_z^2\end{aligned}\quad (2-19)$$

$$\begin{aligned}\hat{H}_4 &= \sum_{\alpha \neq \beta} T_{\alpha \beta} \hat{J}_{\alpha}^2 \hat{J}_{\beta}^2 \\ &= T_{xx} \hat{J}_x^4 + T_{yy} \hat{J}_y^4 + T_{zz} \hat{J}_z^4 + T_{xy} (\hat{J}_x^2 \hat{J}_y^2 + \hat{J}_y^2 \hat{J}_x^2) \\ &\quad + T_{xz} (\hat{J}_x^2 \hat{J}_z^2 + \hat{J}_z^2 \hat{J}_x^2) + T_{yz} (\hat{J}_y^2 \hat{J}_z^2 + \hat{J}_z^2 \hat{J}_y^2)\end{aligned}\quad (2-20)$$

$$\begin{aligned}\hat{H}_6 &= \sum_{\alpha} \phi_{\alpha \alpha \alpha} \hat{J}_{\alpha}^6 + \sum_{\alpha \neq \beta} \phi_{\alpha \alpha \beta} (\hat{J}_{\alpha}^4 \hat{J}_{\beta}^2 + \hat{J}_{\beta}^2 \hat{J}_{\alpha}^4) \\ &\quad + \phi_{xyz} (\hat{J}_x^2 \hat{J}_y^2 \hat{J}_z^2 + \hat{J}_z^2 \hat{J}_y^2 \hat{J}_x^2) \\ &= \phi_{xxx} \hat{J}_x^6 + \phi_{yyy} \hat{J}_y^6 + \phi_{zzz} \hat{J}_z^6 + \phi_{xxy} (\hat{J}_x^4 \hat{J}_y^2 + \hat{J}_y^2 \hat{J}_x^4) \\ &\quad + \phi_{xxz} (\hat{J}_x^4 \hat{J}_z^2 + \hat{J}_z^2 \hat{J}_x^4) + \phi_{yyz} (\hat{J}_y^4 \hat{J}_z^2 + \hat{J}_z^2 \hat{J}_y^4) \\ &\quad + \phi_{yxz} (\hat{J}_y^4 \hat{J}_x^2 + \hat{J}_x^2 \hat{J}_y^4) + \phi_{zzx} (\hat{J}_z^4 \hat{J}_x^2 + \hat{J}_x^2 \hat{J}_z^4) \\ &\quad + \phi_{zzy} (\hat{J}_z^4 \hat{J}_y^2 + \hat{J}_y^2 \hat{J}_z^4) + \phi_{xyz} (\hat{J}_x^2 \hat{J}_y^2 \hat{J}_z^2 + \hat{J}_z^2 \hat{J}_y^2 \hat{J}_x^2)\end{aligned}\quad (2-21)$$

This Hamiltonian may be expanded to higher degrees in \hat{J}_{α} . However, in general, for low quantum numbers the energy contributions from the various terms are such that $\hat{H}_2 \gg \hat{H}_4 \gg \hat{H}_6 \dots$, so that the power series may be truncated according to the needs of the particular system. For highly flexible or light molecules, such a series may not converge at a satisfactory rate and an alternative treatment may be

preferable [40-42].

The coefficients $T_{\alpha\beta}$ are related to Kivelson and Wilson's parameters by $T_{\alpha\alpha\beta\beta} = 4T_{\alpha\beta}$. At this point however, the Hamiltonian has 3 quadratic, 6 quartic and 10 sextic coefficients of which some are not determinable parameters. Unitary transformation of \hat{H}_{rot} affects only the coefficients of the momentum operators while leaving the eigenvalues unchanged. Watson has made use of this fact and demonstrated that by a proper choice of unitary operators it is possible to eliminate many terms from the Hamiltonian so that it yields a set of determinable molecular constants from combinations of the indeterminable coefficients.

Watson constructed a unitary operator by means of the equation

$$\hat{U} = \exp(i\hat{S}) \quad (2-22)$$

where \hat{S} is Hermitian. In order that \hat{U} be invariant to time reversal, S must change sign under time reversal. Hence, \hat{S} is given as an odd power series in the components of the angular momentum [37]

$$\hat{S} = \sum_{pqr} s_{pqr} (\hat{J}_x^p \hat{J}_y^q \hat{J}_z^r + \hat{J}_z^r \hat{J}_x^p \hat{J}_y^q) = \hat{S}_3 + \hat{S}_5 + \hat{S}_7 + \dots \quad (2-23)$$

with p , q , and r all odd, and real coefficients s_{pqr} . As in the case of the standard form \hat{H}_{rot} , this series may be truncated according to the particular case. This work utilizes the first two terms of this series, which are

$$\begin{aligned}\hat{S}_3 &= s_{111}(\hat{J}_x \hat{J}_y \hat{J}_z + \hat{J}_z \hat{J}_y \hat{J}_x) \\ \hat{S}_5 &= s_{311}(\hat{J}_x^3 \hat{J}_y \hat{J}_z + \hat{J}_z \hat{J}_y \hat{J}_x^3) + s_{131}(\hat{J}_x \hat{J}_y^3 \hat{J}_z + \hat{J}_z \hat{J}_y \hat{J}_x^3) \\ &\quad + s_{113}(\hat{J}_x \hat{J}_y \hat{J}_z^3 + \hat{J}_z^3 \hat{J}_y \hat{J}_x)\end{aligned}\quad (2-24)$$

The contact transformation of the rotational Hamiltonian may be written as

$$\tilde{H}_R = U^{-1} \hat{H}_{\text{rot}} U = \tilde{H}_2 + \tilde{H}_4 + \tilde{H}_6 + \dots \quad (2-25)$$

where the terms of the transformed Hamiltonian are given by

[37]

$$\begin{aligned}\tilde{H}_2 &= \hat{H}_2 \\ \tilde{H}_4 &= \hat{H}_4 + i(\hat{H}_2, \hat{S}_3) \\ \tilde{H}_6 &= \hat{H}_6 + i(\hat{H}_4, \hat{S}_3) - 1/4\{(\hat{H}_2, \hat{S}_3), \hat{S}_3\} + i(\hat{H}_2, \hat{S}_5)\end{aligned}\quad (2-26)$$

For each commutation of the type $(A, B) = AB - BA$ the degree of a given term is reduced by one. The rearrangement of each \tilde{H}_n to the standard form produces terms of lower degree. The terms of the same degree are then collected to give

$$\tilde{H}_R = \tilde{H}_2 + \tilde{H}_4 + \tilde{H}_6 + \dots \quad (2-27)$$

\tilde{H}_R has now the same form as \hat{H}_{rot} . The new quadratic and quartic molecular constants are then related to the old ones by

$$\tilde{B}_x = B_x + 4(B_z - B_y)s_{111}$$

$$\tilde{B}_y = B_y + 4(B_x - B_z)s_{111}$$

$$\tilde{B}_z = B_z + 4(B_y - B_x)s_{111} \quad (2-28)$$

$$\tilde{T}_{xx} = T_{xx}, \quad \tilde{T}_{yy} = T_{yy}, \quad \tilde{T}_{zz} = T_{zz}$$

$$\tilde{T}_{yz} = T_{yz} + 2(B_z - B_y)s_{111}$$

$$\tilde{T}_{xz} = T_{xz} + 2(B_x - B_z)s_{111}$$

$$\tilde{T}_{xy} = T_{xy} + 2(B_y - B_x)s_{111} \quad (2-29)$$

The transformed sextic coefficients are listed in Watson's paper [37], while the higher order contributions for the quadratic and quartic terms are given by Typke [43].

Due to the fact that the determinable constants can only be a function of the energies, and cannot depend on the particular choice of unitary transformation, s_{pqr} must not appear in the expression for the determinable parameters. Hence, in equations (2-28) and (2-29) s_{111} should be eliminated by substitution. By doing so one also eliminates one molecular parameter. Consequently, a set of parameters which do not depend on the transformation is obtained:

$$\tilde{B}_x = B_x - 2T_{yx}$$

$$\tilde{B}_y = B_y - 2T_{xz}$$

$$\tilde{B}_z = B_z - 2T_{xy}$$

$$T_{xx}, \quad T_{yy}, \quad T_{zz}$$

$$T_1 = T_{yz} + T_{xz} + T_{xy}$$

$$T_2 = B_x T_{yz} + B_y T_{xz} + B_z T_{xy}$$

$$(2-30)$$

Similarly, the sextic part of the Hamiltonian may be reduced to seven determinable combinations of coefficients. The three rotational constants, the five quartic centrifugal distortion constants, and the seven sextic centrifugal distortion constants give a total of 15 determinable parameters from a sixth order asymmetric Hamiltonian. In general, a Hamiltonian of n^{th} degree has $n(n+4)/4$ determinable parameters (remembering that here n is an even integer).

Finally, in order to reduce the complexity of the matrix elements, the Hamiltonian is written in terms of the operators \hat{J}^2 , \hat{J}_z and \hat{J}_{\pm} . Where, \hat{J} represents the total angular momentum, \hat{J}_z is the component of \hat{J} along the z molecular principal axis, and $\hat{J}_{\pm} = \hat{J}_x \pm i\hat{J}_y$, in the symmetric top basis, acts as the lowering and raising operators of the quantum number K. This representation is given by [37]

$$\begin{aligned}\hat{H}_{\text{rot}} = & B_{200} \hat{J}^2 + B_{020} \hat{J}_z^2 + B_{002} (\hat{J}_+^2 + \hat{J}_-^2) \\ & + T_{400} \hat{J}^4 + T_{220} \hat{J}^2 \hat{J}_z^2 + T_{040} \hat{J}_z^4 + T_{202} \hat{J}^2 (\hat{J}_+^2 + \hat{J}_-^2) \\ & + 1/2 T_{022} \{ \hat{J}_z^2 (\hat{J}_+^2 + \hat{J}_-^2) + (\hat{J}_+^2 + \hat{J}_-^2) \hat{J}_z^2 \} \\ & + T_{004} (\hat{J}_+^4 + \hat{J}_-^4) + \text{higher order terms} \quad (2-31)\end{aligned}$$

where the subscripts of the coefficients refer to the powers of the operators \hat{J} , \hat{J}_z and \hat{J}_{\pm} . In the transformed

Hamiltonian the coefficients for the quadratic and quartic terms then become:

$$\tilde{B}_{200} = B_{200} + 4B_{002}s_{111}$$

$$\tilde{B}_{020} = B_{020} - 14B_{002}s_{111}$$

$$\tilde{B}_{002} = B_{002} + 2B_{002}s_{111}$$

$$\tilde{T}_{400} = T_{400} - 2B_{002}s_{111}$$

$$\tilde{T}_{202} = T_{202}$$

$$\tilde{T}_{220} = T_{220} + 12B_{002}s_{111}$$

$$\tilde{T}_{022} = T_{022} - 2B_{020}s_{111}$$

$$\tilde{T}_{040} = T_{040} - 10B_{002}s_{111}$$

$$\tilde{T}_{004} = T_{004} + B_{002}s_{111}$$

(2-32)

2.4 The Reduced Hamiltonian

It was shown in the previous section that the rotational Hamiltonian may be reduced by a proper choice of s_{pqr} . This however, can be done in many ways [39,44]. To limit the possibilities it is convenient to consider only those reductions that eliminate specific cylindrical components from the Hamiltonian. The two most commonly used reductions, called AS (asymmetric) and NS (nearly symmetric) are obtained using two of Nielsen's molecular constants [45]

$$R_5 = (1/8)(-T_{xx} + T_{yy} + 2T_{xz} - 2T_{yz})$$

$$R_6 = (1/16)(T_{xx} + T_{yy} - 2T_{xy}) \quad (2-33)$$

Under unitary transformation these become

$$\tilde{R}_5 = R_5 - (B_z - (1/2)(B_x - B_y))s_{111}$$

$$\tilde{R}_6 = R_6 + (1/4)(B_x - B_y)s_{111} \quad (2-34)$$

The NS and AS forms may be obtained by setting respectively \tilde{R}_5 and \tilde{R}_6 to zero yielding

$$s_{111} = R_5 / \{B_z - 1/2(B_x + B_y)\} = T_{022}/2B_{020} \quad (2-35)$$

or

$$s_{111} = 4R_6 / (B_x - B_y) = -T_{004}/B_{002} \quad (2-36)$$

Observe that equation (2-35) may not be used for nearly spherical tops, where $B_x = B_y = B_z$ leads to an infinitely large s_{111} . Similarly equation (2-36) used in the AS case goes to infinity for nearly symmetric tops where $B_x = B_y$. Hence, the choice of reduction form is governed by molecular symmetry. The Hamiltonian for formaldehyde was reduced using the AS form.

The choice for s_{111} using Equation (2-36) makes $T_{004} = 0$ so that the operator $(\hat{J}_+^4 + \hat{J}_-^4)$ is eliminated from Equation (2-31). Similarly, with proper choices of s_{113} , s_{131} and s_{311} one may drop three operators from the sextic term of H_{rot} . The reduced Hamiltonian may then be written as

$$\hat{H}^{AS} = \hat{H}_2^{AS} + \hat{H}_4^{AS} + \hat{H}_6^{AS} + \dots \quad (2-37)$$

where

$$\begin{aligned}\hat{H}_2^{AS} &= 1/2(B_x^{AS} + B_y^{AS})\hat{J}^2 + \{B_z^{AS} - 1/2(B_x^{AS} + B_y^{AS})\}\hat{J}_z^2 \\ &\quad + 1/4(B_x^{AS} - B_y^{AS})(\hat{J}_+^2 - \hat{J}_-^2)\end{aligned}$$

$$\begin{aligned}\hat{H}_4^{AS} &= -\Delta_J\hat{J}^4 - \Delta_{JK}\hat{J}^2\hat{J}_z^2 - \Delta_K\hat{J}_z^4 - \delta_J\hat{J}^2(\hat{J}_+^2 - \hat{J}_-^2) \\ &\quad - 1/2\delta_K\{\hat{J}_z^2(\hat{J}_+^2 - \hat{J}_-^2) + (\hat{J}_+^2 - \hat{J}_-^2)\hat{J}_z^2\}\end{aligned}$$

$$\begin{aligned}\hat{H}_6^{AS} &= h_J\hat{J}^6 + h_{JK}\hat{J}^4\hat{J}_z^2 + h_{KJ}\hat{J}^2\hat{J}_z^4 + h_K\hat{J}^6 + h_J\hat{J}^4(\hat{J}_+^2 - \hat{J}_-^2) \\ &\quad + 1/2h_{JK}\hat{J}^2\{\hat{J}_z^2(\hat{J}_+^2 - \hat{J}_-^2) + (\hat{J}_+^2 - \hat{J}_-^2)\hat{J}_z^2\} \\ &\quad + 1/2h_K\{\hat{J}_z^4(\hat{J}_+^2 - \hat{J}_-^2) + (\hat{J}_+^2 - \hat{J}_-^2)\hat{J}_z^4\}\end{aligned}$$

The matrix of this Hamiltonian is in tri-diagonal form, which makes it relatively easy to solve. Therefore, the AS form is the one most commonly used.

2.5 Asymmetric Rotor Notation and Selection Rules

The rigid rotor Hamiltonian given in Equation (2-11) is usually rewritten as

$$\hat{H}_{\text{rigid}} = B_a\hat{J}_a^2 + B_b\hat{J}_b^2 + B_c\hat{J}_c^2 \quad (2-38)$$

where the molecule fixed axes x, y, and z are now represented by some permutation of a, b and c. A further simplification introduces $A=B_a$, $B=B_b$ and $C=B_c$. According to convention $A>B>C$

since $I_a < I_b < I_c$. The original x, y, and z axes may be identified with the new labels in the six ways [46] shown in Table 2-2

Table 2-2
Axis Representation

	right hand permutations			left hand permutations		
	I^r	II^r	III^r	I^l	II^l	III^l
x	b	c	a	c	a	b
y	c	a	b	b	c	a
z	a	b	c	a	b	c

The rotational constants A, B and C may be used to define asymmetry parameters. These in turn indicate to what extent an asymmetric top approximates the limits of a symmetric top, i.e., when any two rotational constant are equal. The Wang asymmetry parameter b is given by

$$b = (B_y - B_x) / (2B_z - B_x - B_y) \quad (2-39)$$

In the I^r axis permutation b becomes

$$b_p = (C - B) / (2A - B - C) \quad (2-40)$$

The range of b_p is $-1 \leq b_p \leq 0$. Now, for a prolate symmetric

top where $A > B = C$, $b_p = 0$. The other limit, $b_p = -1$ occurs for the oblate symmetric top where $A = B > C$. In the III^r representation b is defined as

$$b_o = (B - A) / (2C - A - B) \quad (2-41)$$

The range here is $0 \leq b_o \leq 1$; where b_o is respectively 0 and 1 for oblate and prolate symmetric tops. The utilization of the remaining representations is not necessary due to redundancy.

Another useful definition is given in terms of Ray's asymmetry parameter κ where

$$\kappa = (2B - A - C) / (A - C) \quad (2-42)$$

Here the range is $-1 \leq \kappa \leq +1$, where κ is equal to -1 in the prolate limit and +1 in the oblate limit, $\kappa = 0$ defines the most asymmetric case. The computed Ray parameter for H₂CO is $\kappa = -0.961$, hence formaldehyde is a near prolate asymmetric top. The limits of κ also suggest that an asymmetric top may be described in terms of its symmetric limits. A convenient method of representation consist of the symmetric wavefunctions $\psi_{J,K,M}$ written as $|J,K,M\rangle$. The quantum numbers K and M represent respectively, the $2J+1$ orientations of the total angular momentum in the molecule fixed axis system (J_z) and in the space fixed coordinate system (J_z). In the absence of an external potential field, all M values are degenerate for a given K and they are not considered in the computation used in this thesis.

The matrices of the Hamiltonians discussed thus far are diagonal in J . Hence the only matrix elements required for the calculation of the energy levels are $\langle J, K' | \hat{H} | J, K \rangle$. Therefore the Hamiltonian may be diagonalized individually for each J value. In the rigid rotor representation, the only non-zero matrix elements are

$$\begin{aligned}\langle J, K | \hat{H}_{\text{rigid}} | J, K \rangle &= (1/2)(B_x + B_y)J(J+1) \\ &\quad + [B_z - (1/2)(B_x + B_y)]K^2 \\ \langle J, K \pm 2 | \hat{H}_{\text{rigid}} | J, K \rangle &= (1/4)(B_x - B_y)\{[J(J+1) - K(K \pm 1)] \\ &\quad \times [J(J+1) - (K \pm 1)(K \pm 2)]\}^{1/2} \quad (2-43)\end{aligned}$$

so that H_{rigid} is tri-diagonal. The calculation of the rotational energy level reduces to the diagonalization of this matrix for each value of J . Observe, however, that for a symmetric top ($B_x = B_y$) or a spherical top ($B_x = B_y = B_z$) the Hamiltonian is already diagonal.

The numerical diagonalization of asymmetric top Hamiltonian matrices is facilitated by the use of a new set of basis function $|J, K^+ \rangle$ created by the Wang transformation [47]

$$\begin{aligned}|J, 0^+ \rangle &= |J, 0 \rangle \\ |J, K^+ \rangle &= (1/2)\{|J, K \rangle + |J, -K \rangle\} \quad K > 0 \\ |J, K^- \rangle &= (1/2)\{|J, K \rangle - |J, -K \rangle\} \quad K > 0 \quad (2-44)\end{aligned}$$

Here one takes into account the symmetry properties of the asymmetric wavefunctions which belong to the group $V_{(a, b, c)}$

defined by an identity operator E and three two-fold rotational operators C_2^a, C_2^b, C_2^c , where a, b and c denote the molecular fixed axis. The character table for $V_{(a,b,c)}$ is given in Table 2-3 with +1 and -1 representing respectively symmetric and antisymmetric wavefunctions for the given operator.

Table 2-3
Character Table for the Group $V_{(a,b,c)}$

operation				symmetry		Wang's sub-matrices	
E	C_2^a	C_2^b	C_2^c	K_a, K_c	type	J_{even}	J_{odd}
1	1	1	1	e,e	A_O	E^+	E^-
1	1	-1	-1	e,o	B_a	E^-	E^+
1	-1	1	-1	o,o	B_b	O^+	O^-
1	-1	-1	1	o,e	B_c	O^-	O^+

The rigid-rotor Hamiltonian is invariant to two-fold rotations C_2^α ($\alpha = x, y, z$) which generate the point group $V_{(a,b,c)}$ (or D_2 group). Since the Wang functions are linear combinations of the symmetric top wavefunctions which transform with $V_{(a,b,c)}$ operations, they may be used as a basis set yielding fully symmetrized sub-matrices. If H_{rot} is now set up in this basis, then the Hamiltonian matrix for each J (other than $J=0$ and $J=1$) can be partitioned into four independent tri-diagonal matrices. This can be done because the matrix elements connecting even and odd K 's vanish along

with those connecting $|J, K^+\rangle$ and $|J, K^-\rangle$. Hence for a given J we may write

$$\hat{H}_R^J = E^+ + O^+ + E^- + O^- \quad (2-45)$$

where + and - refer to matrices with only $|J, K^+\rangle$ or $|J, K^-\rangle$ elements. The E and O labels refer to whether K is even or odd. Upon computation, one obtains $2J+1$ energy levels for each J . The advantage of using Wang's transformation lies in the fact that the original $2J+1$ by $2J+1$ matrix is reduced to four much smaller matrices. A general result for the asymmetric top Hamiltonian matrix of a given J is that for even J the E^+ block has dimension $(J+2)/2$ and the other three blocks have dimension $J/2$, whereas for odd J the E^- block has dimension $(J-1)/2$ and the other three blocks have dimension $(J+1)/2$. This results in significant computational efficiencies.

The asymmetric top rotational energy levels are designated J_{K_a, K_c} . This is obtained by considering a process in which the rotational constant B_α is varied smoothly from the prolate to the oblate symmetric conditions. Here K_a and K_c represent respectively the prolate and oblate limits of K . For intermediate values of B_α , the energy levels for a given J do not cross. Thus, J_{K_a, K_c} specifies each energy level uniquely as can be seen in Figure 2-1. The symmetries of the wave functions with respect to C_2^a and C_2^c of $V(a, b, c)$ are determined by K_a and K_c .

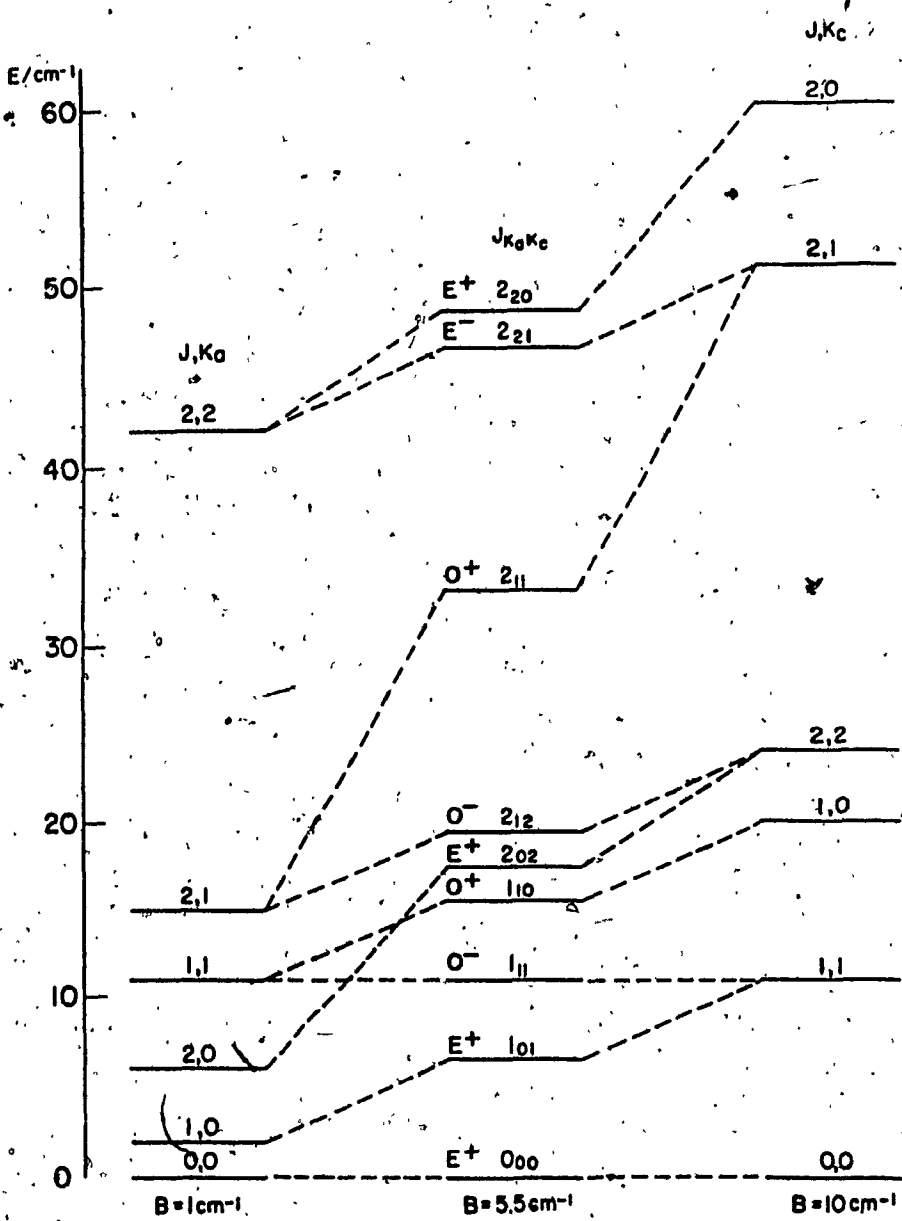


Figure 2-1: Correlation Diagram for the Asymmetric Rotor Energy Levels.

The correlation of $J=0,1$ and 2 energy levels of a rigid asymmetric top molecule having $(A,B,C)=(10,5.5,1) \text{ cm}^{-1}$ i.e., $K=0$, with those for the prolate top having $(A,B,C)=(10,1,1) \text{ cm}^{-1}$ on the left, and with those for the oblate top having $(A,B,C)=(10,10,1) \text{ cm}^{-1}$ on the right.

according to the transformation $C_2^\alpha |J, K^+ \rangle$, where $\alpha = a$ or c . The energy increases with increasing K_a and decreases with increasing K_c . Therefore the energy levels for a given J , in ascending order, have the labels

$$(K_a, K_c) = (0, J), (1, J), (1, J-1), (2, J-1), (2, J-2) \dots \\ \dots (J-1, 2), (J-1, 1), (J, 1), (J, 0) \quad (2-46)$$

Observe that for other than zero, each value of K_a or K_c occurs twice in succession, also that $K_a + K_c$ must equal either J or $J+1$.

In the case of the I^r representation, sixth order AS form Hamiltonian, the only non-zero matrix elements are

$$\langle J, K | \hat{H}_R^{AS} | J, K \rangle = 1/2[B+C]J(J+1) + \{A-1/2[B+C]\}K^2$$

$$- \Delta_J J^2 (J+1)^2 - \Delta_{JK} J(J+1)K^2 - \Delta_K K^4 \\ + h_J J^3 (J+1)^3 + h_{JK} J^2 (J+1)^2 K^2 \\ + h_{KJ} J(J+1)K^4 + h_K K^6$$

$$\langle J, K \pm 2 | \hat{H}_R^{AS} | J, K \rangle = \{1/4[B-C] - \delta_J J(J+1) \}$$

$$- 1/2\delta_K [(K \pm 2)^2 + K^2] + h_J J^2 (J+1)^2 \\ + 1/2h_{JK} J(J+1)[(K \pm 2) + K^2] \\ + 1/2h_K [(K \pm 2)^4 + K^4]$$

$$\times \{[J(J+1)-K(K+1)][J(J+1)-(K+1)(K \pm 2)]\}^{1/2} \quad (2-47)$$

Hence, the form of the energy matrix is identical to that for the rigid rotor.

Transitions between energy levels are designated using $J' K'_a K'_c$ for an upper state energy, and $J'' K''_a K''_c$ for a lower state. In an asymmetric top the type and nature of a given transition is governed by two selection rules. The first rule states that only transitions with $\Delta J = J' - J'' = 0, \pm 1$ are allowed. The second selection rule is a function of the orientation of the dipole moment ($\bar{\mu}$) along the molecular axes a, b and c. Combinations of odd and even K_a and K_c transitions are classified as type a, b and c (Table 2-4). For the case of H_2CO the three vibrational bands ν_3 , ν_4 and ν_6 investigated here are type a, type c and type b respectively and are illustrated in Figure 2-2.

The permanent dipole moment for H_2CO is along the a axis (I^r representation). This gives rise to the pure rotational spectrum of this molecule. For vibrational-rotational transitions one must be concerned with the instantaneous dipole moment induced by the vibration. In this case, the selection rules for changes in K_a and K_c are a function of the transformation of the components of the dipole moment for a given vibration and can be determined from Table 2-3. For the direction cosine matrix (described in the next section) to be non-zero as required for rotational transitions, the product of the characters of the initial and final rotational wave function as well as that

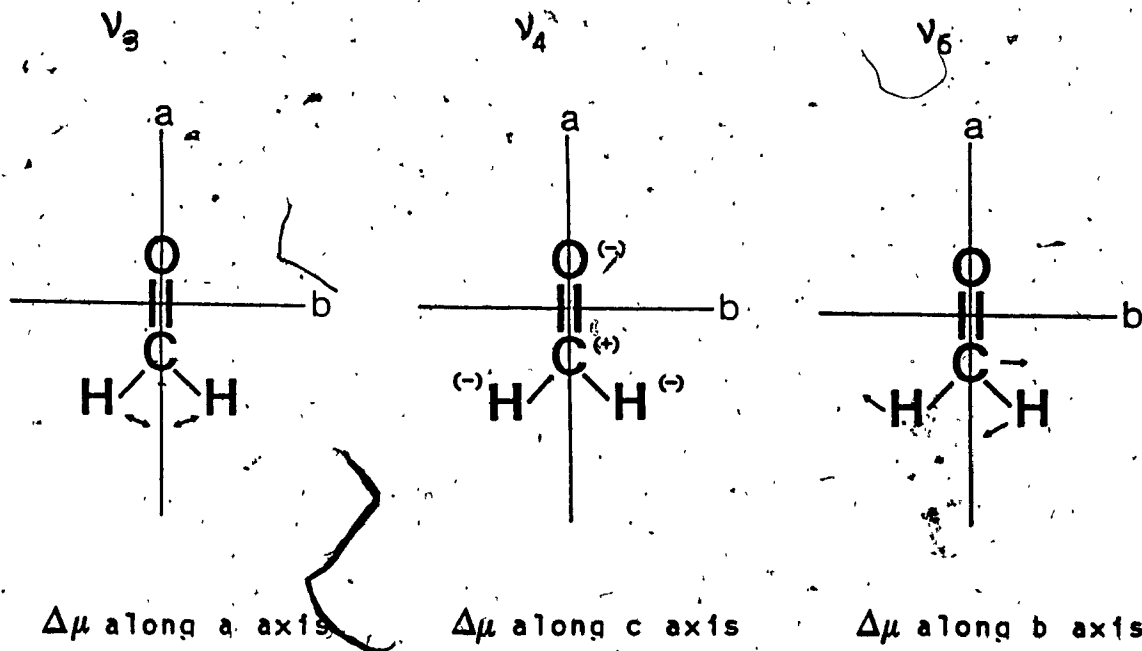
Table 2-4
Asymmetric Top Selection Rules

	ΔK_a	ΔK_c	classification
μ_a	even	odd	type a
μ_b	odd	odd	type b
μ_c	odd	even	type c

Figure 2-2

The v_3 , v_4 and v_6 Vibrations and Their Relation to μ .

c axis is \perp to this page



of the dipole moment change must be +1. This can be seen clearly if Table 2-3 is rewritten as a multiplication table in terms of the transformation of the permanent dipole moment along the a, b, c molecule-fixed axes [46,49] as shown in Table 2-5.

Table 2-5

Direction of the Dipole Moment Permitting Transitions Between Rotational States

$K_a K_c$	A	B_a	B_b	B_c	
	ee	eo	oo	oe	
A	ee	-	a	b	c
B_a	eo	a	-	c	b
B_b	oo	b	c	-	a
B_c	oe	c	b	a	-

For the ν_3 vibration belonging to the B_a symmetry species the instantaneous dipole moment transforms according to B_a , so the selection rules for K_a and K_c are

$$oe \leftrightarrow oo \text{ and } eo \leftrightarrow ee.$$

Similarly, ν_4 with B_c symmetry yields

$$eo \leftrightarrow oo, ee \leftrightarrow oe$$

and ν_6 with B_b symmetry has

$$ee \leftrightarrow oo, eo \leftrightarrow oe$$

For a given vibration $\Delta J=0,+1,-1$ corresponds to the Q, R and P-branches, respectively. However, due to the nature of the asymmetric top, each branch splits into a series of sub-branches as a function of K. In the case of the near prolate top, the sub-branches are governed by K_a , where, for a given K_a one finds a cluster of transitions due to J and K_c . For example, the notation ${}^Q P_5(7)$ in ν_3 represent two possible transitions for $K_a=5$ where Q means that $\Delta K_a=0$; P and 7 stand for $\Delta J=-1$ and $J=7$, respectively. Hence, the notation represent the transitions $(6_{5,1} \leftarrow 7_{5,2})$ and $(6_{5,2} \leftarrow 7_{5,3})$ in the ν_3 band.

2.6 Line Intensities

According to the Beer-Lambert law, the transmission of radiation through a homogeneous gas sample is described by the relation:

$$I = I_0 e^{-k(\nu)X} \quad (2-48)$$

where $k(\nu)$ is the absorption coefficient, $\ln(I/I_0)$ is the absorption ratio and, X is the optical density. The absorption coefficient is a function of both line strength and line shape. The line strength or intensity, S, is defined to be the integral of the absorption coefficient

over the line profile:

$$S = \int_{-\infty}^{\infty} k(\nu) d\nu \quad (2-49)$$

Hence, S is the area under the curve. In terms of fundamental molecular quantities, the strength of a spectral line arising from the transition from state A to state B is given by [46,48]:

$$S_A^B = [8\pi^3/(3hc)] (n/G) \nu_{AB} \text{Exp}(-hcE_A/kT) * [1 - \text{Exp}(-hc\nu_{AB}/kT)] |\langle A | \mu | B \rangle|^2 \quad (2-50)$$

where n is the total number of absorbing molecules per cm^3 per atmosphere, G is the total partition function and $|\langle A | \mu | B \rangle|^2$ is the square of the transition dipole moment matrix element. The rotation-vibration partition function is given by

$$G = \sum_J g_j e^{(-E_J''/kT)} \quad (2-51)$$

where g_j is the statistical weight or degeneracy of the energy state E_j'' of the vibrating-rotating molecule.

The square of the dipole moment matrix element is given by:

$$|\langle A | \mu | B \rangle|^2 = \sum_{f=X,Y,Z} |\langle i | \mu_f | f \rangle|^2 \quad (2-52)$$

where i and f are the initial and final state of all the sublevels in the transition A to B and, μ_f is the component of the dipole moment along the X,Y,Z space fixed axes. In the absence of an external field the X,Y,Z components of the

dipole moment are equal so that only one component has to be evaluated. The chosen component can then be related to the dipole moment relative to the molecule-fixed axis with the direction cosines, ϕ_{Fg} . For example, working with the z component yields

$$|\langle A | \mu | B \rangle|^2 = 3 |\langle i | \mu_z | f \rangle|^2 \quad (2-53)$$

with

$$\mu_z = \sum_g z_g \mu_g$$

where g is summed over the 3 molecule-fixed axes a, b, c.

In the case of H_2CO , if we assume that there is no mixing among the states v_3 , v_4 and v_6 then v_3 has no change in μ_b and μ_c , so only μ_a needs to be considered in Equation (2-53). Similarly, for v_4 and v_6 if it is assumed that there is no mixing then only μ_c and μ_b respectively need to be considered (Figure 2-1). In the case for v_3 Equation (2-53) then becomes:

$$|\langle A | \mu | B \rangle|^2 = 3 |\langle i | \phi_{za} \mu_a | f \rangle|^2 \quad (2-54)$$

If it is assumed that there is no interaction between rotation and vibration, ie., where μ_g does not depend on the rotational coordinates, then Equation (2-54) for v_3 may be written as

$$|\langle A | \mu | B \rangle|^2 = 3 |\langle R_i | \phi_{za} | R_f \rangle|^2 |\langle v_i | \mu_a | v_f \rangle|^2 \times \beta \quad (2-55)$$

where

$$|R_i\rangle |v_i\rangle = |i\rangle \text{ and } |R_f\rangle |v_f\rangle = |f\rangle$$

and β is the nuclear spin degeneracy and is 3 for transitions where K_a is odd and is 1 for transitions where K_a is even in the lower state.

Recalling that we are dealing with the case where there is no mixing between vibrational states we find

$$v_i = \text{ground state}, \quad v_f = v_3 \text{ or } v_4 \text{ or } v_6$$

$$\begin{aligned} R_i^j &= \sum_n T_{jn}^T |J, K\rangle_n \\ R_f^m &= \sum_l S_{ml}^T |J, K\rangle_l \end{aligned} \quad (2-56)$$

where S is the eigenvector transformation matrix that diagonalizes the upper state Hamiltonian (superscript T represents transpose of...), T is the eigenvector matrix that diagonalizes the lower state Hamiltonian, and $|J, K\rangle_n$ represents the n^{th} symmetric top basis set. Thus Equation (2-55) may be written in more compact form as [13,53]

$$\begin{aligned} |\langle A | \mu | B \rangle|^2 &= \{ \langle v_i | \mu | v_f \rangle [\sum_n T_{fn}^T \sum_l S_{ml}^T \langle J'', K'' | \mu | J', K' \rangle] \}^2 \\ &= (\partial \mu / \partial Q)^2 \langle v_i | \Omega | v_f \rangle^2 [T^T U_a S]_{jm}^2 \end{aligned} \quad (2-57)$$

where $[U_a]$ is the dipole moment matrix along the a axis, Ω is the normal coordinate matrix, and $(\partial \mu / \partial Q)$ is the dipole moment derivative.

In the actual case presented in this thesis there is mixing between the vibrational states v_3 , v_4 and v_6 so that Equation (2-55) no longer holds, in the sense that we must consider transition components along more than one axis.

However, the principle is the same and we may still write the intensity in the form of Equation (2-57). But unlike the case of Equation (2-57) the vibrational terms do not simply factor out and the correct expression becomes

$$|\langle i | \mu | f \rangle|^2 = \sum_n T_{in}^T \sum_l U_{nl}^2 S_{if} \quad (2-58)$$

where the full matrix U now has μ_a type term for rotational basis sets in the $v_3=1$ manifold, μ_b terms for the $v_6=1$ manifold and μ_c type terms for the $v_4=1$ manifold. A given transition will be now governed by the expression

$$|\langle i | \mu | f \rangle|^2 = \{(\partial\mu/\partial Q_3)z_3 + (\partial\mu/\partial Q_4)z_4 + (\partial\mu/\partial Q_6)z_6\}^2 \quad (2-59)$$

where z_3 depends only upon the rotational quantum numbers in the $v_3=1$ manifold and the ground state, z_4 depends only upon the rotational quantum numbers in the $v_4=1$ manifold and the ground state, etc. For example, z_3 is represented as

$$z_3 = \sum_i a_i \sum_j b_j \langle v_3=0 | \delta Q | v_3=1 \rangle \langle J'', K'' | F \phi_{Zg} | J', K' \rangle \quad (2-60)$$

where a and b are the basis set coefficients ($\int X \hat{O} p. Y d\tau = \int \sum a_i \phi_i \hat{O} p. \sum b_j \phi_j d\tau$). The z terms are easily calculated from matrix elements given in reference [53].

Equation (2-59) may be used to determine the dipole moment derivatives from measured line strengths for several transitions. This is accomplished by a least-squares fit of the measured strengths to Equation (2-59). Note that not only the magnitude of the derivatives but their relative

signs are important. The results of this type of analysis for 27 lines will be presented at the end of Chapter 5. Once the dipole moment derivatives are determined the entire spectrum may be calculated from the eigenvalues and eigenvectors of the Hamiltonian.

2.7 Coriolis Perturbations

Perturbations between close lying energy levels are common phenomena in molecular spectroscopy. These perturbations may be caused by either Fermi or Coriolis interactions. Fermi resonance is due to mixing of states by terms in the potential energy while Coriolis interaction is due to mixing of states caused by terms in the kinetic energy. Coriolis interactions can occur between vibrational levels of different species while for Fermi resonance only states of the same vibrational and rotational species may interact. Since the effects of Fermi resonance were not observed in the 10 μm bands of H_2CO , it will not be described any further in this section.

When a polyatomic molecule rotates and vibrates simultaneously, two apparent forces can be observed. One is the centrifugal force; the second is the Coriolis force. The magnitude of these forces is given by

$$F_{\text{centrifugal}} = mr\omega^2 \quad (2-56)$$

$$F_{\text{Coriolis}} = 2mv_a \omega \sin\varphi \quad (2-57)$$

where m is the mass of the particle, v_a its apparent velocity with respect to the moving coordinate system, r its distance from the axis of rotation, ω the angular velocity of the coordinate system with respect to a fixed coordinate system, and φ the angle between the axis of rotation and the direction of v_a . The Coriolis force, unlike the centrifugal force, occurs only for a particle moving with respect to the rotating axis ($v_a \neq 0$) and is directed at right angles to both the direction of motion and the axis of rotation. The coupling which has been observed between rotation and vibration has been related to this Coriolis force. Coriolis interaction can be classified as either a rotational or vibrational perturbation [58]. It is a rotational perturbation when the interaction between two vibrational levels of different species results in a specific change in the rotational constant B . In a vibrational perturbation one finds either a change in the rotational constant accompanied by a shift in the vibrational level or a systematic change in the rotational constant alone. A shift of only the vibrational level is always due to Fermi resonance [50]. With ν_3 at 1500.17 cm^{-1} , ν_4 at 1167.26 cm^{-1} , and ν_6 at 1249.09 cm^{-1} , H_2CO is the classic example of rotational perturbations [45,50-52]. These are induced by the proximity of

the bands. The P-branch of ν_6 overlaps the R-branch of ν_4 , and its R-branch overlaps the P-branch of ν_3 . The band overlaps cause two strong Coriolis interactions observed previously. These are between the $K'_a=2$ level in ν_6 and the $K'_a=4$ level in ν_4 , and between the $K'_a=6$ level of ν_6 and the $K'_a=3$ level in ν_3 . The rovibrational model for H₂CO must include the relevant Coriolis terms to account for these perturbations. The following quantum mechanical description of Coriolis interaction is based on derivations by Nielsen [45], Allen and Cross [46], Mills et al. [53, 54] and Nakagawa et al. [13, 52].

Coriolis interaction is caused by the coupling of the total angular momentum components p_α and the vibrational angular momentum p_α . The main term of interaction for each band is included in its first order Hamiltonian as

$$H_{21}(\text{Cor.}) = - \sum_{\alpha} 2B_{\alpha}^e p_{\alpha} p_{\alpha} \quad (2-58)$$

$$= -2 \sum_{\alpha} B_{\alpha}^e p_{\alpha} \sum_{ss} \zeta_{ss}^{\alpha} (\omega_s / \omega_s)^{1/2} q_s p_s, \quad (2-59)$$

where B_{α}^e stands for the equilibrium rotational constant around the α axis and ζ_{ss}^{α} for the Coriolis coupling constants derived from the vibration-rotation interaction constants α_s^{α} . The normal coordinate q_s , the conjugate momenta p_s and the angular momentum operators p_{α} are all dimensionless. According to Jahn's rule [31], if the product of the symmetry species of two vibrational modes contain the species of rotation, $\Gamma(q_s) \otimes \Gamma(\alpha_s) \in \Gamma(J_{\alpha})$,

Coriolis interaction may take place between the modes ω_s and $\omega_{s'}$, or between the states $(v_s, v_{s'})$ and $(v_{s'+1}, v_{s'}, -1)$.

The first order Hamiltonian component H_{21} is usually isolated by a perturbation method [45], and contains the $\xi_{ss'}$ terms which represent the extent of interaction between the states in question. The transformed Hamiltonian may now be written as the sum of two terms

$$\tilde{H}_{21}(s, s') = \tilde{H}_{21} + H_{21}^* \quad (2-60)$$

in which \tilde{H}_{21} is the resonance term with nonvanishing matrix elements only between the resonating states, and H_{21}^* is a term with no such matrix elements. The contact transformation with a proper S_{21}^* function [56] eliminates H_{21}^* from the first order Hamiltonian and transforms H_{21} into

$$\begin{aligned} \tilde{H}_{21} = & -[(\omega_s + \omega_{s'})/(\omega_s \omega_{s'})^{1/2}] \\ & \times (q_s p_s - q_{s'} p_{s'}) \sum_{\alpha} \tilde{B}_{\alpha} \xi_{ss'}^{\alpha} p_{\alpha} \end{aligned} \quad (2-61)$$

The transformation yields a somewhat modified vibration-rotation interaction constant, α_s^{α} . The unperturbed α_s^{α} may be obtained [56] by replacing $\xi_{ss'}^{\alpha}$ by

$$-(\xi_{ss'}^{\alpha})^2 (B_{\alpha}/\omega_s) (\omega_s - \omega_{s'})^2 [\omega_s, (\omega_s + \omega_{s'})]^{-1} \quad (2-62)$$

The term \tilde{H}_{21} can then be evaluated by solving a secular equation obtained from a matrix with off-diagonal elements

$$\langle v_s, v_{s'} | \tilde{H}_{21} | v_{s'+1}, v_{s'}, -1 \rangle = i \xi_{vv} p_{\alpha} \quad (2-63)$$

where

$$\xi_{vv} = 2B_\alpha \xi_{ss}^\alpha [(\omega_{s'}/\omega_s)^{1/2} + (\omega_s'/\omega_s)^{1/2}] \times [(v_s+1)v_s/4]^{1/2} \quad (2-64)$$

In cases of strong Coriolis resonance as for ν_4 with ν_6 of H_2CO , a second order correction constant, η , may be extracted from the term \tilde{H}_{22} . Using a derivation similar to that of ξ_{vv} , η_{vv} may be obtained from the \tilde{H}_{22} term by solving a secular matrix with off-diagonal elements

$$\langle v_s, v_s, | \tilde{H}_{22} | v_s+1, v_s, -1 \rangle = \eta_{vv}, (P_\alpha P_\beta + P_\beta P_\alpha) \quad (2-65)$$

The type of Coriolis interactions in H_2CO are governed as usual by symmetry. Formaldehyde belongs to the C_{2v} point group (Table 2-6). For the I' representation the axes are labeled as $z=a$, $x=b$, and $y=c$. Therefore, since ν_4 belongs to the B_1 representation, ν_6 to the B_2 representation, and ν_3 to the A_1 representation one obtains

a type Coriolis interaction for ν_4/ν_6 since

$$B_1 \otimes B_2 = 1 \ 1 \ -1 \ -1 = A_2 (P_a)$$

b type Coriolis interaction for ν_3/ν_4 since

$$A_2 \otimes B_1 = 1 \ -1 \ -1 \ 1 = B_2 (P_b)$$

and c type Coriolis interaction for ν_6/ν_3 since

$$B_2 \otimes A_2 = 1 \ -1 \ 1 \ -1 = B_1 (P_c)$$

Symmetry also restricts the interaction between the rotational species in each set of bands to be as shown below.

Band	Symmetry Type	Angular Momentum comp.	C_{2v} Point group			
			E	C_2 (a)	σ_v (ba)	σ_v (ca)
ν_3	A_1	A	1	1	1	1
ν_4	B_1	P_b	-1	-1	-1	1
ν_6	B_2	P_c	1	-1	1	-1
	A_2	P_a	1	1	-1	-1

Table 2-6: The C_{2v} Point Group Table in The I^r Representation.

ν_6/ν_4 , a type	ν_3/ν_4 , b type	ν_3/ν_6 , c type
Coriolis	Coriolis	Coriolis
$E^+ P_a E^-$	$E^+ P_b O^+$	$E^+ P_c O^-$
$E^- P_a E^+$	$E^- P_b O^-$	$E^- P_c O^+$
$O^+ P_a O^-$	$O^+ P_b E^+$	$O^+ P_c E^-$
$O^- P_a O^+$	$O^- P_b E^-$	$O^- P_c E^+$

The matrix elements for rotation in the symmetric top basis are

$$\langle J, K | P_a | J, K \rangle = \hbar K \quad (2-66)$$

$$\langle J, K | P_b | J, K \pm 1 \rangle = 1/2(\hbar) [J(J+1) - K(K \pm 1)]^{1/2} \quad (2-67)$$

$$\langle J, K | P_c | J, K \pm 1 \rangle = \pm i/2(\hbar) [J(J+1) - K(K \pm 1)]^{1/2} \quad (2-68)$$

and the second order in the same basis may be stated as

$$\begin{aligned} \langle J, K | (P_b P_c + P_c P_b) | J, K \pm 2 \rangle &= \pm \hbar^2 / 2 [J(J+1) - K(K \pm 1)]^{1/2} \\ &\times [J(J+1) - K(K \pm 1)(K \pm 2)]^{1/2} \end{aligned} \quad (2-69)$$

The Coriolis interaction is one of vibration-rotation. Hence vibrational angular momentum must be taken into consideration. It has been shown [13] that by doing so one obtains

$$\begin{aligned} \langle v, J, K | \hat{H} | v', J, K \rangle &= i \xi_{vv}^a, K \\ \langle v, J, K | \hat{H} | v', J, K \pm 1 \rangle &= i/2 \xi_{vv}^b, [J(J+1) - K(K \pm 1)]^{1/2} \\ \langle v, J, K | \hat{H} | v', J, K \pm 1 \rangle &= \mp i/2 \xi_{vv}^c, [J(J+1) - K(K \pm 1)]^{1/2} \end{aligned} \quad (2-70)$$

$$\begin{aligned} \langle v, J, K | \hat{H} | v', J, K \pm 2 \rangle &= \mp i/2 \eta_{vv}^{bc}, [J(J+1) - K(K \pm 1)]^{1/2} \\ &\times [J(J+1) - (K \pm 1)(K \pm 2)]^{1/2} \end{aligned} \quad (2-71)$$

The matrix elements shown above are imaginary, but they can be made real by the proper choice of phase factors. The phase factors may be chosen corresponding to symmetry species of the vibrational states [13,45]; for example, 1 for A_1 , -i for A_2 , i for B_1 , and -1 for B_2 . Introducing these factors into the vibrational-rotational products and labeling the interacting modes observed in H_2CO yields the final matrix elements used by Johns [14] in an earlier analysis of the Coriolis interactions in formaldehyde.

$$\langle v_4, J, K | \hat{H} | v_6, J, K \rangle = \xi_{64}^{aK} \quad (2-72)$$

$$\begin{aligned} \langle v_4, J, K | \hat{H} | v_6, J, K \pm 2 \rangle = & \eta_{64}^{bc} [J(J+1) - K(K \pm 1)]^{1/2} \\ & \times [J(J+1) - (K \pm 1)(K \pm 2)]^{1/2} \end{aligned} \quad (2-73)$$

$$\langle v_4, J, K | \hat{H} | v_3, J, K \pm 1 \rangle = -1/2 \xi_{34}^b [J(J+1) - K(K \pm 1)]^{1/2} \quad (2-73)$$

$$\langle v_6, J, K | \hat{H} | v_3, J, K \pm 1 \rangle = \mp 1/2 \xi_{36}^c [J(J+1) - K(K \pm 1)]^{1/2} \quad (2-74)$$

The first and second order Coriolis interaction constants, ξ and η , are obtained from the least squares fit to the observed transitions.

The quintic third order Hamiltonian term, H_{23} , can be used to characterize the accidental Coriolis interaction between $K_a'=3$ of v_3 and $K_a'=6$ of v_6 . For asymmetric tops H_{23} is purely off-diagonal in v_s , and is calculated from a series of other Hamiltonian terms including H_{21} and H_{22} discussed above. Hence, H_{23} is a mixed Coriolis Hamiltonian term which allows for $\Delta K=\pm 3$ interactions needed to treat

this particular local resonance. The expression for \tilde{H}_{23} is given by Aliev and Watson [57] as

$$\tilde{H}_{23} = \sum_{\alpha\beta\gamma} \sum_{s,s'} Y_{ss'} a_s p_s \alpha^\gamma \beta^\alpha \gamma^\beta \quad (2-75)$$

where Y is the third order Coriolis coupling constant. The derivation of \tilde{H}_{23} and its contact transformation, as well as the evaluation of Y are described in detail in the literature [31, 56, 57].

The molecular symmetry and the particular Coriolis interaction govern the choice of axis assignment in equation (2-75) i.e. α , β , and γ for $p_\alpha^\gamma \alpha^\beta \beta^\gamma$. As in the case for the first order Coriolis between v_3 and v_6 the vibrational angular momentum p becomes p_c (along the c axis). To get $\Delta K=\pm 3$ coupling one must have the condition that the axes $\beta\gamma\neq a$ since P_a is diagonal in K (Equation (2-72)). The possible products are:

$$P_c P_c P_c^2, P_c P_c P_b^2, P_c P_c P_b P_c, P_c P_c P_c P_b, \dots \text{etc.}$$

Since the entire term should be symmetric and so terms such as $P_c P_c P_b P_c$ must drop out yielding only $P_c P_c P_c^2 = P_c P_c^3$ and $P_c P_c P_b^2$. Both these products give the same J and K dependence. For pure rotational transitions using P_c^3 one obtains

$$\langle J, K | P_c^3 | J, K \pm 3 \rangle = \langle J, K | P_c | J, K \pm 1 \rangle \langle J, K \pm 1 | P_c | J, K \pm 2 \rangle \\ \times \langle J, K \pm 2 | P_c | J, K \pm 3 \rangle$$

$$\begin{aligned}
 &= -i\hbar/8 [J(J+1)-K(K\pm 1)]^{1/2} \\
 &\quad \times [J(J+1)-(K\pm 1)(K\pm 2)]^{1/2} \\
 &\quad \times [J(J+1)-(K\pm 2)(K\pm 3)]^{1/2} \quad (2-76)
 \end{aligned}$$

Introducing Y, p_c , and q, from Equation (2-75), i.e. the interacting vibrational modes, the final off-diagonal term of the Hamiltonian takes the form

$$\begin{aligned}
 \langle v_6, J, K | \hat{H} | v_3, J, K\pm 3 \rangle &= z_{36} [J(J+1)-K(K\pm 1)]^{1/2} \\
 &\quad \times [J(J+1)-(K\pm 1)(K\pm 2)]^{1/2} \\
 &\quad \times [J(J+1)-(K\pm 2)(K\pm 3)]^{1/2} \\
 &= z_{36} \hbar(J, K) \quad (2-77)
 \end{aligned}$$

where z_{36} is a third order Coriolis coupling constant for the interaction between v_3 and v_6 and may be obtained from the least squares fit of the observed transitions.

CHAPTER 3

INSTRUMENTATION AND DATA ACQUISITION

3.1 Introduction

The qualitative and quantitative analysis of H₂CO has been carried out using two very high resolution techniques: Fourier transform infrared (FT-IR), and Doppler limited, tunable diode laser (TDL) spectroscopies. The FT-IR has been used for wide range survey spectroscopy, while the diode laser spectrometer has been used for the determination of individual line strengths, pressure broadened widths, and analytical trace analysis.

This chapter begins with a brief description of the FT-IR spectra. The laser spectrometer as well as the procedures used to obtain a spectrum are described in the next section. Several examples of TDL spectra are then shown and discussed to illustrate the capabilities of this technique and to show typical characteristics of the spectrum of H₂CO.

3.1 FT-IR Survey Spectra

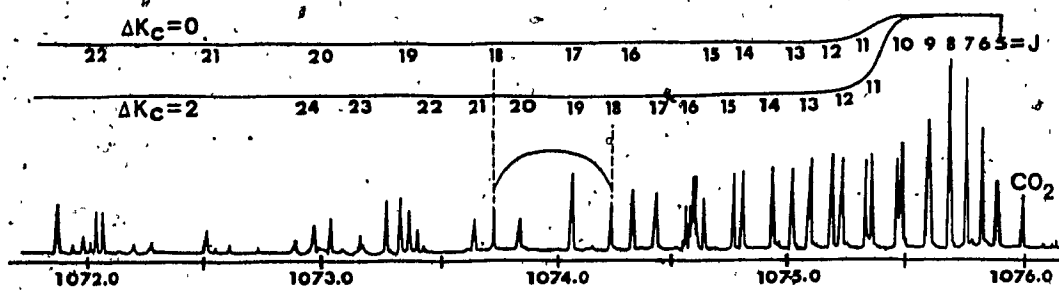
High resolution FT-IR spectra of H₂CO from 890 to 1580 cm⁻¹ have been recorded with a Bomem interferometer at the Herzberg Institute of Astrophysics in Ottawa. This

instrument has an unapodized resolution of $\sim 0.0024 \text{ cm}^{-1}$. The spectrum reported was apodized with a Happ-Genzel function yielding an observed width of $\sim 0.004 \text{ cm}^{-1}$. The spectrum contained nearly 4000 transitions arising from the ν_3 , ν_4 , and ν_6 bands. A peak finder program running on the PDP-11 computer of the Bomem interferometer provided a measured wavenumber listing for these transitions. A trace of CO_2 gas introduced into the sample cell provided for absolute calibration [59]. A typical FT-IR spectrum of H_2CO is shown in Figure 3-1.

3.3. TDL Experimental Apparatus

The Pb-salt tunable semiconductor diode lasers (TDL's) used in this work were fabricated by Spectra Physics/Laser Analytics division. Lasing in these semiconductors results from stimulated emission across the energy gap between the conduction and valence bands. A population inversion is achieved by applying a forward-bias current to the diode and thereby injecting charge carriers across the p-n junction. The recombination of these charge carriers facilitate the gain mechanism for laser action. The end faces of the laser crystals made by cleaving along natural crystal planes form the laser resonator. The TDL crystals are typically $400 \mu\text{m}$ long with a cross-section of $200 \times 200 \mu\text{m}$. The lasing frequencies of TDLs is governed by the specific composition of the crystal. $\text{Pb}_{1-x}\text{Sn}_x\text{Se}$ lasers can be made to operate

$\text{H}_2\text{CO } \nu_4 \text{ PQ}_5$



$\text{H}_2\text{CO } \nu_3$

Q-BRANCHES AT BAND CENTER

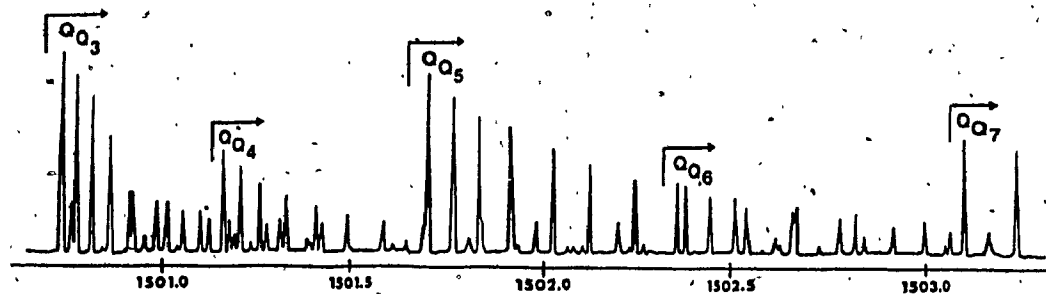


Figure 3-1: Two Typical Examples of FT-IR Spectra.

from about 300 to 1200 cm^{-1} and $\text{PbS}_{1-x}\text{Se}_x$ from 1200 to 2500 cm^{-1} by selective variation of x during fabrication. Both types of TDL's were used in this experimental work.

The output of any one TDL can be tuned across a range of 20-200 cm^{-1} by varying the crystal temperature from 10K to 100K, which in turn changes the band gap energy in the semiconductor and to some extent its index of refraction. Most diode lasers oscillate in several modes simultaneously, separated in wavelength by the cavity mode spacing of several wavenumbers. In most cases, however, single modes may be isolated by a grating monochromator. Several reviews of Pb-salt TDL's detailing their fabrication and operation have been published [23,60].

Line parameter measurements for H_2CO were made using a modified Laser analytics Model LS-3 spectrometer and the following procedure. One of the four tunable diode lasers mounted in a closed-cycle cryogenic refrigerator is temperature tuned to the desired wavelength within the tuning range of the laser emission. At this set wavelength, fine tuning of up to 1 cm^{-1} is accomplished with small temperature variations (I^2R heating) induced by the laser current control module (LCM). The laser current is sawtooth modulated at ~50 Hz and is synchronized to both a sectored blade chopper and a signal averager in a manner similar to that described by Jennings [15]. The output from the grating spectrometer is detected with a liquid nitrogen cooled

HgCdTe (or InSb) detector and is amplified by an EG&G Model 113 pre-amplifier. The signal is then sent to an EG&G Model 4203 signal averager and transmitted either to an X-Y recorder or via an RS-232 interface to an IBM PC computer. The relative calibration of the wavenumber scale was provided by a 3" solid germanium etalon with a fringe spacing in the region studied of $\sim 0.016 \text{ cm}^{-1}$. The precise transition wavenumbers of H_2CO and etalon fringe spacings were obtained by reference to well known N_2O lines [63].

A Laser Analytics Model LO-3 multiple traversal absorption cell was used as the sample cell. This cell has White's optical configuration [61,62], and is adjustable for optimal pathlengths of 4.17 to 100.17 meters. Formaldehyde vapour was generated by heating analytical grade para-formaldehyde and introduced into the White cell through a liquid nitrogen trap. In order to prevent both sample polymerization and insure absorption lines having Doppler widths, the pressure of all H_2CO samples was maintained at $< 0.1 \text{ Torr}$. The optical path of the White cell was adjusted so as to allow 15-20% transmission for all transitions being measured. Pressure measurements were made with a Datametrics Model 572A capacitance manometer which was frequently calibrated with reference to a Kontes McLeod gauge (0.001-1.000 mm Hg). A block diagram of the spectrometer and support equipment is shown in Figure 3-2.

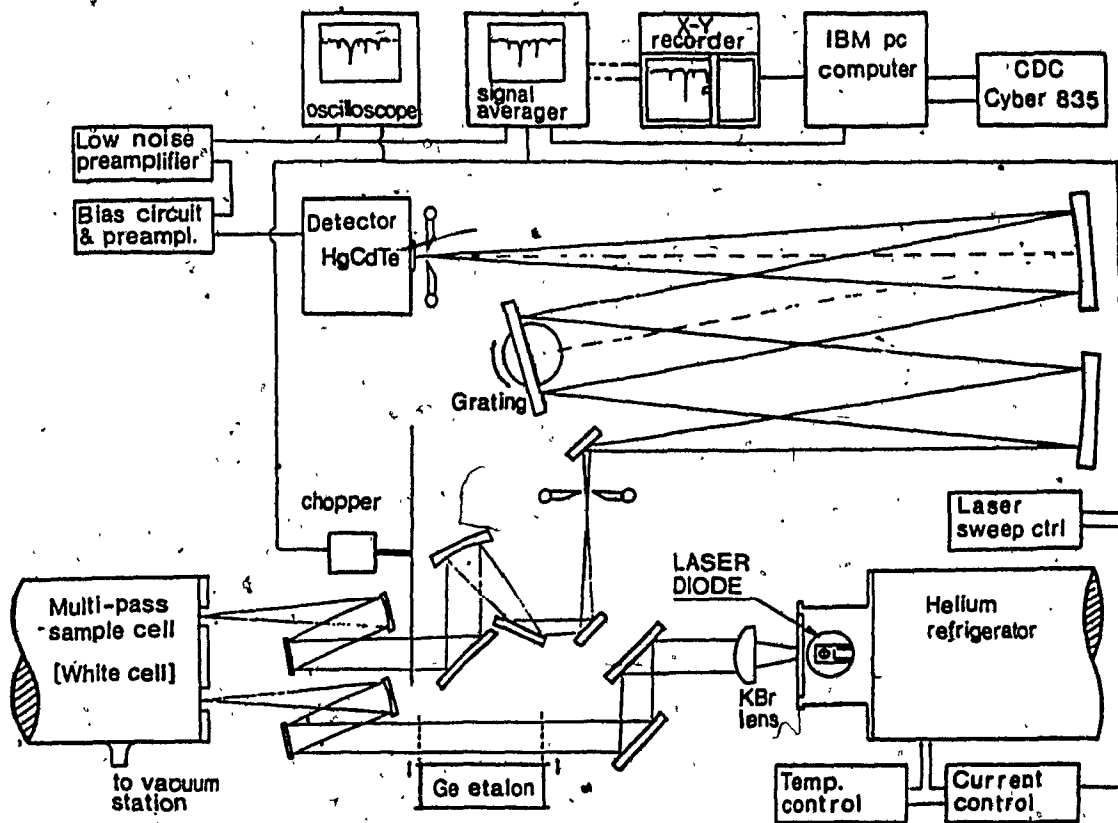


Figure 3-2: Schematic Diagram of the TDE Spectrometer.

3.4 Data Acquisition

Experimental data were obtained from six sets of spectra, taken in duplicate on three different occasions. This allowed analysis of variance within and between runs. A typical spectrum is shown in Figure 3-3. Maximum energy (I_0) was recorded through the evacuated White cell at the beginning and end of each set of spectra and compared with the I_0 obtained for the individual traces. Pressure broadening effects were evaluated using an average of only the initial and final I_0 values since the 100% transmission (background) at elevated pressures became indeterminable. A saturation absorption scan was made in order to verify whether the shutter zero was equivalent to the 100% absorption level. It has been found that the two agreed well, and so the shutter zero was used as the $I=0$ level. The full width at half height (FWHM) at $(1/2)\ln(I_0/I)$ (i.e. FWHM at $I' = \sqrt{I_0}I$) was measured by direct comparison with the Ge etalon transmission peaks (fringes) nearest each spectral feature. Etalon fringes were generally used for both the conversion of the tuning current axis (x-axis) to wavenumbers and the linearization of this axis. The need for linearization arises from the fact that the lasers do not tune linearly with current. The spacings between the fringes were calibrated using well known N_2O lines taken from Guelachvili [63]. The separation of the interference fringes of the Ge etalon vary as a function of both wave

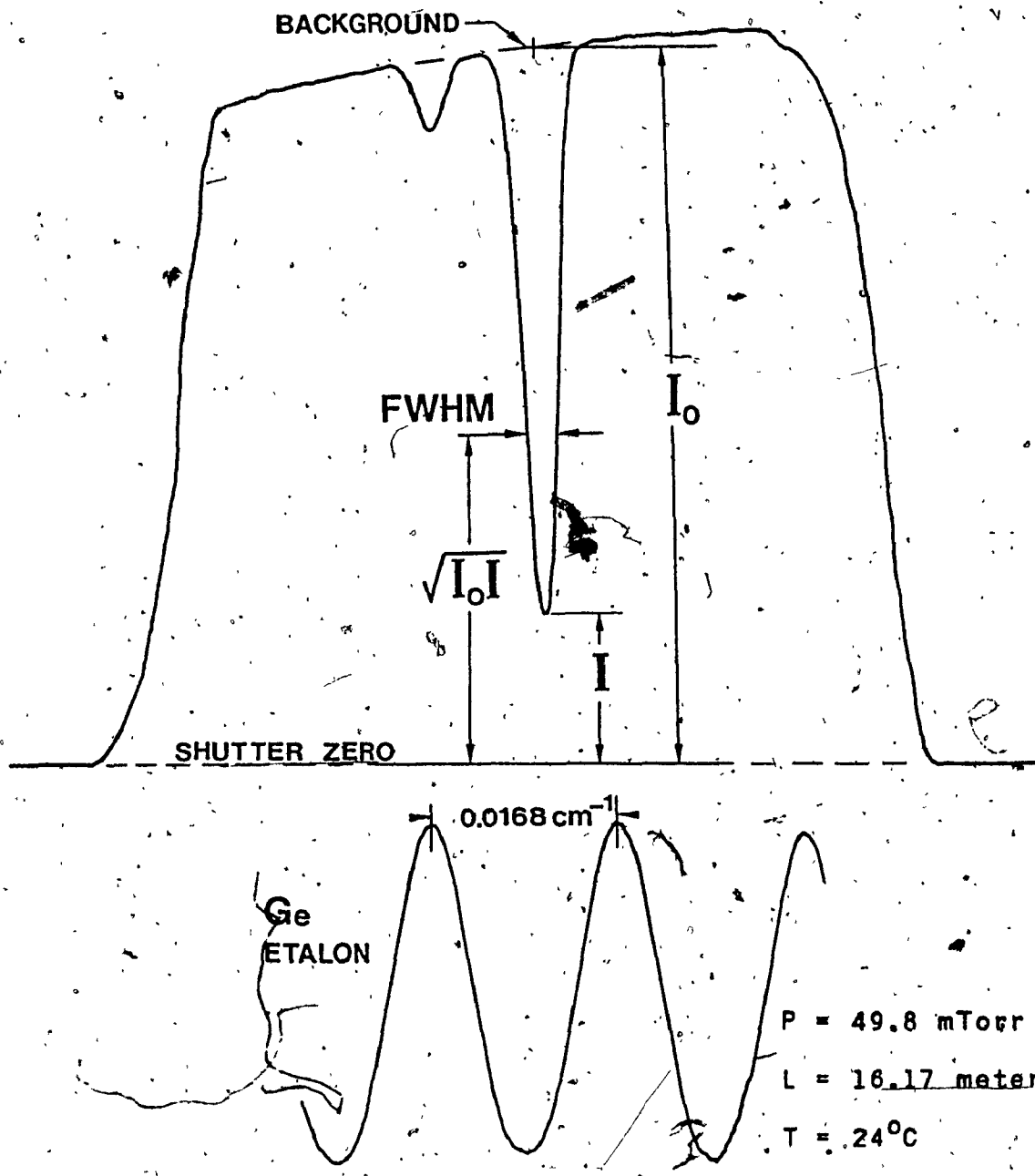


Figure 3-3: Measurable Parameters From TDL Spectra.

Absorption spectrum of the $18_{2,17} \leftarrow 18_{1,17}$ transition in the ν_4 band of H_2CO at $1172.38603 \text{ cm}^{-1}$. Interference fringes from Ge 7.62 cm etalon are used to provide relative calibration of the wavelength scale.

length and temperature and therefore needed frequent calibration. The above procedure for data collection was repeated at several different pressures: 0 to 70 mTorr H₂CO for line intensity studies; and 0 to 25 Torr for foreign gas broadening measurements. Each series of data points collected formed the basis for a Beer's law plot and statistical evaluation of the results.

The identification of individual transition lines prior to analysis was obtained by comparing survey (~0.5 cm⁻¹) TDL scans with the FT-IR data. Single isolated lines were identified using N₂O lines and etalon fringes. Typical TDL survey spectra are shown in Figures 3-4 and 3-5.

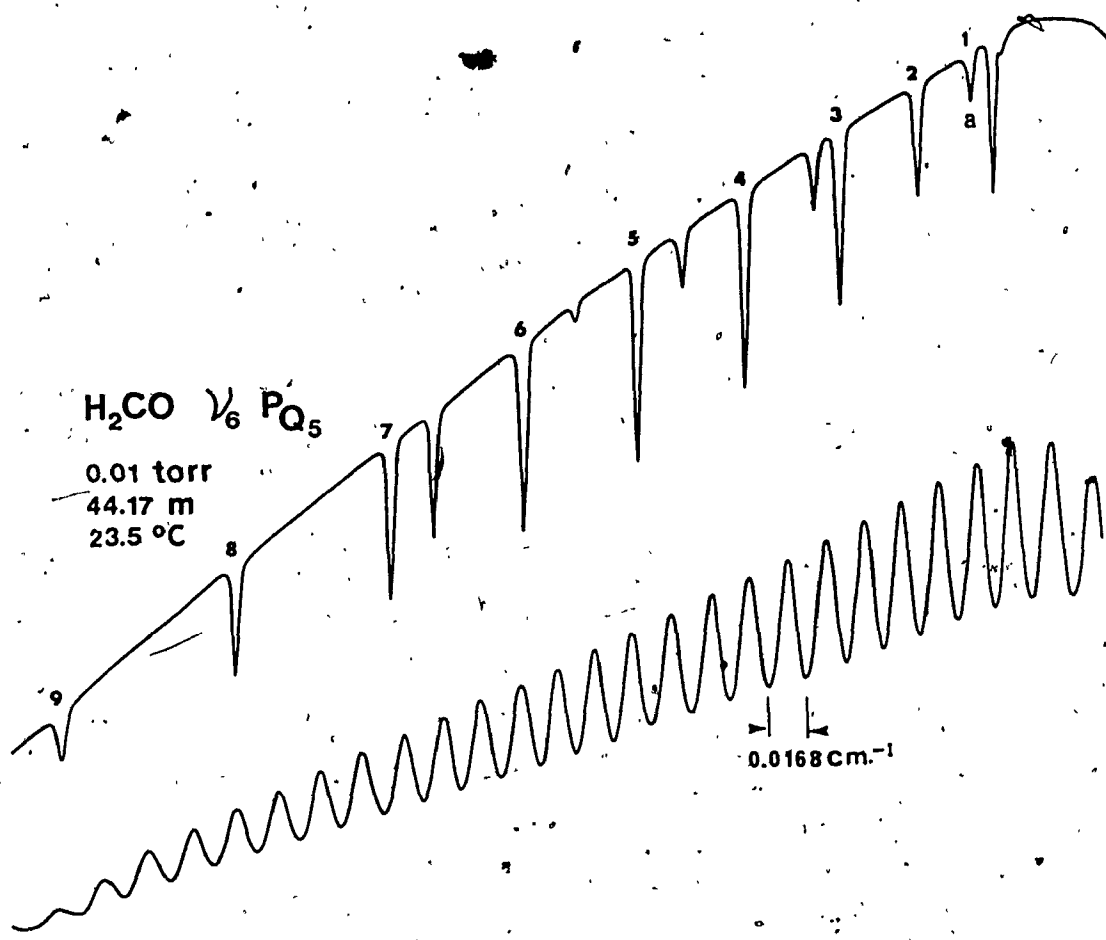


Figure 3-4: Survey Spectra of a Selected Region in the ν_6 band of H_2CO Recorded with a TDL.

- a. The numbers 1-9 are used only as identifiers of the PQ_5 series, i.e. 1 represents the transitions $5_{4,1}^{\circ} \leftarrow 5_{5,0}$ and $5_{4,2} \leftarrow 5_{5,1}$ at $1192.84237 \text{ cm}^{-1}$

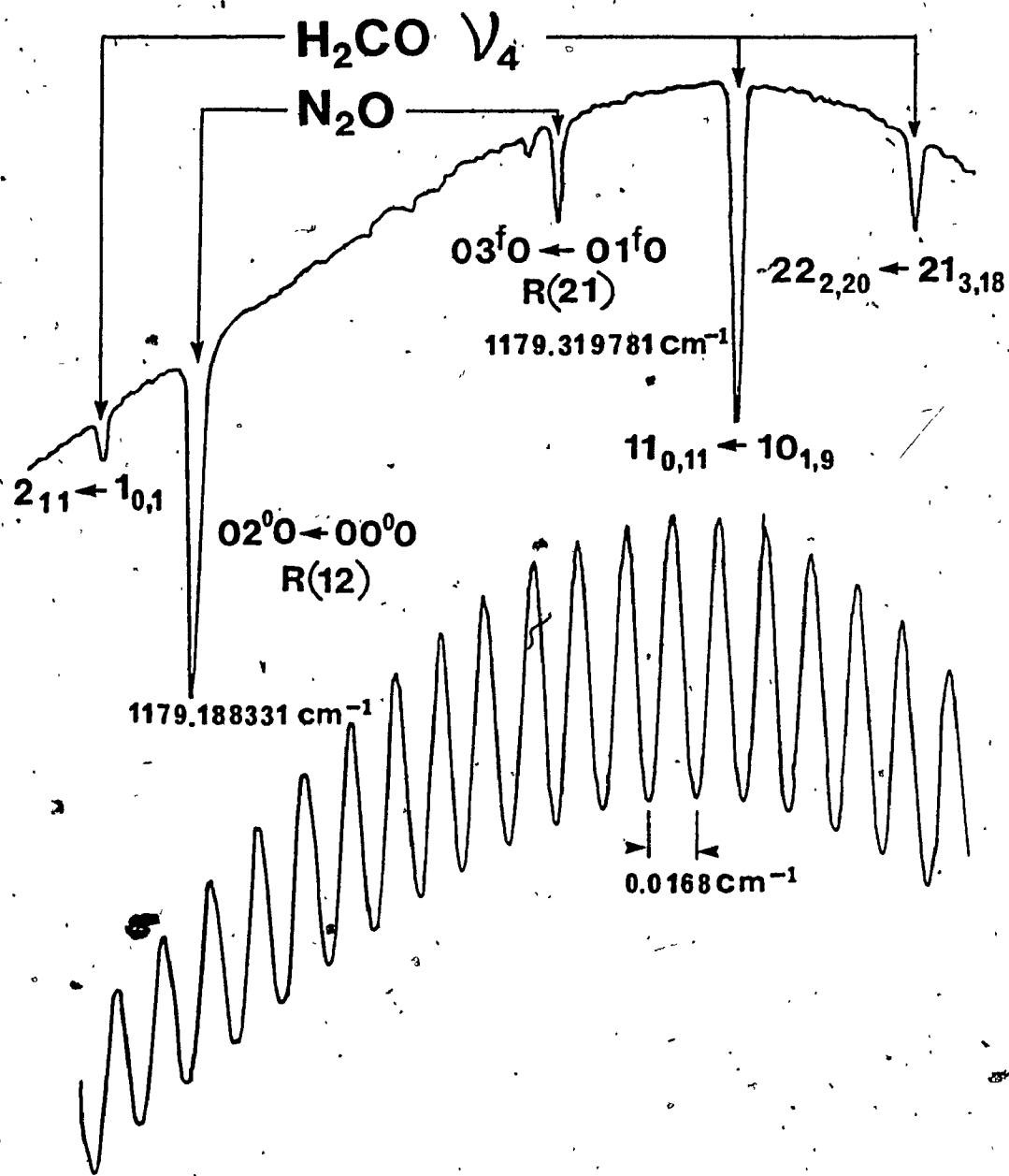


Figure 3-5: TDL Survey Spectra: Identification of Transitions in v_4 of H_2CO Using Ge Etalon Fringes for Relative Calibration and N_2O for Absolute Calibration.

CHAPTER 4

EXPERIMENTAL RESULTS - H₂CO LINE ASSIGNMENTS, AND DETERMINATION OF LINE STRENGTHS AND BROADENING COEFFICIENTS

4.1 Introduction

In this chapter, a description of the method used for the assignment of the H₂CO transitions will be presented. These quantum number assignments were used in the simultaneous analysis of the ν₃, ν₄ and ν₆ vibration-rotation bands discussed in Chapter 5. The techniques used for evaluation of line strengths and foreign-gas pressure broadening parameters, and the final results will also be presented.

4.2 Frequency Assignments

The observed transitions obtained from the FT-IR spectrum were assigned using the ground-state-combination-difference (GSCD) technique. This method determines the upper state energy levels by combination of observed infrared transition wavenumbers and the appropriate calculated, ground state energy values obtained from microwave spectra. Governed by the selection rules, an upper energy state may be reached by several different paths. Hence, the known

parts of a combination may be used to predict the frequencies of the unknown parts. An example of this powerful technique is shown in Figure 4-1 where, using the selection rules for ν_4 , a transition diagram was constructed for $K_a''=1$. The six energy levels for the lower states were calculated from molecular constants derived from recent microwave data [64]. The two R_{Q_1} infrared transition energies were selected using an educated guess. Using these values, the energies x_1 , x_2 , x_3 , and x_4 were computed. These agreed within several milliwavenumbers with the existing FT-IR data, indicating that the transition model and the original guess for R_{Q_1} were correct. Hence, the transitions shown in Figure 4-1 were assigned to these six IR wavenumbers.

The ground state energy levels were generated from the ground state rotational constants reported by Cornet and Winnewisser [64], using a computer program written by Maki [65]. The energy levels generated consisted of all values up to $J''=30$ and $K_a''=10$.

Over 1000 assigned IR transitions given by Allegrini et al. [14], for $J<15$ in ν_3 , ν_4 , and ν_6 of H_2CO , took much of the guess work out of the initial utilization of the ground state combination difference. Using the GSCD technique, 3400 transitions were assigned of which over 3000 were used in the determination of the rotational constants for the three H_2CO bands. The observed wavevenumbers and their respective assignments are listed in Appendix A.

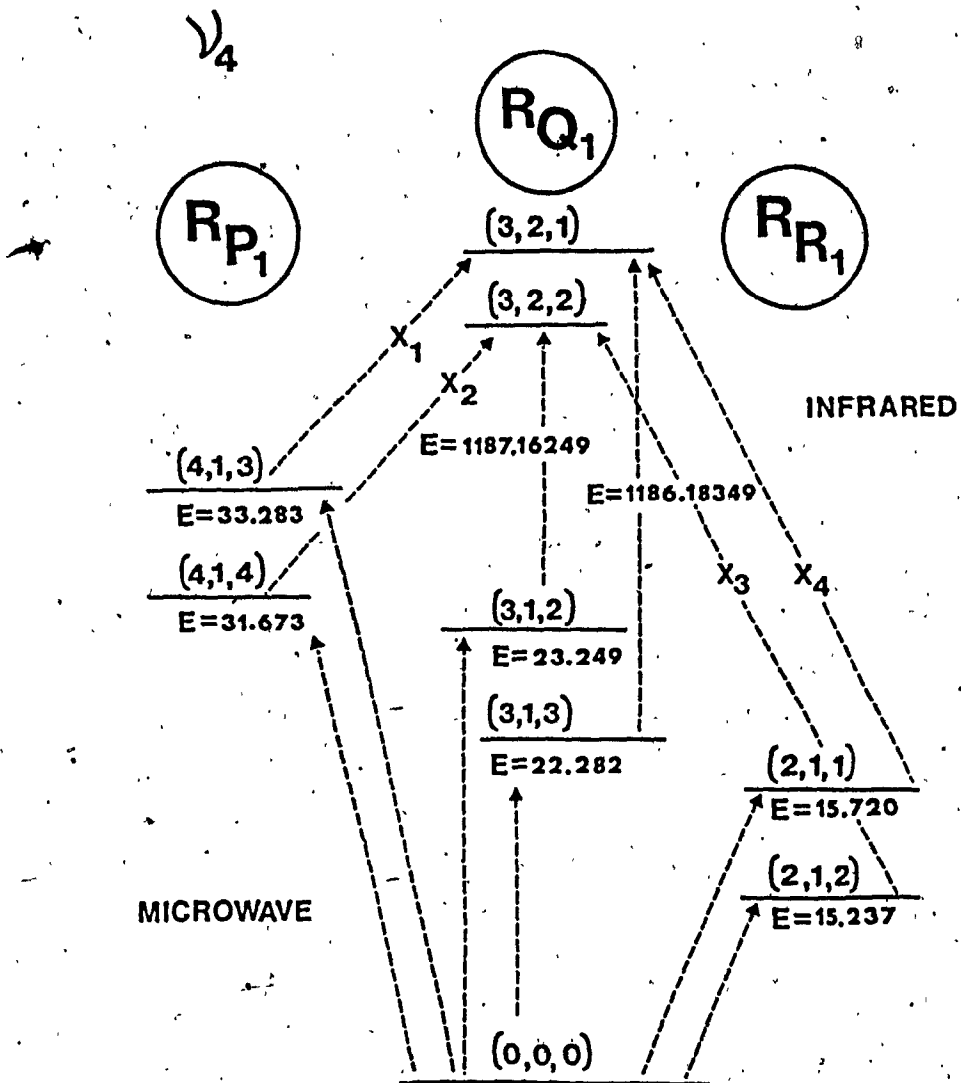


Figure 4-1: A Schematic Diagram of the Ground-State-Combination-Difference Technique.

4.3 Line Strength Determinations

The measurement of line strength is simplified considerably when performed with a laser spectrometer, since the instrument function defined by the laser profile is usually much narrower in bandwidth than typical observed linewidths. Hence, rather than using the somewhat cumbersome equivalent width technique [66-68], the strength of a line can be determined by the direct method from the line center absorption [15,69]. A brief description of the direct method follows.

The intensity $I(\nu)$, of a single absorption line is given by Beer's law as

$$I(\nu) = I_0(\nu) \text{ Exp}[-k(\nu) X] \quad (4-1)$$

where I_0 is the intensity if there is no absorption, $k(\nu)$ is the absorption coefficient, and X is the optical density i.e. the pressure-pathlength product (PL). For a Doppler line shape the absorption coefficient has the form

$$k(\nu) = (S/\gamma_D)(\ln 2/\pi)^{1/2} \text{ EXP}[-\ln 2((\nu - \nu_0)/\gamma_D)^2] \quad (4-2)$$

where γ_D is the Doppler half width and is equal to HWHM of the $k(\nu)$ profile, ν_0 is the frequency at line center, and S is the line strength. The Doppler half width is given by

$$\gamma_D = \nu_0 [(2kT\ln 2)/(mc^2)] \quad (4-3)$$

where k is the Boltzmann constant, T is the temperature, m

is the molecular mass, and c is the speed of light. From the line center transmission, $\tau_0 = I(\nu_0)/I_0(\nu_0)$ one can solve for the line strength S as

$$S = - (\gamma_D \ln \tau_0) / [PL(\ln 2/\pi)^{1/2}] \quad (4-4)$$

In terms of line center wavenumbers one finds [15]

$$S = - (2\pi kT/mc^2)^{1/2} (\nu_0/PL) \ln \tau_0 \quad (4-5)$$

$$= - (0.5794) (\nu_0/PL) (T/M)^{1/2} \ln \tau_0 \quad (4-6)$$

where ν_0 is in cm^{-1} , P is the pressure in milliTorr, L is the absorption pathlength in cm, and M is the molar mass in grams.

The line strength for the 28 transitions measured were determined using Equation (4-6). Each transition was evaluated at several pressures (minimum 5) yielding a Beer's Law plot of $\ln(1/\tau_0)$ versus optical density (PL). Since the pathlength used was fixed, corrections to the pressure reading could be calculated from the X-intercept of the plot. The pressure correction to the capacitance manometer (-6 to -15 millitorr) obtained from the plots were in good agreement with spot calibrations using a McLeod Gauge. All pressure readings were corrected prior to use in the line intensity calculations. A typical Beer's Law plot is shown in Figure 4-2 for the transition $^{18}_{2,17} \leftarrow ^{18}_{1,17}$ of ν_4 .

The resulting line strengths are listed in Table 4-1.

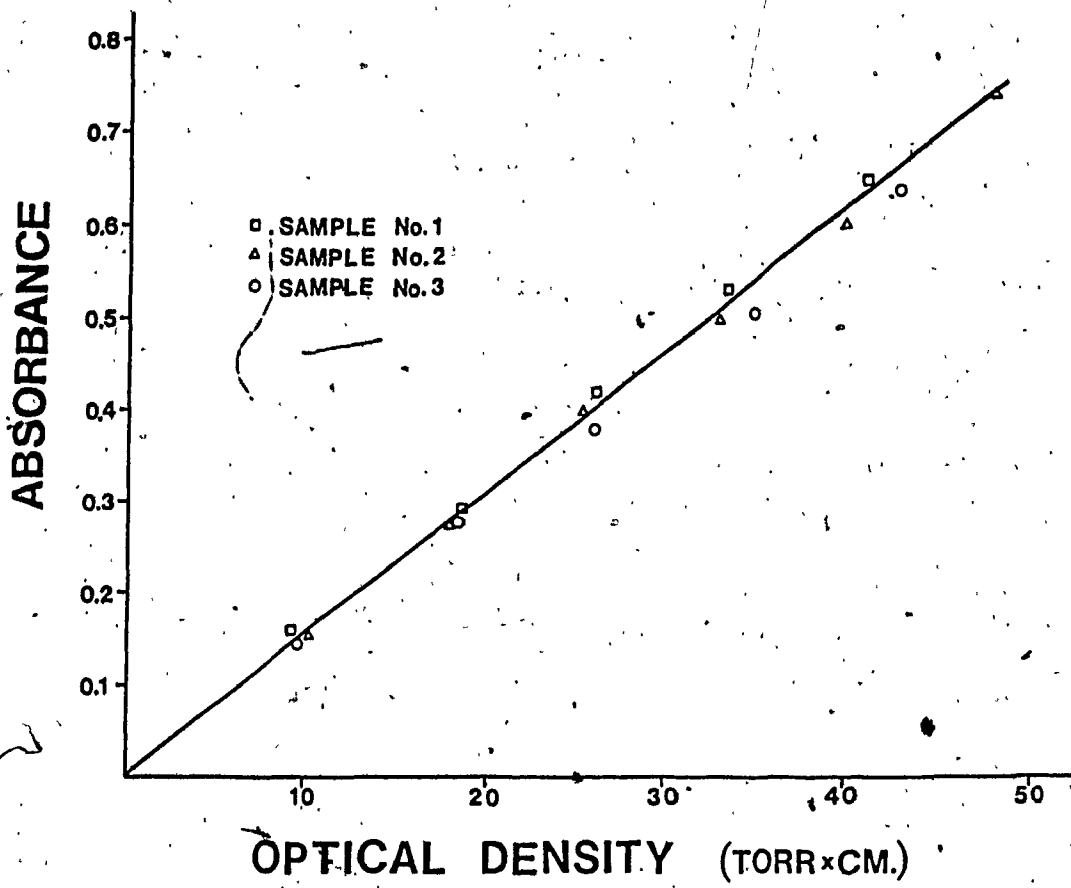


Figure 4-2: Beer's Law Plot of Absorbance vs. Optical Density for the $18_{2,17} \leftarrow 18_{1,17}$ Transition, at $1172.38603 \text{ cm}^{-1}$ in the v_4 band of H_2CO .

Table 4-1: Observed Line Strengths in the v_4 and v_6 Bands
of H₂CO at 24±1°C.

FREQUENCY cm ⁻¹	BAND	TRANSITION UPPER (J', K' _a , K' _c)	LOWER (J'', K'', K'' _a , K'' _c)	AVERAGE INTENSITY cm ⁻² atm ⁻¹
1148.33511	v_6	(17, 4, 14)	(18, 5, 13)	(3.225±0.126)×10 ⁻³
1148.34523	v_4	(11, 2, 9)	(10, 3, 7)	(2.113±0.050)×10 ⁻²
1148.36004	v_6	(17, 4, 13)	(18, 5, 14)	(3.395±0.151)×10 ⁻³
1148.47042	v_4	(3, 0, 3)	(4, 1, 3)	(4.737±0.195)×10 ⁻²
1148.50854	v_4	(16, 1, 15)	(16, 2, 15)	(1.866±0.075)×10 ⁻²
1159.13578	v_4	(1, 0, 1)	(1, 1, 1)	(2.953±0.170)×10 ⁻²
1159.27164	v_4	(2, 0, 2)	(2, 1, 2)	(4.846±0.304)×10 ⁻²
1159.29738	v_4	(28, 2, 27)	(28, 1, 27)	(5.936±0.405)×10 ⁻³
1159.39157	v_4	(15, 2, 13)	(14, 3, 11)	(1.883±0.064)×10 ⁻²
1159.41214	v_6	(6, 6, 1) (6, 6, 0)	(7, 7, 0) (7, 7, 1)	(1.488±0.056)×10 ⁻²
1159.43953	v_4	(9, 1, 9)	(8, 2, 7)	(7.429±0.327)×10 ⁻³
1159.47176	v_4	(3, 0, 3)	(3, 1, 3)	(6.663±0.463)×10 ⁻²
1172.38603	v_4	(18, 2, 17)	(18, 1, 17)	(3.208±0.062)×10 ⁻²
1172.52555	v_4	(6, 1, 6)	(6, 0, 6)	(2.843±0.148)×10 ⁻²
1180.64464	v_6	(12, 2, 11)	(13, 3, 10)	(1.898±0.100)×10 ⁻²
1180.73250	v_6	(4, 4, 1) (4, 4, 0)	(5, 5, 0) (5, 5, 1)	(3.841±0.235)×10 ⁻²
1180.80804	v_4	(24, 0, 24)	(23, 1, 22)	(2.613±0.074)×10 ⁻³
1180.83214	v_4	(11, 2, 10)	(11, 1, 10)	(3.400±0.208)×10 ⁻²
1180.88324	v_6	(13, 2, 11)	(14, 3, 12)	(1.651±0.116)×10 ⁻²

continued.....

Table 4-1 (cont'd)

FREQUENCY cm ⁻¹	BAND	TRANSITION UPPER (J', K' _a , K' _c)	LOWER (J'', K'' _a , K'' _c)	AVERAGE INTENSITY cm ⁻² atm ⁻¹
1192.60831	V ₆	(10, 4, 7) (10, 4, 6)	(10, 5, 6) (10, 5, 5)	(2.800+0.091)x10 ⁻²
1192.62677	V ₆	(3, 3, 1) (3, 3, 0)	(4, 4, 0) (4, 4, 1)	(2.000+0.092)x10 ⁻²
1192.66566	V ₆	(9, 4, 6) (9, 4, 5)	(9, 5, 5) (9, 5, 4)	(2.800+0.096)x10 ⁻²
1192.71773	V ₆	(8, 4, 5) (8, 4, 4)	(8, 5, 4) (8, 5, 3)	(2.492+0.123)x10 ⁻²
1192.73689	V ₆	(18, 1, 17)	(19, 2, 18)	(6.010+0.228)x10 ⁻³
1192.76481	V ₆	(7, 4, 4) (7, 4, 3)	(7, 5, 3) (7, 5, 2)	(2.165+0.075)x10 ⁻²
1192.79547	V ₆	(10, 1, 10)	(11, 2, 9)	(5.890+0.173)x10 ⁻³
1192.80640	V ₆	(6, 4, 3) (6, 4, 2)	(6, 5, 2) (6, 5, 1)	(1.648+0.060)x10 ⁻²
1192.84237	V ₆	(5, 4, 2) (5, 4, 1)	(5, 5, 1) (5, 5, 0)	(9.772+0.202)x10 ⁻³

The absorptivity coefficient obtained from the slope (least squares fit) of the Beer's law function for a given data set routinely yielded a relative standard deviation of less than 3% and a linear correlation of >0.998. However, when absorption coefficients for a given transition obtained in several experiments (days apart) were averaged, the error increased to between 3 and 8% of the mean value. This is clearly demonstrated in the scatter obtained from 3 different H₂CO samples shown in figure 4-2. The error in reproducibility may be attributed to vibrations caused by the helium refrigerator and possibly to shifts in lasing modes [15,70,71].

The overall reliability of the TDL system and technique used was initially evaluated on transitions in the N₂O calibrating gas [72]. The results obtained for five transitions in the 2ν₂ band were in excellent agreement with literature values obtained by other techniques [73,74].

4.4 Pressure Broadening by Foreign Gases

Foreign-gas collision broadening parameters were evaluated by recording the absorption lineshapes of a fixed amount of H₂CO at a number of different pressures of the broadening gas. Pressure induced widths were then determined from a plot of line width versus the partial pressure of the foreign-gas. The H₂CO pressure was again maintained sufficiently low (<100 milliTorr) to insure an initial

Doppler lineshape. The low sample pressure limited the amount of foreign gas used to < 30 Torr, since the absorption lines became weaker as they get wider. This effect is illustrated in Figure 4-3.

The lineshape of a pressure broadened line is governed by the perturbation of exterior systems upon the absorber molecule. A smearing of the energy levels results from these disturbances which produces a probability distribution of the energy level shifts. For a collision broadened line, the lineshape function takes the form

$$k(\nu) = (1/\pi) \{ \gamma_L / [(\nu - \nu_0)^2 + \gamma_L^2] \} \quad (4-7)$$

where γ_L , the half width at half height, is the reciprocal of the relaxation time and is proportional to the pressure. This function is known as the Lorentz lineshape. The observed spectra of a broadened line however, is generally a convolution of Doppler and Lorentzian functions called a Voigt profile. At elevated pressures the lineshape is governed by the Lorentzian function yielding a linear relationship between the HWHM and the applied pressure (Figure 4-4). However, since the pressure range used here was limited to < 30 Torr, the contribution of the Doppler function is still significant. The Lorentzian widths were obtained from the empirical relationship [80]

$$\gamma_L = \gamma_V \{ 7.7254 - 6.7254 [1 + 0.3195 (\gamma_D / \gamma_V)^2]^{1/2} \} \quad (4-8)$$

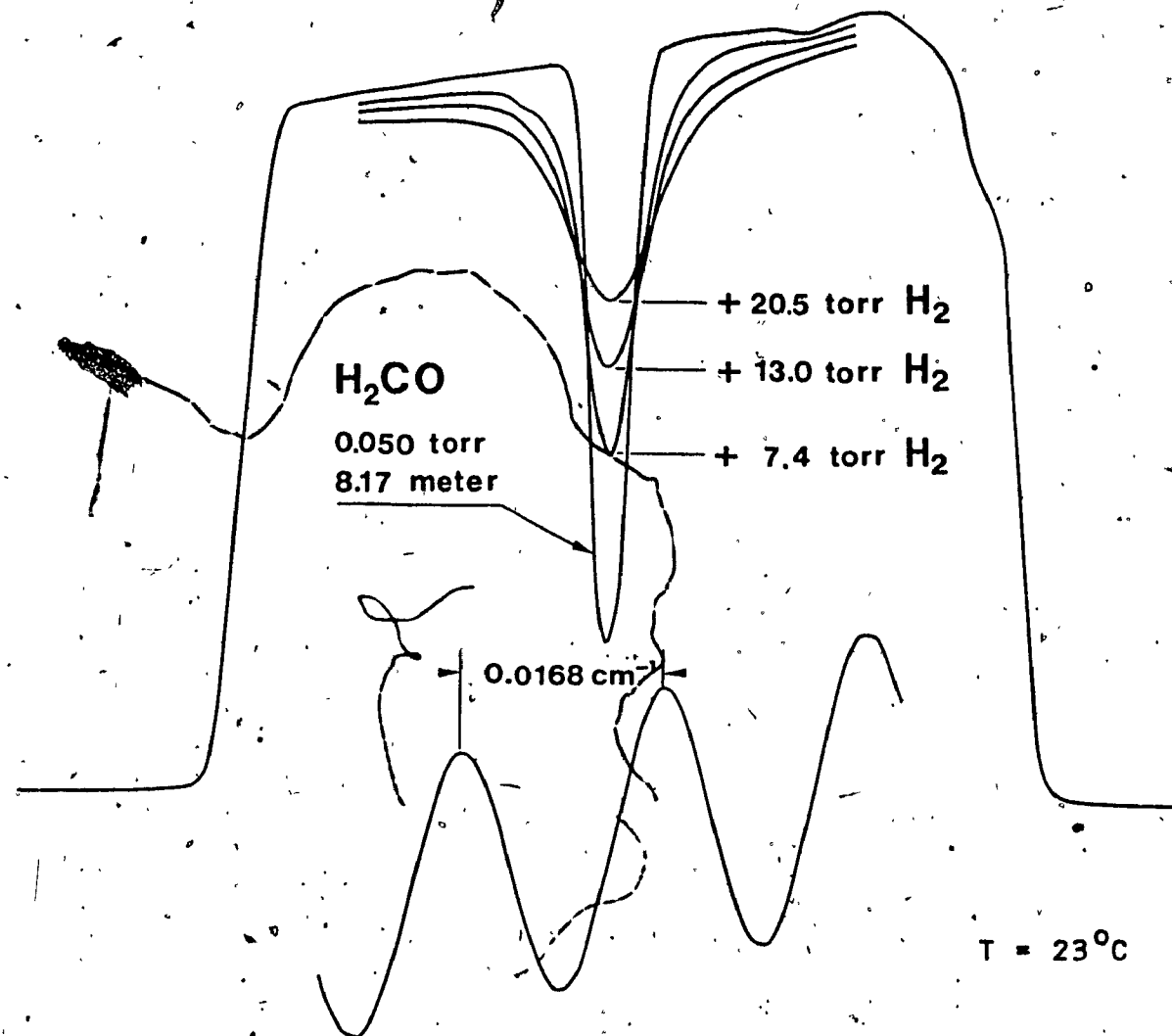


Figure 4-3: TDL Spectra for Hydrogen Pressure Broadening
Experiments on the $3_{0,3} \leftarrow 3_{1,3}$ transition at
 $1159.47176 \text{ cm}^{-1}$ of the ν_4 band of H_2CO .

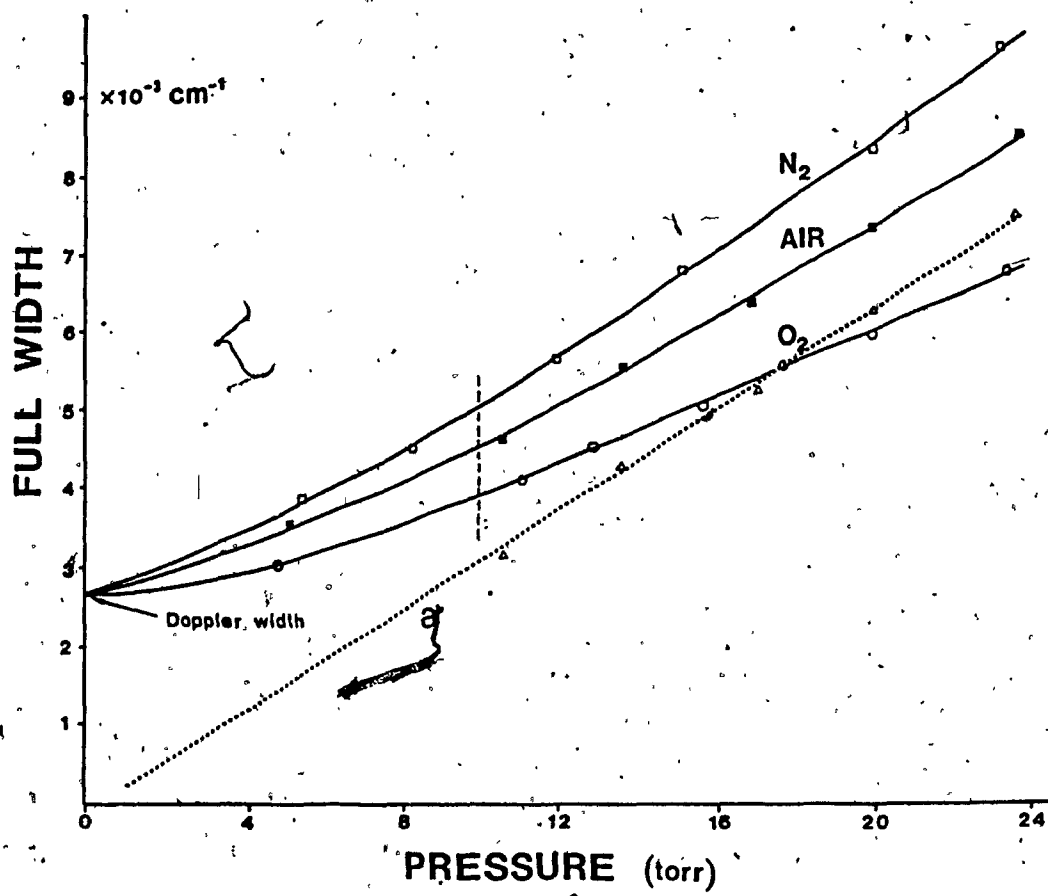


Figure 4-4: Plots of Foreign Gas Broadening Collision Widths (FWHM) of $\text{X}-\text{H}_2\text{CO}$ ($\text{X}=\text{air}, \text{N}_2$ or O_2) as a Function of Pressure.

a. Dotted line represents the Lorentzian full-width as a function of pressure for air broadening derived from Voigt profile calculations.

where γ_V is the half-width of the observed Voigt profile. The Lorentzian results obtained here were then verified by use of a numerical convolution simulation similar to that described by Blass and Halsey [79]. Plotting the Lorentzian widths as a function of applied pressure yielded a linear relationship with an intercept close to zero (10^{-4} to 10^{-6} cm $^{-1}$). From the slopes of these plots all pressure broadening coefficients were evaluated. A typical plot (line marked a) is shown in Figure 4-4 for air broadening. It should be noted here that the kinetic theory of gases does not account for all observed phenomenon concerning halfwidth measurements. It is necessary to treat the problem at a higher level [75], where interactions such as the dependence of the halfwidth on J , the rotational quantum number are also considered [76].

The results for pressure broadening due to collision with air, H₂, O₂, and N₂ at room temperature (24 1°C) are listed in Table 4-2. The effect of air broadening may also be evaluated from the broadening contributions of O₂ and N₂ by the use of the relation

$$\gamma_{\text{air}} = P_{O_2} \gamma_{O_2} + P_{N_2} \gamma_{N_2} \quad (4-9)$$

where the P_i are the partial atmospheric pressures of O₂ and N₂ (0.20946 and 0.78084 atm., respectively) and γ_i are the respective HWHM. Using this relationship yielded a computed air broadening coefficient of 0.128 cm $^{-1}$ /atm. for the

transition $3_{0,3} \leftarrow 3_{1,3}$ of ν_4 . This agrees quite well with the observed value of $0.126(10) \text{ cm}^{-1}/\text{atm}$.

The results obtained for air, O_2 , and N_2 are in reasonable agreement with theoretical values obtained by Tejwani et al. [77]. The theoretical values listed in Table 4-2 represent average, intensity weighted broadening coefficients. The broadening coefficients for H_2 are also in reasonable agreement with the results of the experimental millimeter work reported by Nerfe [78].

Table 4-2: Foreign Gas Pressure Broadening Coefficients
for H_2CO .^a

WAVENUMBER (cm ⁻¹)	TRANSITION	BROADENING GAS			
		air	H_2	O_2	N_2
1159.47176	$\nu_4: 3_{0,3} \leftarrow 3_{1,3}$	0.126(10)	0.139(9)	0.090(8)	0.140(9)
1192.76481	$\nu_6: 7_{4,4} \leftarrow 7_{5,3}$ $7_{4,3} \leftarrow 7_{5,2}$	0.119(10)	0.158(18)		
1192.71773	$\nu_6: 8_{4,5} \leftarrow 8_{5,4}$ $8_{4,4} \leftarrow 8_{5,3}$	0.117(7)	0.166(18)		
1105.93457	$\nu_4: 14_{1,13} \leftarrow 15_{2,13}$	0.115(8)			
Millimeter broadening (avg.)			0.139 ^b		
Theoretical Broadening (avg.)		0.107 ^c		0.062 ^c	0.120 ^c

a. These values are half width at half height and for a temp. of $24+1^\circ\text{C}$.

b. From Nerfe [78]

c. From Tejwani et al. [77]

CHAPTER 5

ROTATIONAL ANALYSIS OF ν_3 , ν_4 AND ν_6 BANDS OF FORMALDEHYDE5.1 Introduction

In this Chapter, the least-squares analysis of the observed transitions of the ν_3 , ν_4 , and ν_6 bands of H_2CO will be presented. The aim of this analysis is to find a set of molecular constants that can most accurately reproduce the measured wavenumbers for a given Hamiltonian model. Generally, if sets of data for a molecule exist for both ultraviolet and microwave transitions or both infrared and microwave transitions, then the data sets can be combined to determine more accurate molecular constants for the common vibrational level(s); subsequent predictions and identifications of previously unassigned transitions are then aided. In this study the molecular constants were evaluated using a combination of vibrational (IR) and pure rotational (microwave) data.

The analysis technique involves an iterative process in which the RMS (root-mean-square) differences between the observed and calculated wavenumbers are minimized using the least-squares technique. The RMS minimization is obtained by iterative adjustment of the parameters of the Hamiltonian. A block diagram of the process is shown in Figure 5-1. To predict the transitions (calculated values)

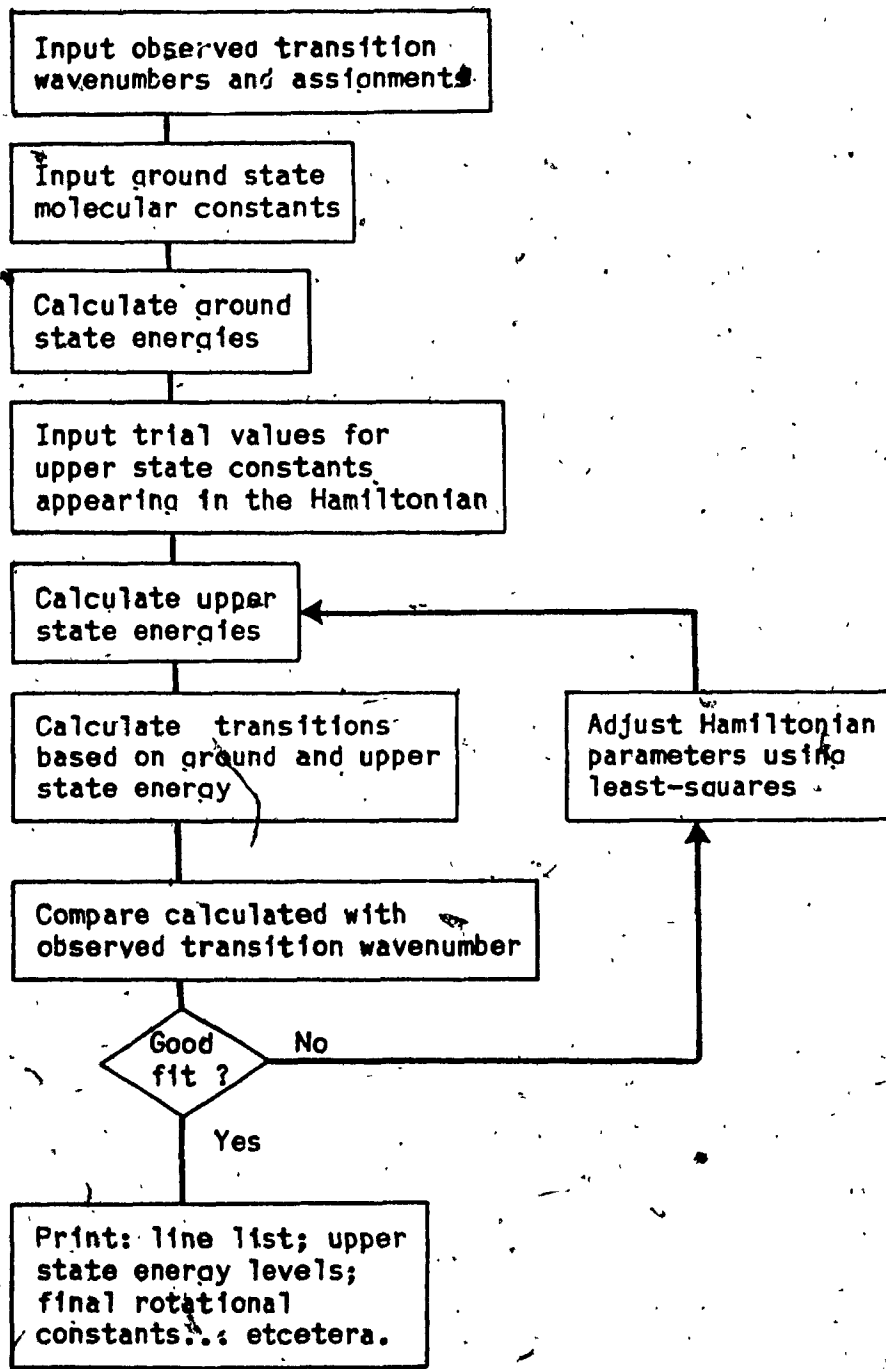


Figure 5-1: Block diagram of computer program used for the determination of asymmetric top molecular constants by least-squares fitting.

one needs both the ground and upper vibrational state molecular constants. The upper state set of constants are the quantities being adjusted and optimized in the fit.

The least-squares fitting technique was also applied to the observed line strengths. This fit computed the dipole moments for the three bands under study and facilitated the prediction of their spectra.

5.2 Least-Square Fitting to the Model Hamiltonian

Least-squares fitting to the rotational Hamiltonian of the transition wavenumbers was performed simultaneously for the ν_3 , ν_4 and ν_6 bands using a computer program written and described by Johns [14] and modified by Reuter [81]. Hence only a summary will be presented here, stressing those points important for the interpretation of the results.

The aim of the program is to find a set of statistically significant molecular constants, C_i , that can most accurately predict the measured wavenumbers from the Hamiltonian

$$\tilde{H}_R = \sum_i C_i \Omega_i \quad (5-1)$$

where Ω_i is a quantum mechanical operator. An iterative approach is used in the least-squares fitting routine since the calculated wavenumbers, ν_i^{cal} , are not a linear function

of the C_i . This is done by making an initial "guess" for the C_i and then finding the set of corrections, δC_i , that best solve the linear equations

$$\nu_i^{\text{obs}} - \nu_i^{\text{cal}} = \sum_k x_{ik} \delta C_k \quad (5-2)$$

where ν_i^{obs} is the observed frequency, i runs over N transitions, k runs over M coefficients, and x_{ik} is the wave-number derivative of transition i with respect to coefficient k ($\partial \nu_i^{\text{cal}} / \partial C_k$). The best set of corrections, δC_k , in a least-squares sense are those that minimize the goodness of fit (RMS) relationship

$$(\text{RMS})^2 = \chi^2 = \sum_{i=1}^N w_i (\nu_i^{\text{obs}} - \nu_i^{\text{cal}})^2 \quad (5-3)$$

where $w_i = 1/\sigma_i^2$ is the weight of the i^{th} transition, and σ_i is the error assigned to that transition. The weighting is particularly important when the fitting involves mixed data sources. e.g. microwave and IR; where the σ in the microwave data is usually several orders of magnitude smaller than that for IR data. Upon minimization of χ^2 a new set of constants are generated, $C_i(\text{new}) = C_i(\text{old}) + \delta C_i$, which in turn are used to generate a new set of ν_i^{cal} . The iteration procedure is repeated to convergence, when the changes δC_i are smaller than some desired measure of precision. In this analysis δC_i had to satisfy the relationship $|\delta C_i| < \sigma(C_i)$, where $\sigma(C_i)$ is the least-squares estimate of the standard deviation of the C_i constants.

In order to minimize the RMS given by Equation (5-3)

the fitting program has to compute ν_i^{cal} , δc_i , and $\partial \nu_i / \partial c_k$. The fitting program uses a full Wang factorization described in Chapter 2, and using the Hellman-Feynmann theorem [82] calculates the required Jacobian matrix of partial derivatives of wavenumbers with respect to molecular parameters ($\partial \nu / \partial c$) by the eigenvector transformation method. The wavenumber derivatives are differences between the energy derivatives $\partial E_i / \partial c_i$. Since the energy levels are eigenvalues of \tilde{H}_R which is a linear function of the c_i parameters, the frequency derivatives may be given as follows.

Starting with the reduced Hamiltonian given by Equation (5-1), $\tilde{H}_R = \sum_k c_k \Omega_k$, where c_k is the k^{th} molecular constant and Ω_k is the k^{th} quantum mechanical operator, the i^{th} eigenvalue, E_i , is then

$$E_i = \sum_k c_k \langle i | \Omega_k | i \rangle \quad (5-4)$$

where i is the i^{th} upper state eigenfunction. The derivative of E_i with respect to the k^{th} molecular constant is,

$$\partial E_i / \partial c_k = \langle i | \Omega_k | i \rangle \quad (5-5)$$

Now, for pure rotational transitions, the i^{th} frequency is

$$\nu_{ij}^{\text{cal}} = E_i - E_j$$

therefore

$$\begin{aligned} \partial \nu_{ij}^{\text{cal}} / \partial c_k &= \partial E_i / \partial c_k - \partial E_j / \partial c_k \\ &= \langle i | \Omega_k | i \rangle - \langle j | \Omega_k | j \rangle \end{aligned} \quad (5-6)$$

where j is the j^{th} upper state wavefunction. For vibrational transitions the i^{th} frequency is given by

$$\nu_{ij} = \nu_{0,n} + E'_i - E''_j \quad (5-7)$$

The band center is represented by $\nu_{0,n}$ and is the separation between the $J'=0$ and $J''=0$ levels. The rotational eigenvalues E'_i and E''_j are measured relative to the $J'=0$ and $J''=0$ levels, respectively. In addition, the derivatives of the lower state energy are a function of the ground state molecular parameters which are kept fixed in the fit. Thus, the derivative with respect to molecular parameter k becomes simply

$$\frac{\partial \nu_{ij}}{\partial C_k} = \frac{\partial E'_i}{\partial C_k} = \langle i | \Omega_k | i \rangle \quad (5-8)$$

In summary, the diagonalization process yields both—the eigenvalues and the eigenvectors. The latter quantities are used for the construction of the Jacobian matrix having the elements described by Equations (5-6) and (5-8).

To find the set of C_i that minimizes χ^2 one generates the needed normal equations from the conditions $(\partial \chi^2 / \partial C_j) = 0$. The normal equations are [83,84]

$$Y = A \delta C \quad (5-9)$$

where

$$Y_k = \sum_j w_j y_j x_{jk}$$

$$A_{ki} = \sum_j w_j x_{jk} x_{ji}$$

The corrections δC_i may be found by inverting the normal matrix A to give

$$\delta C = A^{-1} Y \quad (5-10)$$

The inverse of A can be determined rapidly by matrix inversion techniques designed for the computer. However, if the determinant of A is very small, numerical errors may creep into the calculation of the inverse. This can be due to near linear dependence in the independent variables [85] or from a lack of sufficient experimental data to determine some of the C_i independent of the others. This analysis used matrix inversion to solve Equation (5-9) although other techniques are available, e.g. the Graham-Schmidt ortho-normalization procedure [84,86,87]. Problems which could have arised from matrix inversion were eliminated by inserting a numerical ridge, i.e. the diagonal elements of A were not allowed to drop below a certain value.

Quantities determined for each fit were: the best fit values for the Hamiltonian coefficients, C_i ; the estimated standard deviation of each coefficient, $\sigma(C_i)$; the correlation coefficient matrix, ρ_{ik} ; the calculated wave-number, ν_i^{cal} ; the residuals, $\nu_i^{\text{obs}} - \nu_i^{\text{cal}}$; the standard deviation of the fit, σ_R ; and the weighted standard deviation of the fit, σ_F . The standard deviation of the fit is given as

$$\sigma_R = \left\{ (N-M)^{-1} \sum_{i=1}^N (\nu_i^{\text{obs}} - \nu_i^{\text{cal}})^2 \right\}^{1/2} \quad (5-11a)$$

the weighted standard deviation of the fit is given by

$$\sigma_F = \{(N-M)^{-1} \sum_{i=1}^N \hat{w}_i (\nu_i^{\text{obs}} - \nu_i^{\text{cal}})^2\}^{1/2} \quad (5-11b)$$

A reasonable fit for a set of accurately weighted observations will yeild a value near unity for σ_F .

5.3 Input To The Fitting Program

The input data consisted of the following.

1. Ground state molecular constants.
2. Initial values for the upper state molecular constants.
3. The observed FT-IR transition wavenumbers, their assigned quantum numbers, and their respective weights, and
4. Some observed excited state microwave transitions for the $v_3=1$, $v_4=1$, and $v_6=1$ states.

The rotational constants for the ground state of H_2CO were taken from Cornet and Winnewisser [64]. The constants included all the sextic coefficients. The initial upper states constants for the three bands were taken from Allegrini et al. [14]. These included quartic terms and 1st and 2nd order Coriolis coefficients. Both ground and upper state constants are listed in Table 5-1. A total of 3214 observed IR transitions in the v_3 , v_4 , and v_6 bands were used in the fit. Although the FT-IR spectra contained several hundred additional absorptions, we decided to limit

Table 5-1: Ground State, and Initial Upper States
Rotational Constants.

	Ground State ^a in MHz	Upper States ^b in cm ⁻¹		
		v ₄ = 1	v ₆ = 1	v ₃ = 1
v ₀		1167.258	1249.091	1500.176
A	281970.5723	9.2890	9.4881	9.46697
B	38836.04557	1.287243	1.298244	1.300078
C	34002.20344	1.135716	1.129886	1.129318
Δ _K	19.42374	2.346	11.861	7.586 x10 ⁻⁴
Δ _{JK}	1.29050	2.413	8.025	2.421 x10 ⁻⁵
Δ _J	0.0752953	2.412	2.539	2.825 x10 ⁻⁶
δ _K	1.0260307	2.33	4.64	5.00 x10 ⁻⁵
δ _J	0.0104567	2.71	3.53	5.11 x10 ⁻⁷
h _K	4.499x10 ⁻³			
h _{KJ}	-1.1218x10 ⁻⁴			
h _{JK}	2.9019x10 ⁻⁵			
h _J	3.1435x10 ⁻⁸			
h _K	1.3721x10 ⁻³			
h _{JK}	1.5666x10 ⁻⁵			
h _J	4.2399x10 ⁻⁸			
ξ ₆₄ ^a		10.0728		
η ₆₄ ^{bc}		0.002498		
ξ ₃₄ ^b		1.28841		
ξ ₃₆ ^c		0.75368		

a) From Reference 64. b) From Reference 14.

the fit to transitions with $J \leq 29$. These transitions were the most accurately measured and were sufficient to yield an accurate and reliable set of molecular constants which in turn could be used to predict all the transitions in their respective bands. The observations used (ν_i^{obs}) along with their respective quantum numbers and weights are listed in Table A-1 of Appendix A.

The observed microwave transitions for the $v_3=1$, $v_4=1$, and $v_6=1$ excited vibrational states were taken from Oka et al [88], Chardon et al [89], and Dangoisse et al [90]. The observations included 14 transitions in v_3 , 31 transitions in v_4 , and 29 transitions in v_6 . These transitions along with their respective quantum numbers and weights are listed at the end of Table A-1 of Appendix A. The microwave data which were given in MHz were converted to wavenumbers using a value for the speed of light of $c = 2.99792458 \times 10^{10}$ cm/sec.

5.4 Wavenumbers Fit, Results and Discussion

In this section the results of two separate fits are discussed. These fits are hereafter called fit A and fit B.

Fit A was obtained using the input described in the previous section and included in the fit all transitions up to 10 standard deviations from the fit. The results obtained from this fit are listed in Table A-1 of Appendix A. Out of the 3214 IR transitions fitted, 187 lines had residuals >

0.002 cm^{-1} and only 45 lines had residuals $> 0.005 \text{ cm}^{-1}$.

Most of these transitions were blended lines or transitions with high J and K_a values. Overall this fit yielded excellent results with a RMS standard deviation of

$$\sigma_R = 0.00093 \text{ cm}^{-1}$$

and a weighted standard deviation of $\sigma_F = 1.13$.

The rotational parameters obtained from this simultaneous analysis of the ν_3 , ν_4 , and ν_6 bands (fit A) are listed in Table 5-2. The correlation matrix for fit A shown in Table 5-3 reveals, however, that some of the 53 fitted constants are dependent on each other. There are 26 dependencies (underscored in the Table) with correlations > 0.800 . Allegrini [14] also noted these dependencies and reported very high correlations between rotational parameters of ν_4 and ν_6 and their Coriolis coupling constants ξ_{64} and η_{64} . The relevance of high correlations between the independent variables in least squares fits is discussed in detail by Albritton et al. [83] and will not be dealt with here. From the point of view of our Hamiltonian model, however, it means that different sets of coefficients (rotational constants) might yield equivalent fits. This prompted a series of additional least squares fits culminating in fit B.

Fit B differs from fit A only in its initial upper state constants. The initial parameters for fit B were obtained from the results of a fit A modified to fit only transitions up to $J'=15$ and $K_a'=5$. The resulting rotational

Table 5-2: Molecular Constants for the ν_4 , ν_6 and ν_3
Bands of H_2CO .

Results of fit A and Fit B.

The constants are given in cm^{-1} . The uncertainties in parentheses are 1 from the least-squares fits, right-adjusted to the last digit of the parameter.

** These parameters were fixed to the ground state values.

	Fit A $\nu_4 = 1$	Fit B $\nu_4 = 1$	
ν_0	1167.25657 (6)	1167.25652 (6)	
A	9.287915 (27)	9.274998 (27)	
B	1.288481 (4)	1.288090 (2)	
C	1.1356828 (7)	1.1356943 (7)	
Δ_K	1.0116 (61)	0.7293 (61)	$\times 10^{-4}$
Δ_{JK}	3.5932 (70)	3.4893 (69)	$\times 10^{-5}$
Δ_J	2.3851 (15)	2.3772 (15)	$\times 10^{-6}$
δ_K	1.963 (20)	1.750 (20)	$\times 10^{-5}$
δ_J	2.7902 (52)	2.7559 (52)	$\times 10^{-7}$
H_K	-7.818 (78)	-9.224 (76)	$\times 10^{-7}$
H_{KJ}	-4.65 (17)	-3.92 (18)	$\times 10^{-8}$
H_{JK}	-2.34 (35)	-4.12 (35)	$\times 10^{-9}$
H_J	**	**	$\times 10^{-12}$
h_J	**	**	$\times 10^{-12}$
h_{JK}	2.20 (42)	2.06 (42)	$\times 10^{-9}$
h_K	1.07 (23)	2.13 (23)	$\times 10^{-7}$

continues....

Table 5-2: Continued

	Fit A $V_6 = 1$	Fit B $V_6 = 1$	
ν_0	1249.09454 (6)	1249.09465 (6)	
A	9.473186 (27)	9.501472 (26)	
B	1.2981327 (8)	1.2981322 (8)	
C	1.1314955 (9)	1.1316572 (9)	
Δ_K	1.2098 (6)	1.2368 (6)	$\times 10^{-3}$
Δ_{JK}	5.2081 (58)	5.3599 (57)	$\times 10^{-5}$
Δ_J	2.5598 (13)	2.5589 (13)	$\times 10^{-6}$
δ_K	4.156 (26)	4.166 (26)	$\times 10^{-5}$
δ_J	3.6950 (66)	3.675 (66)	$\times 10^{-7}$
H_K	1.097 (71)	1.236 (71)	$\times 10^{-6}$
H_{KJ}	7.28 (15)	5.90 (14)	$\times 10^{-8}$
H_{JK}	3.48 (36)	4.50 (36)	$\times 10^{-9}$
H_J	**	**	$\times 10^{-11}$
h_J	**	**	$\times 10^{-11}$
h_{JK}	-0.235 (29)	-1.6534 (70)	$\times 10^{-10}$
h_K	5.75 (48)	7.38 (10)	$\times 10^{-8}$

continued....

Table 5-2: Continued.

	Fit A $V_3 = 1$	Fit B $V_3 = 1$	
ν_o	1500.17474 (7)	1500.17456 (7)	
A	9.467042 (11)	9.467124 (11)	
B	1.298742 (4)	1.299127 (4)	
C	1.127668 (1)	1.127517 (1)	
Δ_K	6.8277 (37)	6.8755 (37)	$\times 10^{-4}$
Δ_{JK}	4.2596 (70)	4.2387 (65)	$\times 10^{-5}$
Δ_J	2.7660 (14)	2.7665 (14)	$\times 10^{-6}$
δ_K	5.628 (42)	5.510 (44)	$\times 10^{-5}$
δ_J	4.7232 (75)	4.746 (75)	$\times 10^{-7}$
H_K	1.966 (37)	2.083 (45)	$\times 10^{-7}$
H_{KJ}	-1.121 (19)	-0.753 (22)	$\times 10^{-7}$
H_{JK}	1.422 (72)	1.073 (76)	$\times 10^{-8}$
H_J	**	**	$\times 10^{-12}$
h_J	**	**	$\times 10^{-12}$
h_{JK}	2.36 (36)	2.90 (36)	$\times 10^{-9}$
h_K	9.98 (44)	7.90 (47)	$\times 10^{-7}$

Coriolis Constants

ξ_{64}^a	10.069126 (98)	10.016327 (98)
ξ_{34}^b	-1.43933 (45)	-1.39372 (45)
ξ_{36}^c	0.978624 (38)	0.999699 (39)
η_{64}^{bc}	-0.0032417 (29)	-0.0033324 (29)
z_{36}	-4.02 (16) $\times 10^{-6}$	-5.82 (16) $\times 10^{-6}$

Table 5-3: Correlation Matrix from Least-Squares-Fit: Results From Fit A.

a. The numbers 1-48 represent cyclically the rotational constants for ν_4 , ν_6 and ν_3 . 49-53 represent the Coriolis constants.

WEIGHTED STANDARD DEVIATION = 0.113E+01
UNWEIGHTED STANDARD DEVIATION = 0.933E-03
LEAST SQUARES ITERATIVE PROCEDURE COMPLETE.

constants from fit B are also listed in Table 5-2. These are significantly different from the results obtained from fit A. Yet, the standard deviation of fit B is nearly identical to that of fit A ($\sigma_R = 0.00091 \text{ cm}^{-1}$) and both sets of constants predict the same calculated frequencies. Hence, the high correlation between the parameters does allow for similar results from different sets of molecular constants.

Both A and B fittings were also tried where only transitions within four standard deviations of the fit were included. The resulting rotational constants in these cases were again significantly different but had an improved standard deviation of $\sigma_R < 0.0006 \text{ cm}^{-1}$. These attempts turned out not to be very useful since too many transitions were excluded from the fitting process.

The continuing discussion refers to the parameters obtained from fit A as the final results, although at this point either one of the two sets may be presented as such. Using the sextic Hamiltonian terms significantly improved the overall fit reducing the σ_R of the fit by a factor of 5. The improvements were noticed for transition series with high J and K_a values. Without the sextic terms these series showed an incremental divergence in the residuals as a function of J for $J > 15$. However, preliminary fittings indicated that not all the sextic coefficients could be used in the fit. Two of these coefficients, namely, H_J and h_J , converged in the fit to yield values of the order of 10^{-12} .

cm^{-1} . From the matrix elements shown in Equation (2-47) one can see that H_J and h_J are the coefficients of $J^3(J+1)^3$ and $J^2(J+1)^2$ respectively. As such, even for the highest J used ($J=29$), the products yielded contributions on the order of 10^{-4} and 10^{-7} cm^{-1} . These values are of no significance since they are smaller than the resolution of the FT-IR spectrometer used ($\sim 0.004 \text{ cm}^{-1}$). Consequently, these two coefficients were fixed during the fit to the more accurate ground state values as indicated in Table 5-2.

The 3rd order Coriolis constant, z_{36} , had a surprisingly small effect on the local resonance between ν_3 and ν_6 . It improved the calculated values for many transitions having $J > 15$ by an average of 0.4 milliwavenumbers. Basically it is difficult at this point to estimate the real contribution of z_{36} .

The high correlations between the coefficients of the Hamiltonian are due in large part to the symmetry of the formaldehyde molecule. The near symmetric top ($\kappa = -0.961$) character of H_2CO coupled with the strong Coriolis interactions between the bands is the main cause for the observed correlations. These in turn, allow for some of the fitted Hamiltonian constants to compensate for or contribute to other constants. This being manifested in multiple sets of rotational constants (e.g. fits A and B) and the apparent small contribution of some of the coefficients.

Presently we are searching among the unassigned

transitions of the FT-IR spectra for series having high J and K_a ($K_a > 8$). Fitting such series might cause a convergence to only one set of molecular constants. However, even without these extra transitions the best set of constants may be determined graphically from a predicted spectra, i.e. when both the eigenvalues and eigenvectors obtained from a given fit are used simultaneously.

5.5 Intensity Fitting

The 27 observed line strengths for ν_4 and ν_6 discussed and listed in chapter 4 along with eleven ratio estimated line strengths for ν_3 were used to determine the dipole moment derivatives $\partial\mu/\partial Q_x$ ($x=3,4$ or 6). These derivatives may in turn be used to predict the entire spectrum from the eigenvalues and eigenvectors of the Hamiltonian.

The derivatives $\partial\mu/\partial Q_3$, $\partial\mu/\partial Q_4$, and $\partial\mu/\partial Q_6$ were evaluated using a least-squares fitting program. The fitting involved an iterative process similar to that used for the transition wavenumbers fit. The weighted RMS differences to be minimized is given by

$$(RMS)^2 = \chi^2 = \sum_i^N w_i (s_i^{\text{obs}} - s_i^{\text{cal}})^2 \quad (5-13)$$

where $w_i = 1/\sigma_i^2$ is the weight of the i^{th} line strength, and

σ_i is the error assigned to that observation. s_i^{cal} is obtained from Equation (2-59). The iterative process involves generating estimates of $\partial\mu/\partial Q_x$ such that

$$\partial\mu/\partial Q_x(\text{new}) = \partial\mu/\partial Q_x(\text{old}) + \delta(\partial\mu/\partial Q_x).$$

These in turn are used to generate a new set of s_i^{cal} . The iterative process continues until $\delta(\partial\mu/\partial Q_x) < \sigma(\partial\mu/\partial Q_x)$ where $\sigma(\partial\mu/\partial Q_x)$ is the estimated standard deviation of the dipole moment derivative. The correction factor $\delta(\partial\mu/\partial Q_x)$ is evaluated as follows. From Equation (2-59) one obtains

$$\begin{aligned} s_i^{\text{cal}} = & (\partial\mu/\partial Q_4)^2 z_4^2 + (\partial\mu/\partial Q_6)^2 z_6^2 + (\partial\mu/\partial Q_3)^2 z_3^2 \\ & + 2(\partial\mu/\partial Q_4)(\partial\mu/\partial Q_6)z_4 z_6 + 2(\partial\mu/\partial Q_4)(\partial\mu/\partial Q_3)z_4 z_3 \\ & + 2(\partial\mu/\partial Q_6)(\partial\mu/\partial Q_3)z_6 z_3. \end{aligned} \quad (5-14)$$

Hence, the normal equations may be written as

$$wD^T \Delta S = D^T wD \delta P \quad (5-15)$$

where $\Delta S_i = s_i^{\text{cal}} - s_i^{\text{obs}}$, $\delta P_x = (\partial\mu/\partial Q_x)$ and D , the Jacobian matrix is given by $D_{ix} = \partial s_i^{\text{cal}} / \partial (\partial\mu/\partial Q_x)$ and is evaluated from Equation (5-14) where i runs over the number of observations and $x=3, 4$ or 6 , i.e. the three contributing dipole moment derivatives. For example, the i^{th} row of the matrix contains the following 3 elements

$$\begin{aligned} \partial s_i^{\text{cal}} / \partial (\partial\mu/\partial Q_4) = & 2(\partial\mu/\partial Q_4)z_4^2 + 2(\partial\mu/\partial Q_6)z_4 z_6 \\ & + 2(\partial\mu/\partial Q_3)z_4 z_3 \end{aligned}$$

$$\frac{\partial s_i^{\text{cal}}}{\partial (\partial \mu / \partial Q_6)} = 2(\partial \mu / \partial Q_6) z_6^2 + 2(\partial \mu / \partial Q_4) z_4 z_6 \\ + 2(\partial \mu / \partial Q_3) z_6 z_3$$

$$\frac{\partial s_i^{\text{cal}}}{\partial (\partial \mu / \partial Q_3)} = 2(\partial \mu / \partial Q_3) z_3^2 + 2(\partial \mu / \partial Q_4) z_4 z_3 \\ + 2(\partial \mu / \partial Q_6) z_6 z_3$$

It should be noticed here that in the absence of interactions between the bands the 2nd and 3rd terms of all the elements drop out.

5.6 Intensity fitting; Results and Discussion

The results of the least-squares fitting of the line strengths are listed in Table 5-4. This fit which was based on the eigenvectors obtained from fit A (described above) yielded a standard deviation of $\sigma_R = 0.00404 \text{ cm}^{-2} \text{ atm}^{-1}$. This is a good fit, with an RMS proportional to the experimental error. The σ_R is somewhat smaller when the estimated line strengths for v_3 are not used. However, these were needed for the evaluation of the dipole moment of v_3 which in turn was used in the evaluation of the magnitude of energy mixing between the bands.

The values for the effective dipole moments obtained from this fit are:

$$(\partial \mu / \partial Q_4) = 2.408(44) \times 10^{-3} \text{ cm}^{-1} \text{ atm}^{-1/2}$$

$$(\partial \mu / \partial Q_6) = -3.092(40) \times 10^{-3} \text{ cm}^{-1} \text{ atm}^{-1/2}$$

$$(\partial \mu / \partial Q_3) = 1.69(18) \times 10^{-3} \text{ cm}^{-1} \text{ atm}^{-1/2}$$

JU	KAU	KCU	VU	JL	KAL	KCL	OBS	INT	OBS-CAL	FREQ	WT
17	4	14	2	18	5	13	0.3225E-02	-0.8798E-03	1148.3347	4.7383	
11	2	9	1	10	3	7	0.2113E-01	0.2987E-03	1148.3452	0.3009	
17	4	13	2	18	5	14	0.3395E-02	-0.7146E-03	1148.3602	3.2992	
3	0	3	1	4	1	3	0.4737E-01	0.6102E-02	1148.4702	0.0198	
16	1	15	1	16	2	15	0.1866E-01	0.2189E-02	1148.5083	0.1337	
1	0	1	1	1	1	1	0.2953E-01	0.6159E-03	1159.1356	0.0260	
2	0	2	1	2	1	2	0.4846E-01	0.9827E-03	1159.2716	0.0081	
28	2	27	1	28	1	27	0.5936E-02	0.6334E-03	1159.2876	0.4586	
15	2	13	1	14	3	11	0.1883E-01	-0.6959E-03	1159.3920	0.1837	
9	1	9	1	.8	2	7	0.7429E-02	0.1965E-03	1159.4396	0.7035	
3	0	3	1	3	1	3	0.6663E-01	0.1642E-02	1159.4715	0.0035	
18	2	17	1	18	1	17	0.3208E-01	0.3744E-02	1172.3859	0.1957	
6	1	6	1	6	0	6	0.2843E-01	0.4681E-03	1172.5255	0.0343	
12	2	11	2	13	3	10	0.1898E-01	-0.1705E-02	1180.6443	0.0752	
4	4	1	2	5	5	0	0.1921E-01	-0.2606E-03	1180.7330	0.0540	
24	0	24	1	23	1	22	0.2613E-02	-0.7444E-03	1180.8080	13.7373	
11	2	10	1	11	1	10	0.3400E-01	-0.1982E-02	1180.8324	0.0174	
13	2	11	2	14	3	12	0.1651E-01	-0.3688E-02	1180.8831	0.0559	
10	4	7	2	10	5	6	0.1400E-01	0.1407E-02	1192.6082	0.3555	
3	3	1	2	4	4	0	0.1000E-01	0.4628E-03	1192.6270	0.3555	
9	4	6	2	9	5	5	0.1400E-01	0.1930E-02	1192.6657	0.3265	
8	4	5	2	8	5	4	0.1246E-01	0.1405E-02	1192.7181	0.1957	
18	1	17	2	19	2	18	0.6010E-02	-0.1123E-02	1192.7374	1.4471	
7	4	4	2	7	5	3	0.1083E-01	0.1358E-02	1192.7652	0.5209	
10	1	10	2	11	2	9	0.5890E-02	-0.4981E-03	1192.7954	2.5135	
6	4	3	2	6	5	2	0.8240E-02	0.1029E-02	1192.8068	0.8358	
5	4	2	2	5	5	1	0.4886E-02	0.7429E-03	1192.8428	7.3743	
16	3	14	3	17	3	15	0.3260E-01	0.4423E-02	1460.5795	0.0018	
10	1	10	3	11	1	11	0.6260E-01	-0.9457E-02	1474.5636	0.0005	
7	1	6	3	8	1	7	0.7070E-01	0.2707E-02	1480.5772	0.0004	
6	0	6	3	7	0	7	0.3010E-01	0.6901E-02	1483.4343	0.0021	
3	3	1	3	3	3	0	0.3250E-01	-0.1104E-01	1500.7334	0.0018	
9	5	5	3	9	5	4	0.1840E-01	0.2022E-02	1502.0204	0.0058	
7	7	1	7	7	7	0	0.2010E-01	0.2710E-02	1503.1104	0.0047	
9	1	8	3	8	1	7	0.5524E-01	-0.6834E-02	1523.3220	0.0006	
13	0	13	3	12	0	12	0.2450E-01	0.6134E-02	1531.2509	0.0031	
14	2	13	3	13	2	12	0.2047E-01	0.6708E-02	1534.9392	0.0047	
20	3	17	3	19	3	16	0.1981E-01	0.6861E-02	1552.1402	0.0047	

NUMBER OF LINES FIT = 38

ROTATIONAL PARTITION FUNCTION = 0.282383D+04

Table 5-4: Results From Least-squares Fitting of Line Strengths.

a. The numbers 1,2 and 3 represent respectively ν_4 , ν_6 and ν_3

The ratio of $(\partial\mu/\partial Q_4)/(\partial\mu/\partial Q_6) = -0.779(12)$ representing the magnitude of perturbation [54] between the two bands, compares well with the value of $-0.8(1)$ obtained by Nakagawa and Morino [13]. The effective dipole moments were converted to conventional units ($\text{Debye}/\text{amu}^{1/2}\text{\AA}$). These compare favorably (within $\pm 15\%$) with literature values (Table 5-4).

The least-squares fit also computed the rotational partition function yielding $G=2823.83$. This value is in good agreement with $G_r=2832.91$ obtained from the empirical relationship [91].

$$G_r \approx 1/\sigma [(\pi/ABC)(kT/h)^3]^{1/2} \quad (5-16)$$

where A, B, and C are the ground state rotational constants (MHz), T is the temperature (K), and σ is a measure of symmetry and is equal to 2 for the C_{2v} group.

The band strengths were computed by summations using

$$B_x = \sum_i k(v)_{xi} \quad (5-17)$$

where i runs over all calculated line strengths within a given band, x ($x=3, 4$, or 6). These summations yielded the following band strengths

$$B_4 = 16.013 \text{ cm}^{-2} \text{ atm}^{-1}$$

$$B_6 = 35.424 \text{ cm}^{-2} \text{ atm}^{-1}$$

$$B_3 = 11.632 \text{ cm}^{-2} \text{ atm}^{-1}$$

These values were converted to conventional units of km/mole using the ideal gas law ($\text{cm}^{-2} \text{ atm}^{-1} = T \times 8.2056 \times 10^{-4} \text{ km/atm}$ [48]) and are compared to literature values [6, 17] in Table 5-5.

Table 5-5: Calculated Dipole Moment Derivatives and Band Strengths.

Dipole Moment derivatives

(Debye/amu^{1/2} Å)

derivative	This work	Nakanaga et al [16]
$(\partial\mu/\partial\Omega_4)$	0.332(6) ^a	0.39
$(\partial\mu/\partial\Omega_6)$	0.442(6)	0.47
$(\partial\mu/\partial\Omega_3)$	0.264(28)	

Band Strength
(km/mole)

	This work	Nakagana et al [16] cal. obs.	Histasune and Eggers [17]
ν_4, ν_6	12.53(84)	16.83, 16.41(65)	9.9(5)
ν_4	3.90(37)	7.53, 6.49(64)	
ν_6	8.63(82)	9.30, 9.94(97)	
ν_3	2.83(27)	12.01, 11.1(1.0)	

a. The uncertainties in parentheses are 1 standard deviation, right adjusted to the last digit.

It should be noted here that none of the literature values for either the dipole moments or band strengths were obtained from direct line strength measurements. For example, the values quoted from Nakanaga et al [16] were obtained from low resolution (0.25 cm^{-1}) FT-IR band measurements and band simulation.

Since in this work the line strengths were not measured directly for transitions in ν_3 , we have little confidence in the values of $(\partial\mu/\partial Q_3)$ and B_3 . However, when in several calculations this dipole moment was varied in magnitude from 1/10 to $\times 10$ its current value, little change has been noticed in the band strengths of ν_4 and ν_6 . This indicates that ν_3 has a relatively weak interaction with the other bands. It is estimated that B_3 should be about 3 times the reported value. This will increase $(\partial\mu/\partial Q_3)$ by a factor of $\sqrt{3}$ which in turn will cause only 1.8% change in B_4 and <1% change in B_6 . Based on this reasoning we have high confidence in the values presented here for ν_4 and ν_6 .

The goodness of the fit was checked by comparing the wavenumbers and relative line strengths of the predicted transitions to those of the observed (FT-IR). A stick diagram of such a comparison is presented in Figure 5-2.

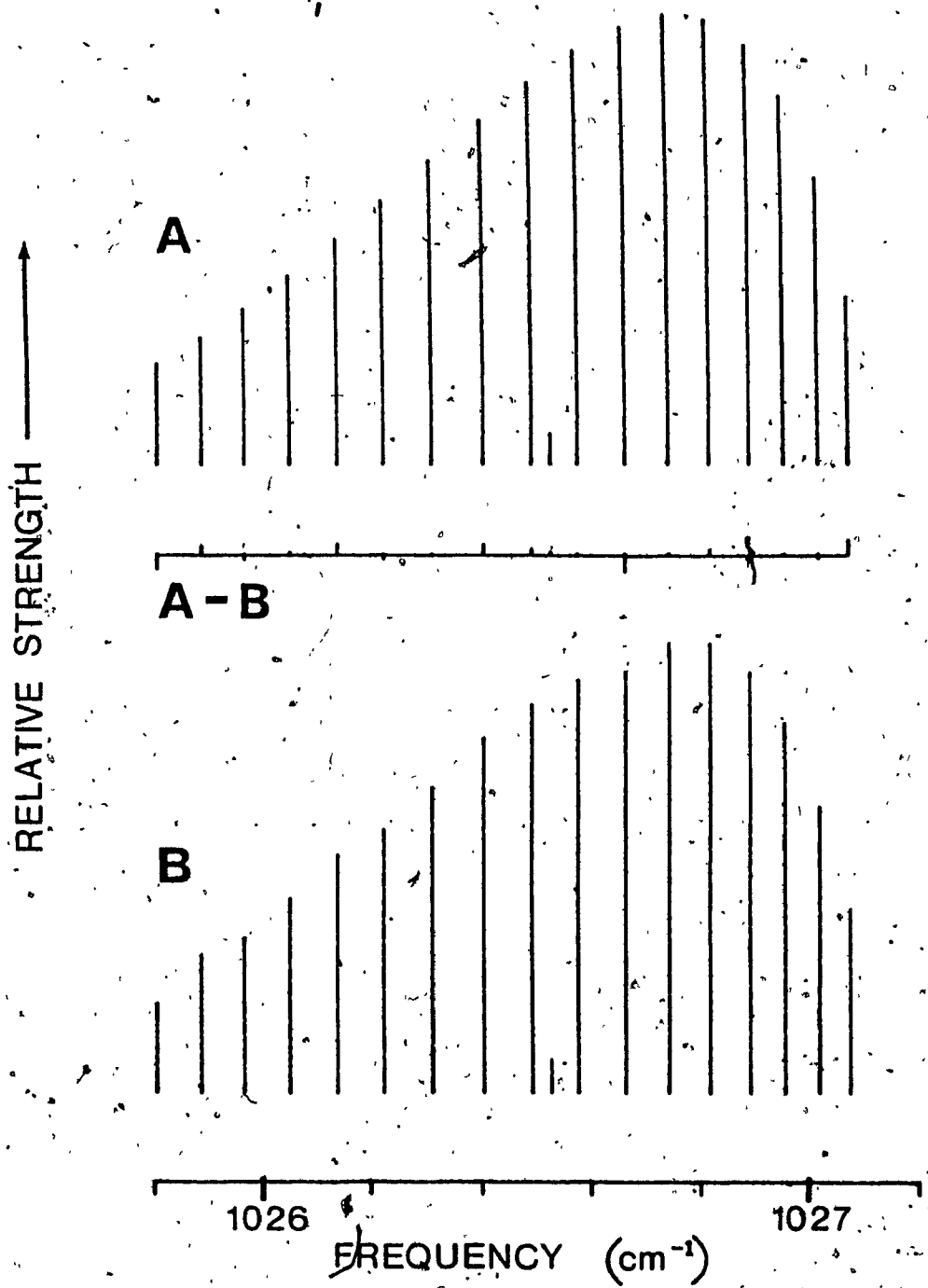


Figure 5-2: Stick Diagram Comparing Observed and Calculated Wavenumbers and Line Strengths for P_{07} of V_4 .

A. Calculated
B. Observed (FT-IR)

CHAPTER 6

TRACE ANALYSIS OF FORMALDEHYDE IN AMBIENT AIR.

6.1 Introduction

In this Chapter, the potential application of the TDL spectrometer to trace analysis of H₂CO in ambient air will be discussed. The aim here is to develop a rapid analysis technique capable of measuring air samples containing H₂CO concentrations at the low ppb level.

In the past decade, TDL systems have been used in a wide range of analytical applications, from trace analysis of gases at the <1 ppb level to fully automated on-line monitoring of gases and liquids [18-25, 92, 93]. Since the techniques and methodology are covered in the literature, the task here is rather heavily oriented to sample collection and handling prior to and during analysis. The ease with which H₂CO polymerizes and adsorbs to surfaces complicates its routine analysis. In addition, due to pressure broadening effect the spectroscopic technique requires reduced sample pressures. These three factors reduce the analyte concentration by several orders of magnitude. Analyte loss may be compensated by increasing the optical path length. This, however, is limited by hardware cost and size.

The results obtained from the TDL determinations were always compared with results obtained from the Laser Thermal

Lens (LTL) [94-98] technique, and to those obtained from the well established NIOSH colorimetric technique [99]. The LTL technique is currently also evaluated and developed at Concordia University by Dr. Langford's group for air pollution monitoring [100-102].

6.2 Preliminary Analysis

The initial attempts at determining H₂CO in air were carried out using a conventional spectroscopic technique. Samples of 10 ppm H₂CO in air prepared in a one liter glass bulb by passing dry air over a pellet of reagent grade paraformaldehyde [101] were introduced into the White cell. The cell pressure was then reduced to <10 Torr and the path length adjusted to 100.17 meters. The result from monitoring several strong transitions in the 10 μm region (ν_4 and ν_6 bands) were always negative, i.e. no absorption was observed.

The next step was to install the cold trap (liquid N₂) shown in Figure 6-1 between the sample cell and the White cell. This allowed for the reduction of pressure without loss of sample since the H₂CO was frozen out in the cold trap. This yielded detections as low as 1 ppm (Figure 6-2). It was observed, however, that identical samples yielded a variety of absorption values. We attributed this to the following potential causes: polymerization, surface adsorption and/or poor trapping mechanism of sample. The steps

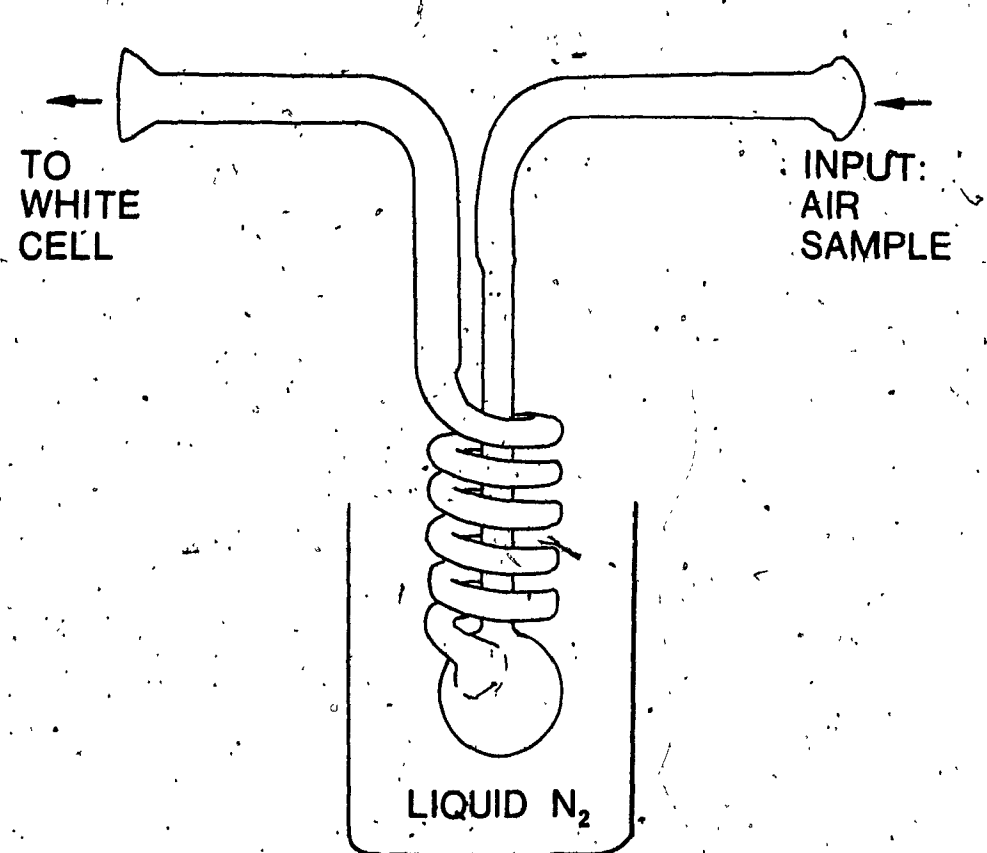


Figure 6-1: Formaldehyde Sampling Apparatus for Trapping H₂CO from a Fixed Volume of Air.

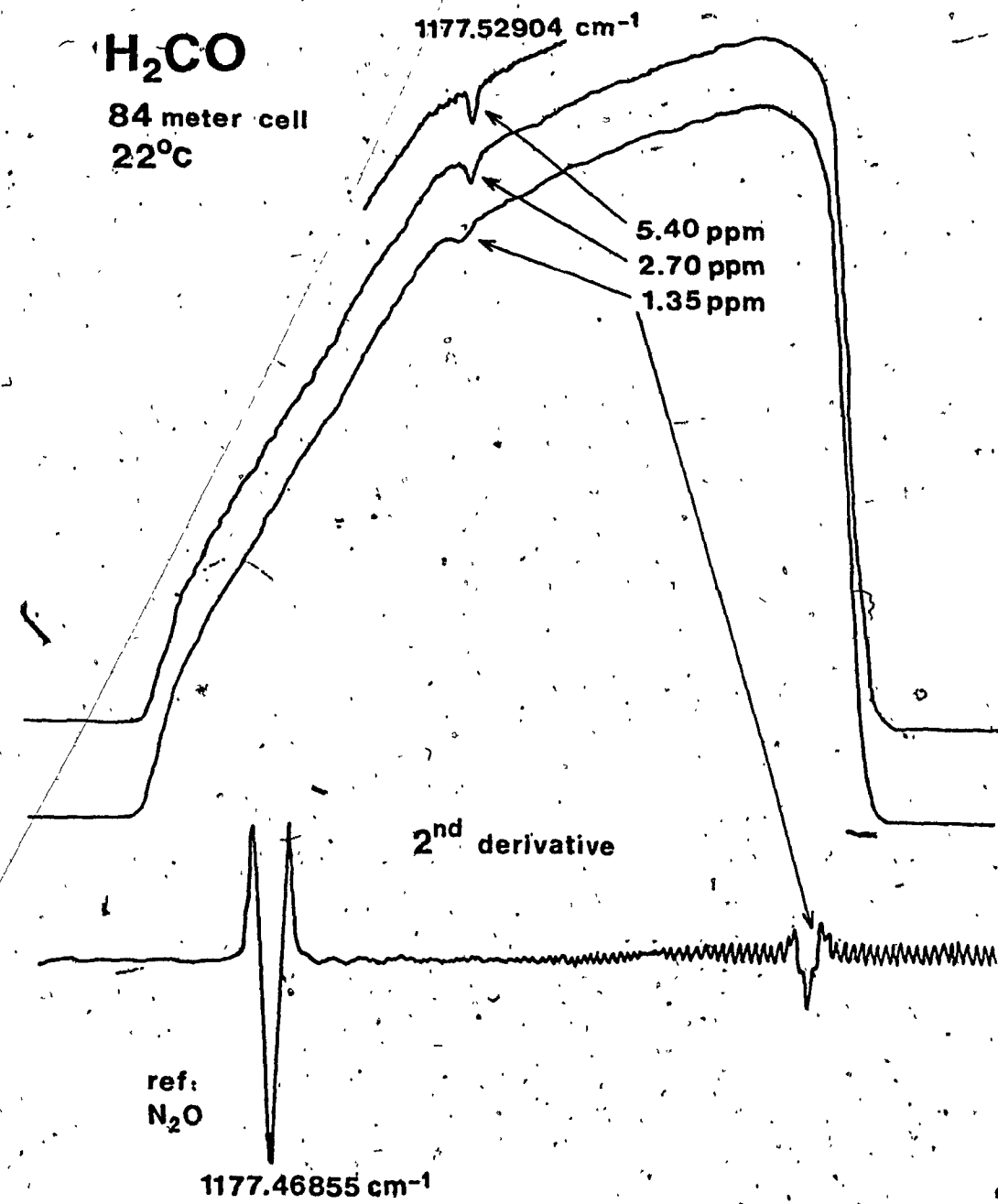


Figure 6-2: First Efforts at Determining H_2CO in Air Concentrations Using the Cold Trap.

taken to eliminate or reduce these problems as well as the measures taken to improve the lower limit of detection are described in the following section.

6.3 Experimental

Two steps were taken to improve the lower limit of detection. The first was to switch to the $3 \mu\text{m}$ spectral region. Transitions in the ν_1 (C-H stretch) band are much stronger than those of the ν_4 and ν_6 bands, [103]. The second step was to use standard 5 liter grab bags. Since the cold trap allows the analysis to be mass based rather than volume based, this increased 5 fold the number of molecules introduced into the White cell for analysis. The reusable multilayer (polyethylene inner layer) gas sampling bags were obtained from Applied Research Products Ltd, Quebec. Samples were obtained routinely from environmental chambers at Technitrol Canada Ltd, from the McGill University Laboratory for Occupational Hygiene, and from several sites at Concordia University.

Several survey spectra were taken in the ν_1 band (Figure 6-3). The strong transitions in the $^0\text{Q}_3$ sub-branch were selected for monitoring. Analytical measurements were taken only from the transition $^3_{3,1} \leftarrow ^3_{3,0}$ (the strongest line in the branch). It should be noted here that the selection of monitoring lines in the ν_1 band is also

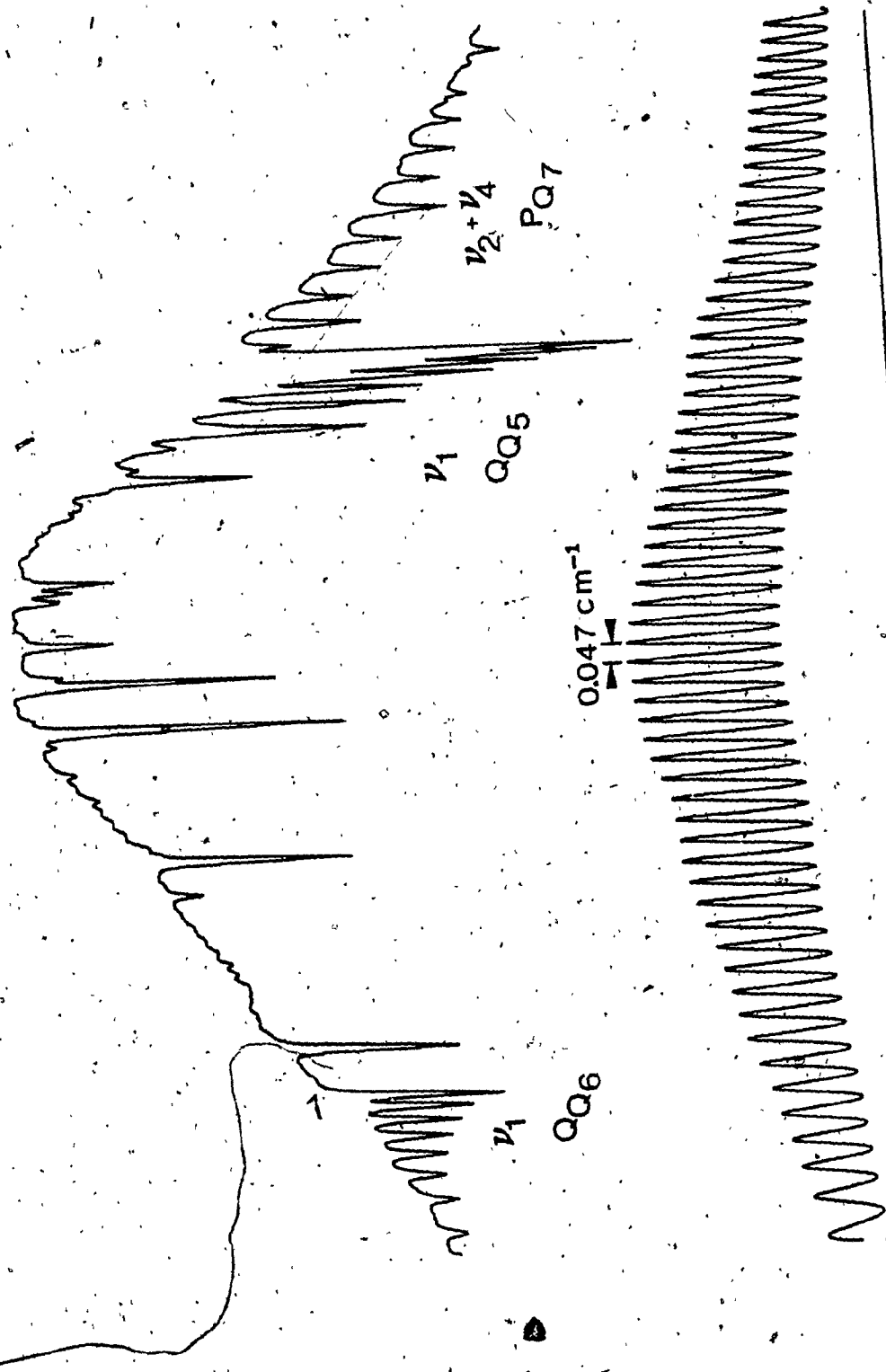
Figure 6-3: Survey Scans of Portions of the ν_1 Band of H₂CO
in the 3 μm Region. The Strong Q₃ Branch Lines
were Selected for Monitoring.

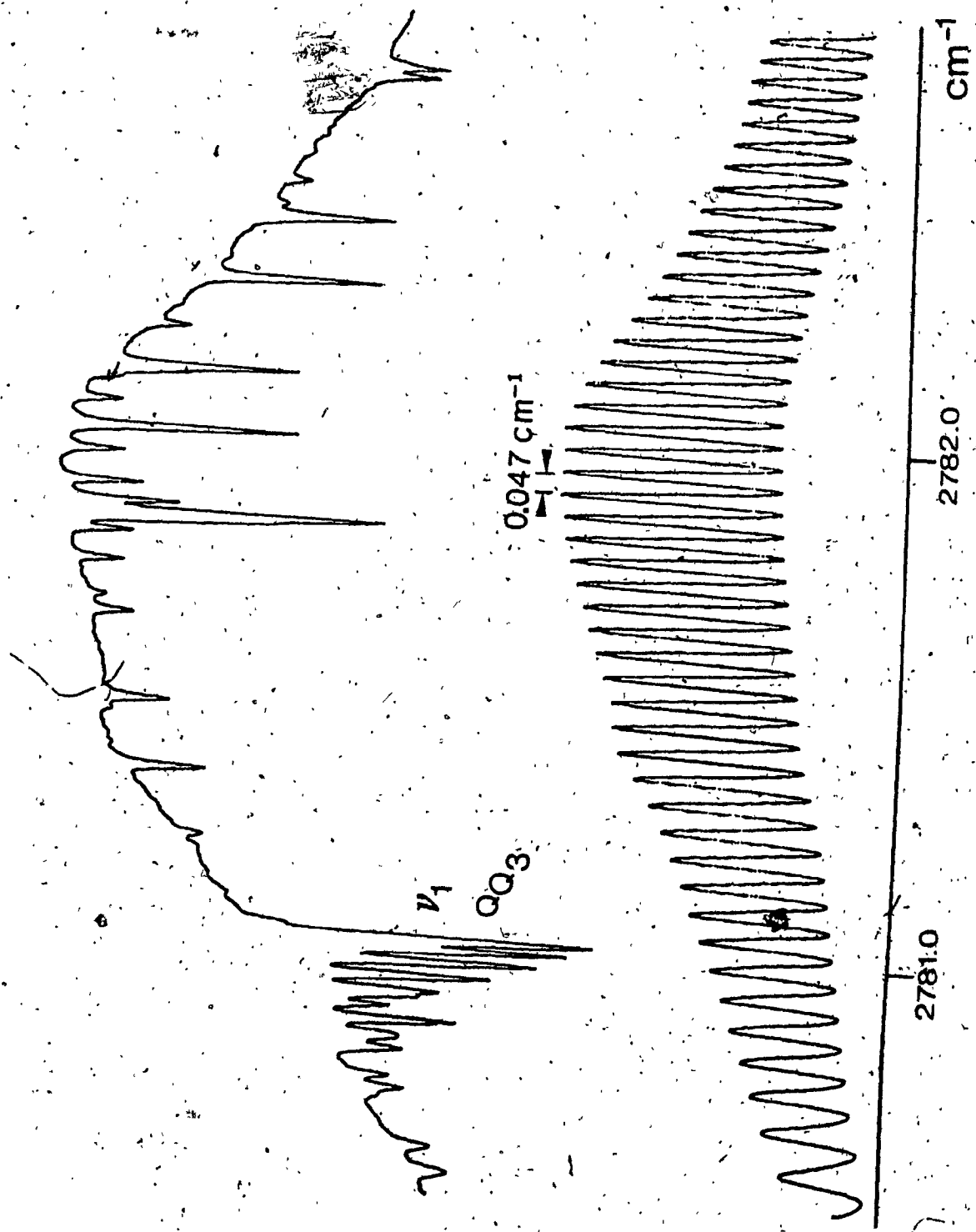
Conditions: 5 Torr H₂CO in 10 cm. cell at 24°C.



2778.5

2777.0

 0.047 cm^{-1} PQ₇QQ₅ $\nu_2 + \nu_4$ ν_1 QQ₆



governed by their distance from interfering H_2O lines. Hence, the Q_{Q_3} sub-branch has been chosen not only for its strong transitions but also because the nearest H_2O line is 0.4 cm^{-1} away [104]. Working with these transitions allowed determinations of < 1 ppm. The results obtained from identical sample bags however, demonstrated very poor reproducibility. Grab bags containing 1 ppm H_2CO have yielded 0.170 ppm on LTL analysis and ~0.03 ppm on TDL determinations. More importantly, the TDL results never agreed with the NIOSH determinations and it was impossible to construct calibration curves. Poor results were still obtained - even after the White cell and access ports were heated (80°C) to reduce adsorption.

Since the cold trap yielded the mass of H_2CO from a given volume of air, it was decided to prepare liquid standards containing equivalent masses (1 ppb in 5 liter = 6.131×10^{-9} grams). The standard solutions were prepared by dissolving paraformaldehyde in water at 120°C (in an autoclave [105]). The concentrations were such that 1 liter contained the equivalent mass of 10 or 20 ppb in 5 liters of air. These standards produced excellent calibration curves (Figures 6-4 and 6-5) with linear correlation coefficients of $R = 0.999$. From the spectra observed detection limits of 6×10^{-3} absorbance units (twice the signal to noise ratio) were determined. The sensitivity determined from the slope of the Beer's plots for a 100 meter optical path length is

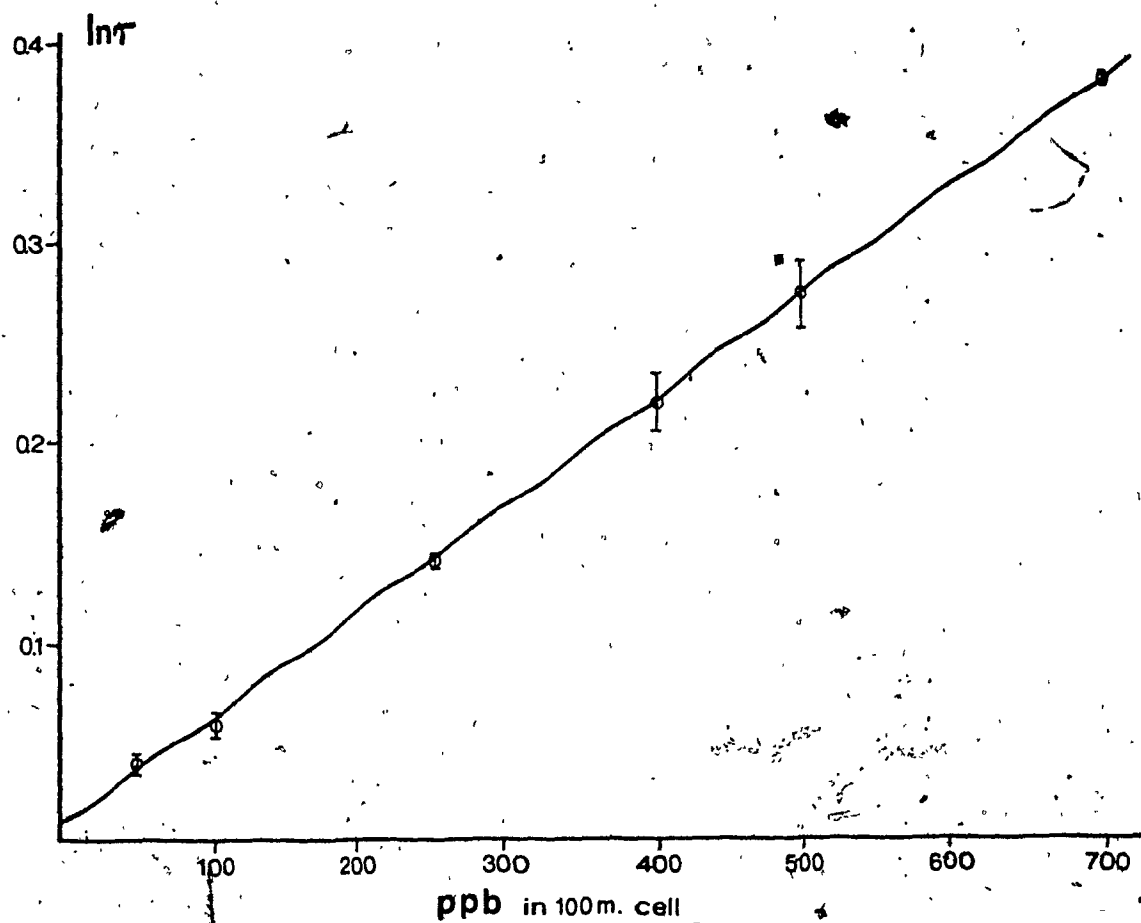


Figure 6-4: Analytical Detection Curve (Beer's plot) for the Transition $3_{3,1} \rightarrow 3_{3,0}$ of ν_1 Using Standard Solutions. The plot was constructed from the following data.

Conc. (ppb)	$\ln(I_0/I)$
50	0.039 (5)
100	0.060 (6)
250	0.142 (3)
400	0.218 (15)
500	0.273 (18)
700	0.381 (3)

* Error bars represent 1 standard deviation.

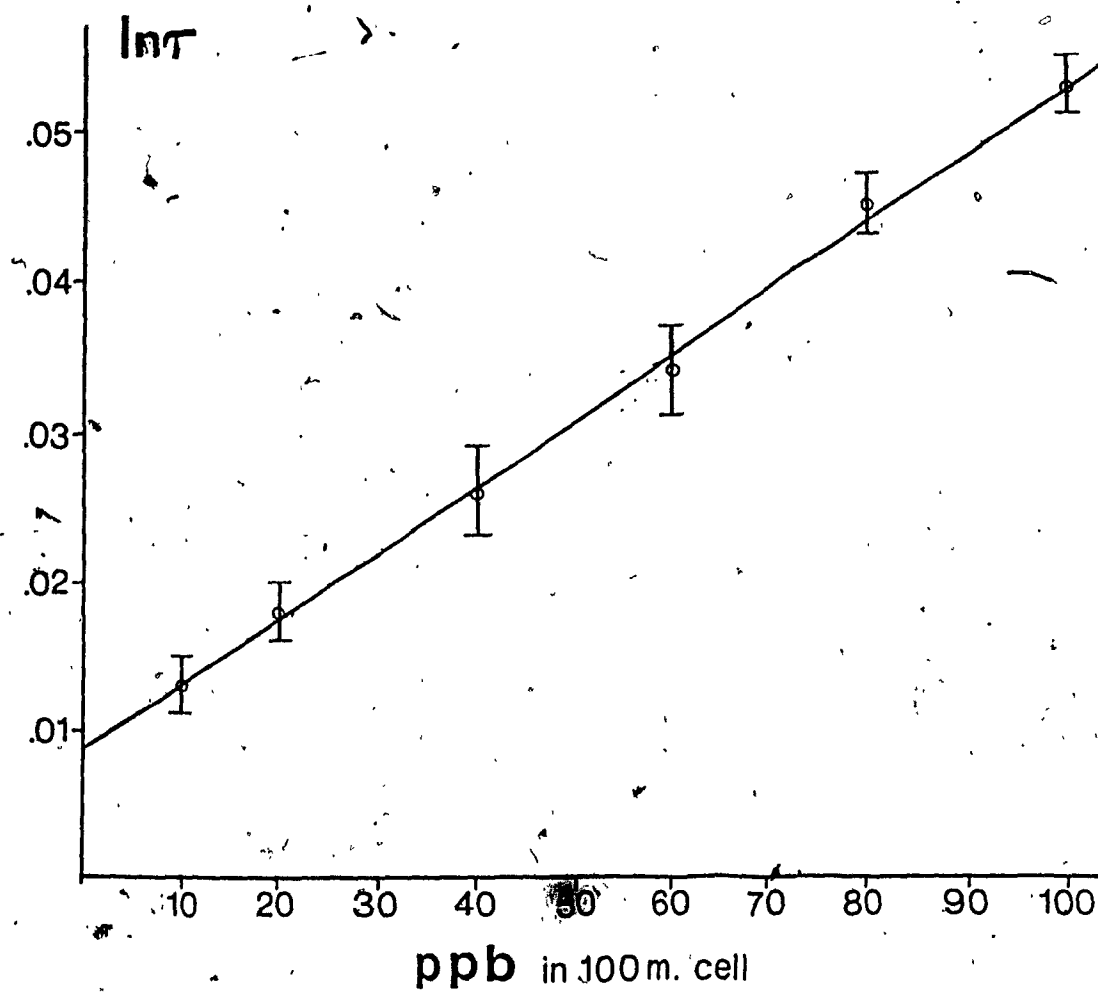


Figure 6-5: Same as Figure 6-4 but For Lower Concentration
of 10-100 ppb.

The plot was constructed from the following data:

Conc. (ppb)	$\ln(I_0/I)$
10	0.013(2)
20	0.018(2)
40	0.026(3)
60	0.034(3)
80	0.045(2)
100	0.053(2)

$4.4 \times 10^{-5} \text{ m}^{-1}$. For the strongest line in O_3 of ν_1 this limits the detection to ~7 ppb/v. This lower limit of detection is based on 5 liter samples. With the use of larger trap designs and by sampling larger volumes such as 10 liters or more the detection limit would come down to 5 ppb. Note, however, that the choice of sample volume is governed by the design of the cold trap, since ice (moisture from air) must be prevented from clogging the trap.

The attention was then focused on the grab bags. Using the same standard solution, an equivalent amount of 100 (and 200) ppb was evaporated into several bags. These were analyzed as a function of time spent within each bag. The 100 ppb bags were evaluated about 1/2 hour after the fill yielding an absorption of about 20 ppb. The 200 ppb bags were evaluated as shown below:

STARTING WITH 200 ppb

TIME (hrs)	YIELD
0.5	~75 ppb
3.0	~80 ppb
6.0	~60 ppb
24.0	~12 ppb

It becomes evident from this behaviour that the main cause for sample loss is due to adsorption and/or polymerization. This opinion was reinforced by proving that the cold trap is quite efficient in both trapping and delivering H_2CO molecules. The combined volume of the White cell and connecting hoses is about 16.5 liters. This volume was

evacuated and laboratory air (room air) was introduced through the cold trap to a final room pressure. Upon analysis (figure 6-6) the trapped sample yielded an absorption of $\ln(I_0/I) = 0.045(5)$. From the calibration curve (Figure 6-5) this is equivalent to 80(9) ppb. Converting this result to the equivalent mass in 5 liters yields 24 ± 3 ppb. This was in good agreement with both the NIOSH analysis (22 ppb) and the LTL (20 ppb) results.

The formaldehyde adsorbs so readily to most surfaces that remote sampling using bulbs, grab bags, etc. seems very suspect (see trace c of Figure 6-6). If the samples are immediately processed on the site by being put into solution as in both the LTL and NIOSH techniques or via a trap in the TDL method they will be acceptable. However, storage and subsequent transportation for even a few hours will give misleading low results as demonstrated above. Eventually all results appear to show 10-20 ppb which is unfortunately close to ambient room air levels and would be interpreted as acceptable.

This problem of sampling means that a mobile system would be the optimum setup for TDL air sampling, especially for H_2CO . A layout for a proposed "Super Sniffer" system is given in the following section

6.4 The Mobile TDL "Super Sniffer" System

The proposed mobile TDL spectrometer is illustrated in

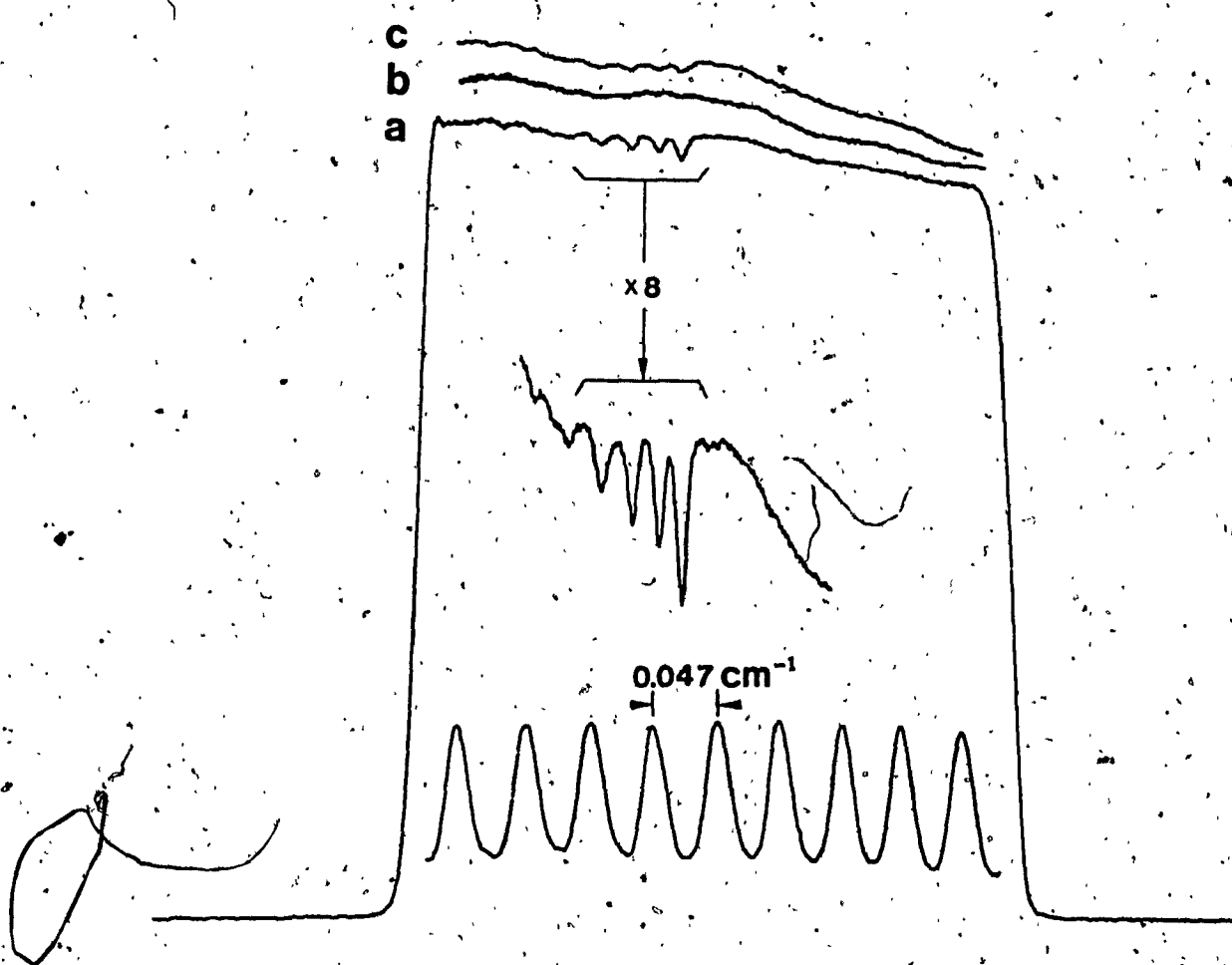


Figure 6-6: Detection of H_2CO in Laboratory air by the TDL System Using the Cold Trap and 100.17 meter Optical Path Length.

Trace a: the H_2CO absorption peaks due to Q_0 ₃ transitions. Measurements were taken only for the transition $3_{3,1} \leftarrow 3_{3,0}$ (strongest line). Trace b: the background. Trace c: the desorption spectra after 3 hrs of heating the White cell under vacuum.

Figures 6-7,8,9. This Super Sniffer is a double beam, frequency locked system and completely self contained. It is flexible enough to allow flowing air methods such as have been proposed by other workers for NO_x and SO_x problems [18,19,24] as well as for a trapping system. The frequency locking allows a simpler setup than in our laboratory system. The system is double beam so that the diode lasers can be locked to a monitoring frequency from the reference cell to prevent drifting. If one wishes to apply this system to other gases besides H_2CO this is easily done. The proposed system would even allow use as a laboratory system by the installation of a small 0.25 meter monochromator if needed for selecting new monitoring frequencies. Once the proper frequencies have been chosen it could be removed for the remote field work. Systems of this type have been demonstrated already by other groups for mobile astronomical and tropospheric monitors [15,106].

An integral alignment system containing a HeNe laser and pellicle beam splitter is also included. This facilitates quick alignment and peaking up the system (mobile units are in need of frequent alignment). The alignment system will also permit rapid switching of monitoring lasers. Four lasers can be mounted in the refrigerator cold head allowing the monitoring of up to four gases. The White cell can be either 0.5 or 1.0 meter in base length depending on how small a cart one wishes to construct. The analytical

pressures would be monitored by several capacitance manometers, covering the desired working range.

The electronic system (Figure 6-9) provides for feed-back stabilization of the diode wavelength and if one wishes to incorporate a microcomputer then it would be possible to automate the switching between diodes to monitor more than one gas automatically. The system would use HgCdTe detectors for work in the 5-16 μm range and InSb detectors in the 3-5 μm region.

In summary, the proposed mobile Super Sniffer would be a multi-purpose state-of-the-art analytical spectrometer. The system could be easily upgraded and/or modified to meet specific needs. The size of the unit would be governed mainly by the choice of White cell. e.g. using a 1 meter cell the dimensions would be $l=1.5$ m, $h=1.0$ m, and $w=0.85$ m. The system has been designed to be self contained except for plugging in to the electrical outlet where it is used. Requirements are for 110V for everything except the helium compressor which requires 220V. The design is more elaborate than that used by other groups with the intention that it can double as the laboratory system.

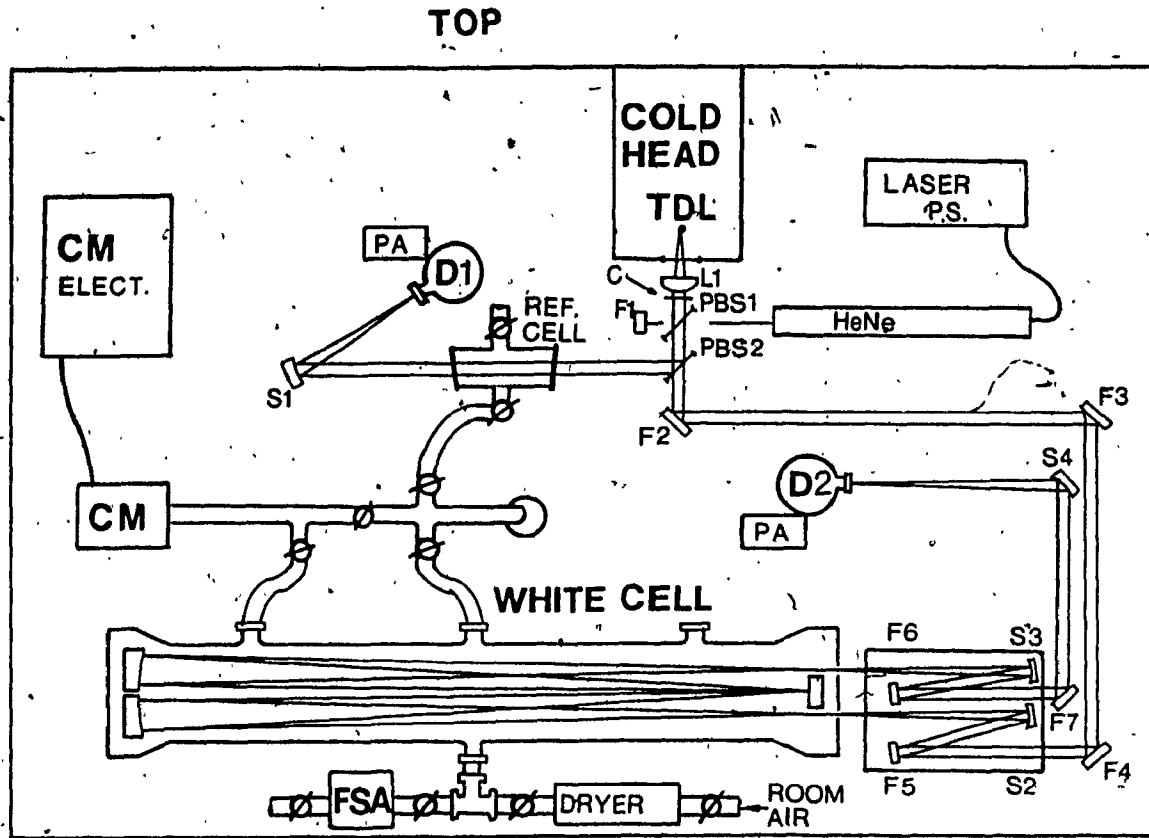
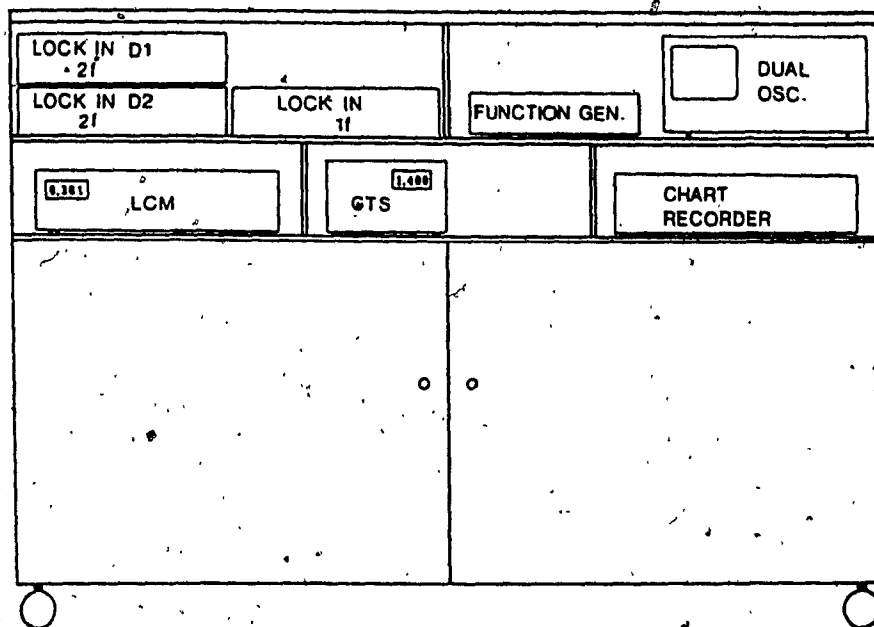


Figure 6-7: Top View of the Proposed Mobile TDL System; The "Super Sniffer".

The labels are interpreted as: detectors (D1, D2), diode lasers (TDL), capacitance manometer (CM), formaldehyde sampling apparatus (FSA), flat mirrors (F1-F7), spherical mirrors (S1-S4), pellicle beam splitter (PBS1), ZnSe beam splitter (PBS2), chopper (C), KBr lens (L1), and preamplifiers (PA). The scale is mainly determined by the base length of the White cell (0.5 m or 1.0 m).

FRONT



BACK

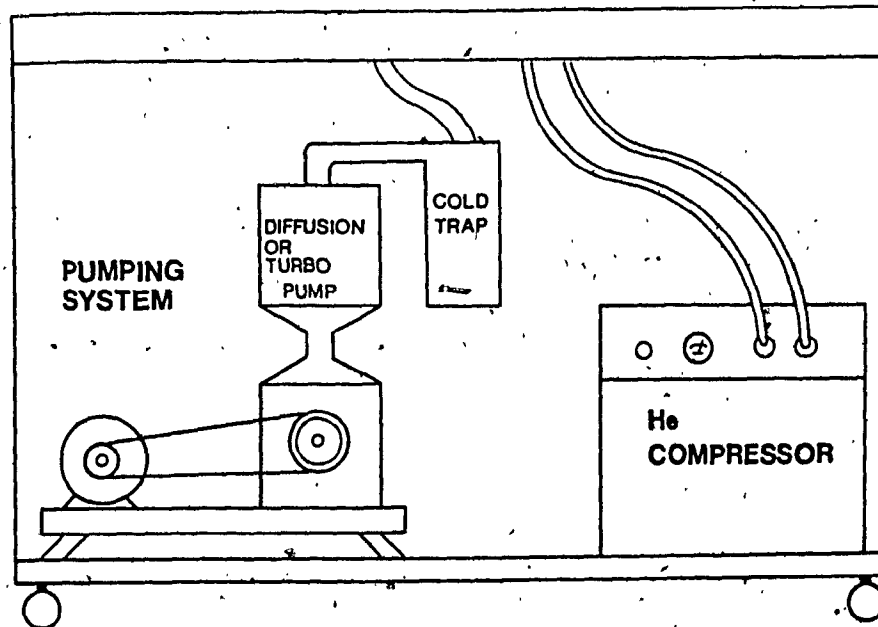


Figure 6-8: Side Views of the Mobile TDL System.

The CTS is the laser temperature control and the LCM is the laser current control.

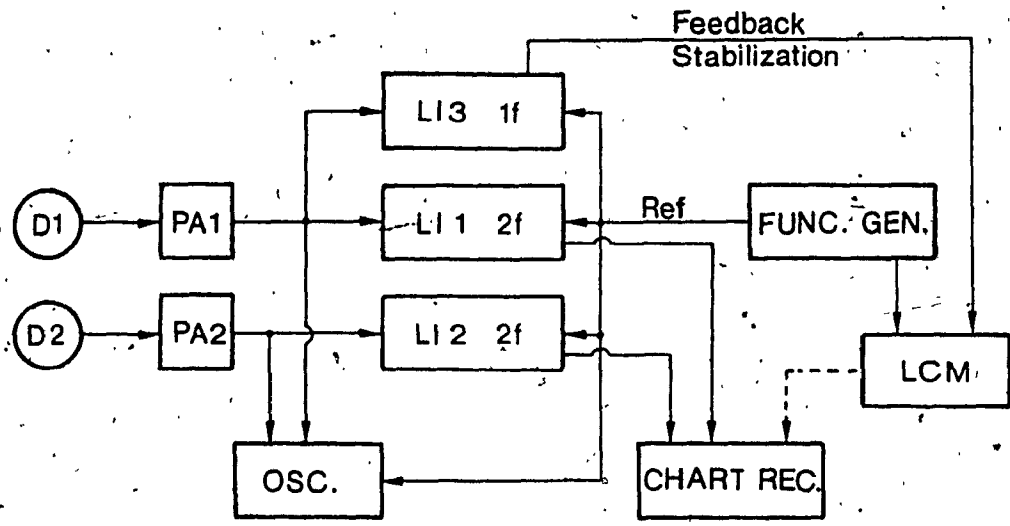


Figure 6-9: Schematic of the System Electronic Connections.

These in fact can be varied in several ways so that the system can operate with a chopper in slow scan modes or with frequency modulation at 1f or 2f. LI1-LI3 are the lock-in amplifiers. In this configuration, LI3 is used for frequency locking while LI1 and LI2 are used for 2f point monitoring of sample and reference signal.

CHAPTER 7

GENERAL CONCLUSIONS AND SUGGESTIONS FOR FUTURE RESEARCH

7.1 Conclusions7.1.1 The Molecular Constants of Formaldehyde

The simultaneous least-squares fitting of transitions in the ν_3 , ν_4 and ν_6 bands yielded excellent results ($\sigma_R = 0.00093 \text{ cm}^{-1}$). Both the sixth order (Hamiltonian) and the third order Coriolis interaction constants are reported for the first time. High correlation between some of the rotational constant lead to redundancy in the fitting process. That is to say, different sets of molecular constants yield the same results. Each set, however, may be used to predict with great accuracy all the wavenumbers for transitions up to $J'=30$ and $K_a'=8$. Means to reduce the computational redundancies are proposed in section 7.2.

In light of these redundancies as well as the fact that direct measurements of line strengths in the ν_3 band were not available, the dipole moment derivatives obtained in this work should be considered tentative. Similar consideration should be given to the reported band strengths, remembering that these depend both on the dipole moment derivatives and the eigenvectors obtained from the least-squares fittings.

7.1.2 Line Strengths and Foreign-Gas Pressure Broadening

This study reports tunable diode laser measurements of several transitions in the ν_4 and ν_6 bands of H_2CO . Line strengths and foreign-gas (air, N_2 , O_2 and H_2) broadening coefficients for these bands are reported for the first time. The Doppler-limited spectra obtained using the diode laser spectrometer facilitated straightforward data analysis and evaluation of absorption parameters. The broadening coefficients for air, N_2 , O_2 , and H_2 compare favorably with reported microwave and theoretical values.

7.1.3 Analytical

The trace analysis technique developed here is capable of detecting formaldehyde in ambient air at the low ppb levels. The mass based technique allows for analysis in relatively shorter optical path lengths. The lower limits of detection (~7 ppb) for formaldehyde obtained in this work is similar to the results obtained by other workers for N_2O [107,108], NO_2 , and SO_2 [18,19,24]. Sampling and calibration problems have been reported for these gases as well, although they are not as difficult to handle as H_2CO .

Based on existing technology the construction of a mobile TDL "Super Sniffer" system is proposed. This is a multi-faceted system easily modified to suit the particular needs. For the specific application of H_2CO detection the

sniffer may be equipped with several detachable cold traps and a sampling pump (with control for the rate of intake). This will facilitate analysis at locations with difficult access.

7.2 Suggestions for Future Research

From the results and conclusions drawn in this thesis, as well as from the work of other researchers, the scope and range of application of TDL's is obvious. The following suggestions pertain specifically to the study of the H₂CO molecule. In order to close the present stage of work on the 10 μm region of H₂CO we suggest the following additional research.

Line strengths for transitions in the ν₃ band should be measured. This would allow an accurate evaluation of the dipole moment derivative for this band. That in turn, would give a more accurate value of the ν₃ band strength and the extent of its interaction with ν₄ and ν₆. At that point a complete spectrum for the 10 μm region could be generated. This would reduce the problem encountered in the least-squares fitting by pinpointing the most suitable molecular constants for the three bands, i.e. help find the set of constants that yields a calculated spectrum closest to the observed.

Both sets of rotational constants obtained and described in this thesis yielded similar results. For high J values and $K_a > 8$ these sets of constants also differ in their prediction of transition wavenumbers. These are weak transitions and consequently did not appear in the FT-IR spectra studied in this thesis. Thus, we suggest that the spectra of several selected sections of the $10 \mu\text{m}$ region should be recorded at higher sample (H_2CO) pressure-pathlength. This will facilitate the identification of the weaker transitions and again help to isolate a final set of molecular constants.

REFERENCES

1. S. H. Msiao and J. E. Williams, "Occupational Health and Safety and Environmental Aspects of Urea Formaldehyde Resins," Report No. A10711, Vol. 6, Science Institute Service Dept., The Franklin Institute Research Laboratories, Philadelphia, PA (1978).
2. "Cancer Risks of Formaldehyde remains Controversial", Chem. Eng. News, p. 17 (Apr. 30, 1984).
3. F. Perára and C. Petito, Science 216, 1285 (1982).
4. L. E. Snyder, D. Buhl, B. Zuckerman and P. Palmer, Phys. Rev. Letts. 22, 679 (1969).
5. B. Zuckerman, P. Palmer, L. E. Snyder and D. Buhl, Astrophys. J. 157, L167 (1969).
6. A. Wootten, R. B. Loren and J. Bally, Astrophys. J. 277, 189 (1984).
7. D. R Johnson, F. J. Lovas and W. H. Kirchoff, J. Phys. Chem. Ref. Data 1, 1011 (1972).
8. T. Nakagawa, K. Yamada and K. Kuchitsu, J. Mol. Spectrosc. 63, 485 (1976).
9. A. S. Pine, J. Mol. Spectrosc. 70, 167 (1978).
10. L. R. Brown, R. H. Hunt and A. S. Pine, J. Mol. Spectrosc. 75, 406 (1979).
11. R. H. Toth, J. Mol. Spectrosc. 46, 470 (1973).
12. D. M. Sweger and R. L. Sams, J. Mol. Spectrosc. 87, 18 (1981).
13. T. Nakagawa and Y. Morino, J. Mol. Spectrosc. 38, 84 (1971).
14. M. Allegrini, J. W. C. Johns and A. R. W. McKeller, J. Mol. Spectrosc. 67, 476 (1977).
15. D. E. Jennings, Appl. Optics 19, 2695 (1980).
16. T. Nakanaga, S. Kondo and S. Saeki, J. Chem. Phys. 76, 3860 (1982).
17. C. Hisatsune and D. F. Eggers, J. Chem. Phys. 23, 487 (1955).
18. J. Reid, M. El-Sherbiny, B. K Garside and E. A. Ballik, Appl. Optics. 19, 3349 (1980).

19. J. Reid, J. Shewchun, B. K Garside and E. A. Ballik, Appl. Optics. 17, 300 (1978).
20. D. T. Cassidy and J. Reid, Appl. Optics. 21, 2527 (1982).
21. R. T. Ku, E. D. Hinkley and J. O. Sample, Appl. Optics. 14, 854 (1975).
22. J. Reid and D. Labrie, Appl. Phys. B26, 203 (1981).
23. R. S. Eng, J. F. Butler and K. J. Linden, Optical Eng. 19, 945 (1980).
24. H. I. Schiff, D. R. Hastie, G. I. Mackay, T. Iguchi and B. A. Ridley, J. Am. Chem. Soc. 105, 352A (1983).
25. G. T. Forrest, D. L. Wall and A. W. Mantz, Photonic Spectra, (Nov. 1982).
26. M. Born and J. R Oppenheimer, Z. Physik. 84, 457 (1927).
27. C. Eckart, Phys. Rev. 47, 552 (1935).
28. E. B. Wilson and J. B. Howard, J. Chem. Phys. 4, 260 (1936).
29. B. T. Darling and D. M. Dennison, Phys. Rev. 57, 128 (1940).
30. J. K. G. Watson, Mol. Phys. 15, 479 (1968).
31. G. Amat and H. H. Nielsen, J. Chem. Phys. 36, 1859 (1962).
32. L. D. Landau and E. M. Lifshitz, "Quantum Mechanics-Non Relativistic Theory", 2nd ed., section 103, Pergamon Press, (Oxford, 1965).
33. D. Kivelson and E. B. Wilson, J. Chem. Phys. 21, 1229 (1953).
34. D. Kivelson and E. B. Wilson, J. Chem. Phys. 20, 1575 (1952).
35. J. M. Dowling, J. Mol. Spectrosc. 6, 550 (1961).
36. J. K. G. Watson, J. Chem. Phys. 46, 1935 (1967).
37. J. K. G. Watson, in "Vibrational Spectra and Structure", vol. 6, ed. J. R. Durig, Elsevier Sci. Pub. Co., (N.Y., 1977).
38. E. P. Wigner, "Group Theory", Academic Press, (N.Y., 1959).
39. J. K. G. Watson, J. Chem. Phys. 48, 4517 (1968).
40. P. R. Bunker and J. M. R. Stone, J. Mol. Spectrosc. 41, 310 (1972).
41. A. R. Hoy and P. R. Bunker, J. Mol. Spectrosc. 52, 439 (1974).

42. P. R. Bunker, "Molecular Symmetry and Spectroscopy", Academic Press Inc., (N.Y., 1979).
43. V. Typke, J. Mol. Spectrosc. 63, 170 (1976).
44. K. K. Yallabandi and P. M. Parker, J. Chem. Phys. 49, 410 (1968).
45. H. H. Nielsen, Rev. Modern Phys. 23, 90 (1951).
46. H. C. Allen and P. C. Cross, "Molecular Vib-Rotors", John Wiley and Sons Inc., (N.Y., 1963).
47. S. C. Wang, Phys. Rev. 34, 243 (1929).
48. K. N. Rao, "Molecular Spectroscopy: Modern Research", Vol. 2, Academic Press, (N.Y., 1976).
49. G. W. King, "Spectroscopy and Molecular Structure", Holt, Rinehart and Winston Inc., (N.Y., 1965).
50. E. S. Ebers and H. H. Nielsen, J. Chem. Phys. 5, 822 (1937).
51. H. H. Blau and H. H. Nielsen, J. Mol. Spec. 1, 124 (1957).
52. T. Nakagawa, H. Kashiwagi, H. Kurihara and Y. Morino, J. Mol. Spectrosc. 31, 436 (1969).
53. C. Di Lauro and I. M. Mills, J. Mol. Spectrosc. 21, 386 (1966).
54. I. M. Mills, in "Molecular Spectroscopy - VIII I.U.P.A.C.", Butterworths, (London, 1965).
55. H. A. Jahn, Phys. Rev. 56, 680 (1939).
56. D. Papousek and M. R. Aliev, "Molecular Vibrational-Rotational Spectra", Elsevier Sci. Pub. Co., (N.Y., 1982).
57. M. R. Aliev and J. K. G. Watson, J. Mol. Spectrosc. 75, 150 (1979).
58. G. Herzberg, "Infrared and Raman Spectra", D. Van Nostrand Co., (N.Y., 1960).
59. C. Freed, L. C. Bradley and R. G. O'Donnell, IEEE J. Quant. Elec. QE-16, 1195 (1980).
60. E. D. Hinkley, K. W. Mill and F. A. Blum, in "Laser Spectroscopy of Atoms and Molecules", H. Walther Ed., Springer-Verlag, (Heidelberg, 1980).
61. J. U. White, J. Opt. Soc. Am. 32, 285 (1942).
62. T. H. Edwards, J. Opt. Soc. Am. 51, 98 (1961).

63. G. Guelachvili, Can. J. Phys. 60, 1334 (1982).
64. R. Cornet and G. Winnewisser, J. Mol. Spectrosc. 80, 438 (1980).
65. A. G. Maki and W. J. Lafferty, National Bureau of Standards, private communication.
66. W. S. Benedict, R. Herman, G. E. Moore and S. Silverman., Can. J. Phys. 34, 834 (1956).
67. C. L. Korb, R. H. Hunt and E. K. Plyler, J. Chem. Phys. 48, 4252 (1968).
68. V. M. Devi, P. P. Das, A. Bano and K. N. Rao, J. Mol. Spectrosc. 87, 578 (1981).
69. M. El-Sherbiny, E. A. Ballik, J. Shewchun, B. K. Garside and J. Reid, Appl. Optics 18, 1198 (1979).
70. D. E. Jennings and J. J. Hillman, Rev. Sci. Instrum. 48, 1568 (1978).
71. J. A. Mucha, Appl. Spectroscopy. 36, 141 (1982).
72. L. W. Tang, S. Nadler and S. J. Daunt, "Diode Laser study of Line Strength in $2\nu_2$ Band of Nitrous Oxide", 1985, in preparation.
73. R. A. Toth, Appl. Optics 23, 1825 (1984).
74. A. Levy, N. Lacome and G. Guelachvili, J. Mol. Spec. 103, 160 (1984).
75. M. A. H. Smith, C. P. Rinsland and B. Fridovich, in "Molecular Spectroscopy: Modern Research" Vol. 3, K. N. Rao Ed., Academic Press Inc., (N.Y., 1985).
76. W. V. Smith, J. Chem. Phys. 23, 339 (1955).
77. G. D. T. Tejwani and E. S. Yeung, J. Chem. Phys. 66, 4915 (1977).
78. R. B. Nerfe Jr., J. Mol. Spectrosc. 58, 451 (1975).
79. W. E. Blass and G. W. Halsey, "Deconvolution of Absorption Spectra", Academic Press, (N.Y., 1981).
80. J. J. Olivero and R. L. Longbothum, J. Quant. Spec. Radiat. Transf. 17, 233 (1977).
81. D. C. Reuter, NASA/Goddard Space Flight Center, private communication.
82. P. W. Atkins, "Molecular Quantum Mechanics", 2nd ed. Oxford University Press, (N.Y., 1983).

83. D. L. Albritton, A. L. Schmelzkopf and R. N. Zare, in "Molecular Spectroscopy: Modern Research", vol 2, K. N. Rao Ed., Academic Press, (N.Y., 1976).
84. W. H. Kirchhoff, J. Mol. Spectrosc. 41, 333 (1972).
85. R. M. Gees, J. Mol. Spectrosc. 33, 124 (1970).
86. S. M. Kirschner, Ph.D. dissertation, Ohio State University, 1975.
87. P. J. Walsh, Commun. Assn. Comput. Mach. 5, 511 (1962).
88. T. Oka, K. Takagi and Y. Morino, J. Mol. Spectrosc. 14, 27 (1964).
89. J. Chardon and D. Guichon, J. Phys. Paris 38, 113 (1977).
90. D. Dangois, E. Willemot and J. Bellet, J. Mol. Spectrosc. 71, 414 (1978).
91. W. Gordy, and R. L. Cook, "Microwave Spectroscopy", Interscience Publishers, (N.Y., 1970).
92. R. K. Hanson, P. A. Kuntz and C.H. Kruger, Appl. Optics. 16, 2045 (1977).
93. E. Max and S. T. Eng, Opt. and Quant. Elec. 11, 97 (1979).
94. J. M. Harris and N. J. Dovichi, Anal. Chem. 51, 695A (1980).
95. J. R. Whinnery, Acc. Chem. Res. 7, 225 (1974).
96. K. Fujiwara, W. Lei, H. Uchiki, F. Shimokoshi and T. Kobayashi, Anal. Chem. 54 2026 (1982).
97. N. Ishibashi, T. Higashi and T. Imasaka, Anal. Chem. 55, 1907 (1983).
98. C. E. Buffett and M. D. Morris, Appl. Spectrosc. 37, 455 (1983).
99. D. G. Taylor, "NIOSH Manual of Analytical Methods", Phys. & Chem. method No. 125, National Institute for Occupational Safety and Health, (Cincinnati, Ohio 1977).
100. J. A. Alfheim and C. H. Langford, Anal. Chem. 57, 861 (1985).
101. J. A. Alfheim, M. Sc. dissertation, Concordia University, 1985.
102. D. K. Sharma, F. Villamagna and C. H. Langford, Can. J. Spectrosc. 28, 181 (1983).
103. A. S. Pine, "Tunable Laser Survey of Molecular Air Pollutants", Lincoln Laboratory, MIT (Jan. 1980).

104. J. M. Flaud, C. Camy-Peyret and R. H. Toth, "Parametres des Raies de la Vapeur d'Eau des Micro Ondes à l'Infrarouge Moyen", Pergamon (Oxford, 1981).
105. B. K. Hunter, K. M. Nicholls and J. K. M. Sanders, Biochemistry 23, 508 (1984).
106. D. Glehar, D. Deming, D. E. Jennings, T. Kostiuk and M. J. Mumma, Astrophys. J. 269, 309 (1983).
107. P. S. Connell, R. A. Perry and C. J. Howard, Geophys. Res. Letts. 7, 1093 (1980).
108. G. Restelli and F. Cappellani, Appl. Optics 24, 2480 (1985).

Appendix A.

A.1 Least-Squares-Fitting: Results for Fit A

The molecular constants obtained from fit A were described in chapter 5. Consequently, the following pertains only to the comparison of observed and calculated wavenumbers obtained from this fit.

The observed and calculated wavenumbers are listed in Table A-1. The observed transitions were assigned their respective weights as follows: all transitions up to $J'=15$ and $K_a'=5$ were assigned a standard deviation of 0.0005 cm^{-1} , the standard deviation for the higher J and K_a transitions were estimated to be 0.001 cm^{-1} .

Table A-1: Observed vs. Calculated Results From Fit A.

- a. Number in bracket is the band identifier.
- b. PREC. refers to the standard deviation of the observation.
- c. RESID = Observed-Calculated.
- d. The symbol * denotes blended transitions. These lines were not included in the fit.

Continues

a

UPPER STATE			LOWER STATE			OBSERVATION PREC.	CALCULATION PREC.	CALCULATION RESID.	
J	KA	KC	J	KA	KC	(6)	11	5	
921	8	14	-22	9	14	922.6348	0.001	922.6355	-0.0007
922	8	13	-21	9	13	922.6348	0.001	922.6355	-0.0007
923	8	12	-21	9	12	925.1591	0.001	925.1590	-0.0001
924	8	11	-20	9	11	927.6804	0.001	927.6802	-0.0003
925	8	10	-19	9	10	930.1990	0.001	930.1987	-0.0004
926	8	9	-18	8	9	932.7145	0.001	932.7141	-0.0004
927	8	8	-17	8	8	935.2267	0.001	935.2263	-0.0003
928	8	7	-16	9	7	937.7353	0.001	937.7349	-0.0003
929	8	6	-15	9	6	940.2401	0.001	940.2397	-0.0004
930	8	5	-14	9	5	942.7404	0.001	942.7402	-0.0001
931	8	4	-13	8	4	945.2364	0.001	945.2366	-0.0002
932	8	3	-12	9	3	947.7279	0.001	947.7280	-0.0001
933	8	2	-11	9	2	950.2144	0.001	950.2146	-0.0002
934	8	1	-10	9	1	952.6960	0.001	952.6962	-0.0003
935	8	0	-9	10	9	952.7150	0.001	952.7159	-0.0009
936	7	9	-8	11	9	955.1721	0.001	955.1726	-0.0004
937	7	8	-7	10	9	955.1721	0.001	955.1726	-0.0004
938	7	7	-6	11	9	955.2366	0.001	955.2375	-0.0009
939	7	6	-5	11	9	957.7565	0.001	957.7569	-0.0006
940	7	5	-4	11	9	960.2732	0.001	960.2738	-0.0006
941	7	4	-3	11	9	962.7869	0.001	962.7876	-0.0007
942	7	3	-2	10	9	965.2974	0.001	965.2980	-0.0006
943	7	2	-1	10	9	967.6066	0.001	967.6086	-0.0006
944	7	1	-1	10	9	967.6066	0.001	967.6055	-0.0013
945	7	0	-1	10	9	967.8038	0.001	967.8045	-0.0006
946	6	9	-1	10	9	970.1068	0.001	970.1082	-0.0014
947	6	8	-1	10	9	970.3061	0.001	970.3071	-0.0007
948	6	7	-1	10	9	972.6122	0.001	972.6120	-0.0002
949	6	6	-1	10	9	972.6122	0.001	972.6120	-0.0001
950	6	5	-1	10	9	975.7819	0.001	975.7816	-0.0003
951	6	4	-1	10	9	975.8913	0.001	975.8914	-0.0001
952	6	3	-1	10	9	975.8913	0.001	975.8914	-0.0001
953	6	2	-1	10	9	975.9985	0.001	975.9982	-0.0003
954	6	1	-1	10	9	976.1028	0.001	976.1021	-0.0007
955	6	0	-1	10	9	976.2034	0.001	976.2028	-0.0006
956	5	9	-1	10	9	976.2034	0.001	976.2028	-0.0006
957	5	8	-1	10	9	976.3009	0.001	976.3001	-0.0008
958	5	7	-1	10	9	976.3943	0.001	976.3935	-0.0009
959	5	6	-1	10	9	976.3943	0.001	976.3935	-0.0009
960	5	5	-1	10	9	976.4835	0.001	976.4828	-0.0007
961	5	4	-1	10	9	976.4835	0.001	976.4828	-0.0007
962	5	3	-1	10	9	976.5686	0.001	976.5679	-0.0007
963	5	2	-1	10	9	976.5686	0.001	976.5679	-0.0007
964	5	1	-1	10	9	976.6490	0.001	976.6484	-0.0006
965	5	0	-1	10	9	976.6490	0.001	976.6484	-0.0006
966	4	9	-1	10	9	976.7246	0.001	976.7241	-0.0004
967	4	8	-1	10	9	976.7246	0.001	976.7241	-0.0004
968	4	7	-1	10	9	976.7953	0.001	976.7949	-0.0004
969	4	6	-1	10	9	976.8004	0.001	976.8004	-0.0006
970	4	5	-1	10	9	976.8004	0.001	976.8004	-0.0006
971	4	4	-1	10	9	976.8004	0.001	976.8004	-0.0006
972	4	3	-1	10	9	976.8004	0.001	976.8004	-0.0006
973	4	2	-1	10	9	977.7839	0.001	977.7848	-0.0009
974	4	1	-1	10	9	977.7839	0.001	977.7848	-0.0009
975	4	0	-1	10	9	977.7839	0.001	977.7848	-0.0009
976	3	9	-1	10	9	977.7839	0.001	977.7848	-0.0009
977	3	8	-1	10	9	977.7839	0.001	977.7848	-0.0009
978	3	7	-1	10	9	977.7839	0.001	977.7848	-0.0009
979	3	6	-1	10	9	977.7839	0.001	977.7848	-0.0009
980	3	5	-1	10	9	977.7839	0.001	977.7848	-0.0009
981	3	4	-1	10	9	977.7839	0.001	977.7848	-0.0009
982	3	3	-1	10	9	977.7839	0.001	977.7848	-0.0009
983	3	2	-1	10	9	977.7839	0.001	977.7848	-0.0009
984	3	1	-1	10	9	977.7839	0.001	977.7848	-0.0009
985	3	0	-1	10	9	977.7839	0.001	977.7848	-0.0009
986	2	9	-1	10	9	977.7839	0.001	977.7848	-0.0009
987	2	8	-1	10	9	977.7839	0.001	977.7848	-0.0009
988	2	7	-1	10	9	977.7839	0.001	977.7848	-0.0009
989	2	6	-1	10	9	977.7839	0.001	977.7848	-0.0009
990	2	5	-1	10	9	977.7839	0.001	977.7848	-0.0009
991	2	4	-1	10	9	977.7839	0.001	977.7848	-0.0009
992	2	3	-1	10	9	977.7839	0.001	977.7848	-0.0009
993	2	2	-1	10	9	977.7839	0.001	977.7848	-0.0009
994	2	1	-1	10	9	977.7839	0.001	977.7848	-0.0009
995	2	0	-1	10	9	977.7839	0.001	977.7848	-0.0009
996	1	9	-1	10	9	977.7839	0.001	977.7848	-0.0009
997	1	8	-1	10	9	977.7839	0.001	977.7848	-0.0009
998	1	7	-1	10	9	977.7839	0.001	977.7848	-0.0009
999	1	6	-1	10	9	977.7839	0.001	977.7848	-0.0009
999	1	5	-1	10	9	977.7839	0.001	977.7848	-0.0009
999	1	4	-1	10	9	977.7839	0.001	977.7848	-0.0009
999	1	3	-1	10	9	977.7839	0.001	977.7848	-0.0009
999	1	2	-1	10	9	977.7839	0.001	977.7848	-0.0009
999	1	1	-1	10	9	977.7839	0.001	977.7848	-0.0009
999	1	0	-1	10	9	977.7839	0.001	977.7848	-0.0009

UPPER STATE			LOWER STATE			OBSERVATION PREC.	CALCULATION	RESID.	UPPER STATE			OBSERVATION PREC.	CALCULATION	RESID.								
J	KA	KC	J	KA	KC				J	KA	KC											
(4)	11	6	-	11	7	4	1026.8214	0.001	1026.8214	0.000	0.000	(4)	19	5	-	19	5	14	1051.0840	0.001	1051.0846	-0.0005
(4)	11	6	-	11	7	4	1026.8214	0.001	1026.8214	0.000	0.000	(4)	18	6	-	18	6	15	1051.1030	0.001	1051.1023	-0.0007
(4)	10	6	-	10	7	3	1026.8937	0.001	1026.8936	0.000	0.000	(4)	22	5	-	22	6	17	1051.1173	0.001	1051.1171	-0.0002
(4)	10	6	-	10	7	4	1026.8936	0.001	1026.8936	0.000	0.000	(4)	18	6	-	18	6	12	1051.1335	0.001	1051.1371	-0.0036
(4)	9	6	-	9	7	4	1026.9608	0.001	1026.9608	0.000	0.000	(4)	19	5	-	19	6	13	1051.1658	0.001	1051.1649	-0.0009
(4)	9	6	-	9	7	4	1026.9608	0.001	1026.9608	0.000	0.000	(4)	10	6	-	19	6	13	1051.1458*	0.000	1051.1495	-0.0037
(4)	9	6	-	9	7	4	1027.0227	0.001	1027.0226	0.000	0.000	(4)	10	6	-	19	6	16	1051.1531*	0.001	1051.1546	-0.0016
(4)	9	6	-	9	7	4	1027.0227	0.001	1027.0226	0.000	0.000	(4)	18	3	-	17	6	11	1051.1531*	0.000	1051.1516	-0.0015
(4)	8	6	-	8	7	2	1027.0785	0.001	1027.0786	0.000	0.000	(4)	17	5	-	13	6	11	1051.1724	0.001	1051.1723	-0.0001
(4)	8	6	-	8	7	2	1027.0785	0.001	1027.0786	0.000	0.000	(4)	16	5	-	12	6	16	1051.1822	0.001	1051.1828	-0.0042
(4)	8	6	-	8	7	2	1027.3208	0.001	1027.3208	0.000	0.000	(4)	19	5	-	15	5	11	1051.2221	0.001	1051.2264	-0.0012
(4)	8	6	-	8	7	2	1027.3208	0.001	1027.3208	0.000	0.000	(4)	10	6	-	15	6	15	1051.2221	0.001	1051.2209	-0.0037
(4)	8	6	-	8	7	2	1027.5621	0.001	1027.5621	0.000	0.000	(4)	18	3	-	15	6	10	1051.2580	0.001	1051.2580	0.000
(4)	8	6	-	8	7	2	1028.0758	0.001	1028.0761	0.000	0.000	(4)	17	5	-	10	6	15	1051.2779	0.001	1051.2789	-0.0010
(4)	8	6	-	8	7	2	1029.8082	0.001	1029.8077	0.000	0.000	(4)	14	5	-	10	6	8	1051.3089	0.001	1051.3063	-0.0017
(4)	8	6	-	8	7	2	1029.8082	0.001	1029.8077	0.000	0.000	(4)	14	5	-	10	6	9	1051.3089	0.001	1051.3099	-0.0017
(4)	8	6	-	8	7	2	1030.3186	0.001	1030.3187	0.000	0.000	(4)	9	6	-	10	5	5	1051.3373	0.001	1051.3373	0.0002
(4)	8	6	-	8	7	2	1030.3186	0.001	1030.3186	0.000	0.000	(4)	15	5	-	13	6	8	1051.3373	0.001	1051.3367	-0.0007
(4)	8	6	-	8	7	2	1030.6945	0.001	1030.6946	0.000	0.000	(4)	15	5	-	13	6	7	1051.3373	0.001	1051.3367	-0.0007
(4)	8	6	-	8	7	2	1032.2910	0.001	1032.2910	0.000	0.000	(4)	15	5	-	13	6	8	1051.3858	0.001	1051.3851	-0.0007
(4)	8	6	-	8	7	2	1032.2911	0.001	1032.2911	0.000	0.000	(4)	15	5	-	13	6	8	1051.3999	0.001	1051.3999	0.0007
(4)	8	6	-	8	7	2	1033.5077	0.001	1033.5077	0.000	0.000	(4)	12	5	-	10	6	7	1051.3999	0.001	1051.3995	-0.0007
(4)	8	6	-	8	7	2	1033.5047	0.001	1033.5047	0.000	0.000	(4)	12	5	-	10	6	6	1051.4644	0.001	1051.4640	-0.0004
(4)	8	6	-	8	7	2	1034.7696	0.001	1034.7696	0.000	0.000	(4)	11	5	-	9	6	6	1051.5284	0.001	1051.5281	-0.0003
(4)	8	6	-	8	7	2	1035.7238	0.001	1035.7240	0.000	0.000	(4)	10	5	-	8	6	6	1051.5284	0.001	1051.5281	-0.0003
(4)	8	6	-	8	7	2	1035.9068	0.001	1035.9070	0.000	0.000	(4)	10	5	-	8	6	6	1051.5911	0.001	1051.5908	-0.0003
(4)	8	6	-	8	7	2	1036.9711	0.001	1036.9711	0.000	0.000	(4)	9	5	-	7	6	7	1051.5911	0.001	1051.5908	-0.0003
(4)	8	6	-	8	7	2	1037.2421	0.001	1037.2421	0.000	0.000	(4)	9	5	-	7	6	6	1051.6511	0.001	1051.6508	-0.0004
(4)	8	6	-	8	7	2	1037.2421	0.001	1037.2419	0.000	0.000	(4)	10	5	-	8	6	6	1051.6511	0.001	1051.6511	0.0004
(4)	8	6	-	8	7	2	1038.7696	0.001	1038.7694	0.000	0.000	(4)	11	5	-	9	6	6	1051.6511	0.001	1051.6511	0.0004
(4)	8	6	-	8	7	2	1039.9120	0.001	1039.9120	0.000	0.000	(4)	10	5	-	8	6	6	1051.6511	0.001	1051.6508	-0.0004
(4)	8	6	-	8	7	2	1041.0953	0.001	1041.0956	0.000	0.000	(4)	10	5	-	8	6	6	1051.6511	0.001	1051.6508	-0.0004
(4)	8	6	-	8	7	2	1041.0953	0.001	1041.0956	0.000	0.000	(4)	9	5	-	7	6	6	1051.6511	0.001	1051.6508	-0.0004
(4)	8	6	-	8	7	2	1042.8039	0.001	1042.8038	0.000	0.000	(4)	11	5	-	9	6	6	1051.7585	0.001	1051.7580	-0.0005
(4)	8	6	-	8	7	2	1043.6143	0.001	1043.6145	0.000	0.000	(4)	10	5	-	8	6	6	1051.7585	0.001	1051.7580	-0.0005
(4)	8	6	-	8	7	2	1044.6589	0.001	1044.6588	0.000	0.000	(4)	11	5	-	9	6	6	1051.7588	0.001	1051.7587	-0.0005
(4)	8	6	-	8	7	2	1044.9118	0.001	1044.9118	0.000	0.000	(4)	10	5	-	8	6	6	1051.7588	0.001	1051.7587	-0.0005
(4)	8	6	-	8	7	2	1045.0218	0.001	1045.0215	0.000	0.000	(4)	11	5	-	9	6	6	1051.7588	0.001	1051.7587	-0.0005
(4)	8	6	-	8	7	2	1045.6344	0.001	1045.6347	0.000	0.000	(4)	11	5	-	9	6	6	1051.7588	0.001	1051.7587	-0.0005
(4)	8	6	-	8	7	2	1046.1972	0.001	1046.1973	0.000	0.000	(4)	12	5	-	10	6	6	1051.7588	0.001	1051.7587	-0.0005
(4)	8	6	-	8	7	2	1046.2216	0.001	1046.2217	0.000	0.000	(4)	12	5	-	10	6	6	1051.7588	0.001	1051.7587	-0.0005
(4)	8	6	-	8	7	2	1047.0629	0.001	1047.0626	0.000	0.000	(4)	12	5	-	10	6	6	1051.7588	0.001	1051.7587	-0.0005
(4)	8	6	-	8	7	2	1048.4160	0.001	1048.4164	0.000	0.000	(4)	12	5	-	10	6	6	1051.7588	0.001	1051.7587	-0.0005
(4)	8	6	-	8	7	2	1048.7601	0.001	1048.7600	0.000	0.000	(4)	12	5	-	10	6	6	1051.7588	0.001	1051.7587	-0.0005
(4)	8	6	-	8	7	2	1048.7721	0.001	1048.7723	0.000	0.000	(4)	12	5	-	10	6	6	1051.7588	0.001	1051.7587	-0.0005
(4)	8	6	-	8	7	2	1048.7721*	0.000	1048.7721	0.000	0.000	(4)	12	5	-	10	6	6	1051.7588	0.001	1051.7587	-0.0005
(4)	8	6	-	8	7	2	1048.9467	0.001	1048.9413	0.000	0.000	(4)	12	5	-	10	6	6	1051.7588	0.001	1051.7587	-0.0005
(4)	8	6	-	8	7	2	1049.5803	0.001	1049.5806	0.000	0.000	(4)	12	5	-	10	6	6	1051.7588	0.001	1051.7587	-0.0005
(4)	9	6	-	9	7	3	1050.7580	0.001	1050.7580	0.000	0.000	(4)	12	5	-	10	6	6	1051.7588	0.001	1051.7587	-0.0005
(4)	9	6	-	9	7	3	1051.7580	0.001	1051.7580	0.000	0.000	(4)	12	5	-	10	6	6	1051.7588	0.001	1051.7587	-0.0005
(4)	9	6	-	9	7	3	1051.7580	0.001	1051.7580	0.000	0.000	(4)	12	5	-	10	6	6	1051.7588	0.001	1051.7587	-0.0005
(4)	9	6	-	9	7	3	1051.7580	0.001	1051.7580	0.000	0.000	(4)	12	5	-	10	6	6	1051.7588	0.001	1051.7587	-0.0005
(4)	9	6	-	9	7	3	1051.7580	0.001	1051.7580	0.000	0.000	(4)	12	5	-	10	6	6	1051.7588	0.001	1051.7587	-0.0005
(4)	9	6	-	9	7	3	1051.7580	0.001	1051.7580	0.000	0.000	(4)	12	5	-	10	6	6	1051.7588	0.001	1051.7587	-0.0005
(4)	9	6	-	9	7	3	1051.7580	0.001	1051.7580	0.000	0.000	(4)	12	5	-	10	6	6	1051.7588	0.001	1051.7587	-0.0005

UPPER STATE			LOWER STATE			OBSERVATION PREC.	CALCULATION RESID.	UPPER STATE			LOWER STATE			OBSERVATION PREC.	CALCULATION RESID.
J	KA	KC	J	KA	KC			J	KA	KC	J	KA	KC		
(4) 16	3 14	- 17	4 13	1056.5214	0.001	1056.5216	-0.0002	(4) 19	6 14	- 18	7 12	1072.2186	0.001	1072.2181	0.0005
(4) 16	3 13	- 17	4 13	1057.0087	0.001	1057.0089	-0.0001	(4) 19	6 13	- 18	7 11	1072.2186	0.001	1072.2178	0.0008
(4) 25	0 25	- 26	1 25	1057.1706	0.001	1057.1713	-0.0007	(4) 26	6 23	- 26	5 21	1072.2947	0.001	1072.2949	-0.0002
(4) 26	2 24	- 27	3 24	1057.4903	0.001	1057.4910	-0.0007	(4) 25	6 22	- 25	5 20	1072.5074	0.001	1072.5072	-0.0003
(4) 13	6 64	- 12	7 65	1058.1964	0.001	1058.1960	-0.0004	(4) 24	6 21	- 24	5 19	1072.9020	0.001	1072.9019	-0.0001
(4) 6	4 5	- 7	5 3	1058.8431	0.001	1058.8429	-0.0002	(4) 20	6 20	- 20	5 16	1072.9697	0.001	1072.9699	-0.0002
(4) 15	5 13	- 16	4 13	1059.1593	0.001	1059.1596	-0.0003	(4) 23	6 20	- 23	5 18	1073.0390	0.001	1073.0397	-0.0004
(4) 15	5 12	- 16	4 12	1059.5017	0.001	1059.5019	=0.0002	(4) 23	6 20	- 23	5 18	1073.1666	0.001	1073.1670	-0.0004
(4) 15	5 21	- 22	5 20	1060.0122	0.001	1060.0119	-0.0002	(4) 17	6 17	- 16	5 15	1073.3350	0.001	1073.3391	-0.0005
(4) 25	5 23	- 26	5 23	1060.4739	0.001	1060.4752	-0.0013	(4) 19	6 19	- 15	5 15	1073.3792	0.001	1073.3786	-0.0005
(4) 14	6 13	- 13	7 67	1060.5376	0.001	1060.5373	-0.0003	(4) 22	6 19	- 22	5 17	1073.4117	0.001	1073.4121	-0.0003
(4) 15	6 13	- 15	7 6	1060.5376	0.001	1060.5373	-0.0003	(4) 18	6 18	- 21	5 16	1073.6601	0.001	1073.6605	-0.0004
(4) 15	6 12	- 16	5 12	1061.3269	0.001	1061.3269	-0.0002	(4) 20	6 17	- 20	5 15	1073.7404	0.001	1073.7406	-0.0001
(4) 15	5 21	- 22	5 20	1061.3290	0.001	1061.3289	-0.0001	(4) 19	6 19	- 15	5 14	1073.8551	0.001	1073.8551	-0.0001
(4) 25	5 23	- 26	5 23	1061.7726	0.001	1061.7728	-0.0002	(4) 17	6 13	- 17	5 13	1074.0599	0.001	1074.0580	-0.0019
(4) 14	6 11	- 15	4 11	1062.0557	0.001	1062.0558	-0.0001	(4) 18	6 18	- 18	5 15	1074.2509	0.001	1074.2511	-0.0002
(4) 24	5 24	- 24	6 12	1062.1964	0.001	1062.1969	-0.0004	(4) 16	6 16	- 16	5 14	1074.4959	0.001	1074.4960	-0.0001
(4) 15	6 10	- 15	7 7	1062.8762	0.001	1062.8762	-0.0001	(4) 20	6 15	- 15	5 12	1074.5354	0.001	1074.5354	-0.0002
(4) 15	6 9	- 14	6 9	1063.2757	0.001	1063.2757	-0.0005	(4) 19	6 15	- 19	7 12	1074.5547	0.001	1074.5549	-0.0005
(4) 24	5 24	- 25	5 22	1063.2757	0.001	1063.2752	-0.0005	(4) 17	6 14	- 19	7 12	1074.5547	0.001	1074.5543	-0.0004
(4) 20	5 24	- 25	5 22	1063.4891	0.001	1063.4885	-0.0006	(4) 19	6 14	- 17	5 13	1074.5667	0.000	1074.5669	-0.0002
(4) 14	6 11	- 15	4 12	1064.0557	0.001	1064.0558	-0.0001	(4) 18	6 18	- 18	5 15	1074.5850	0.000	1074.5853	-0.0003
(4) 24	5 24	- 24	6 12	1064.1964	0.001	1064.1969	-0.0004	(4) 16	6 16	- 16	5 11	1074.5982	0.001	1074.5982	-0.0001
(4) 15	6 10	- 14	6 10	1064.8762	0.001	1064.8762	-0.0001	(4) 20	6 15	- 15	5 10	1074.6119	0.001	1074.6119	-0.0001
(4) 15	6 9	- 14	6 9	1064.8762	0.001	1064.8759	-0.0003	(4) 19	6 15	- 15	5 10	1074.7806	0.001	1074.7806	-0.0005
(4) 24	5 24	- 25	5 22	1064.8762	0.001	1064.8759	-0.0005	(4) 17	6 14	- 19	7 12	1074.8211	0.001	1074.8211	-0.0008
(4) 20	5 24	- 25	5 22	1065.2125	0.001	1065.2125	-0.0003	(4) 19	6 14	- 14	5 10	1074.9413	0.001	1074.9413	-0.0002
(4) 14	6 11	- 15	4 12	1065.8033	0.001	1063.8034	-0.0001	(4) 19	6 13	- 13	5 9	1075.0185	0.001	1075.0184	-0.0001
(4) 24	5 24	- 25	5 22	1065.8033	0.001	1063.8034	-0.0001	(4) 19	6 13	- 13	5 9	1075.0932	0.001	1075.0934	-0.0001
(4) 15	6 10	- 14	6 10	1066.3663	0.001	1066.3663	-0.0002	(4) 19	6 12	- 12	5 8	1075.1917	0.001	1075.1917	-0.0008
(4) 15	6 9	- 14	6 9	1066.5175	0.000	1066.5175	-0.0003	(4) 19	6 12	- 12	5 7	1075.2253	0.001	1075.2261	-0.0008
(4) 24	5 24	- 25	5 22	1066.5175	0.000	1066.5175	-0.0003	(4) 19	6 12	- 12	5 7	1075.2359	0.001	1075.2359	-0.0008
(4) 20	5 24	- 25	5 22	1066.5175	0.000	1066.5175	-0.0003	(4) 19	6 11	- 11	5 7	1075.3435	0.001	1075.3433	-0.0001
(4) 14	6 11	- 15	4 11	1066.8662	0.001	1066.8662	-0.0008	(4) 19	6 13	- 13	5 9	1075.3677	0.001	1075.3677	-0.0001
(4) 24	5 24	- 25	5 22	1066.8662	0.001	1066.8662	-0.0005	(4) 19	6 13	- 13	5 9	1075.4755	0.001	1075.4755	-0.0001
(4) 15	6 10	- 14	6 10	1066.9375	0.000	1066.9375	-0.0003	(4) 19	6 12	- 12	5 8	1075.4875	0.001	1075.4877	-0.0002
(4) 15	6 9	- 14	6 9	1067.0366	0.000	1067.0366	-0.0001	(4) 19	6 12	- 12	5 7	1075.5930	0.001	1075.5930	-0.0016
(4) 24	5 24	- 25	5 22	1067.0366	0.000	1067.0366	-0.0001	(4) 19	6 11	- 11	5 6	1075.6889	0.001	1075.6874	-0.0015
(4) 20	5 24	- 25	5 22	1067.5175	0.001	1067.5175	-0.0002	(4) 19	6 11	- 11	5 6	1075.6889	0.001	1075.6888	-0.0008
(4) 14	6 11	- 15	4 11	1068.4056	0.001	1068.4056	-0.0010	(4) 19	6 10	- 10	5 5	1075.7709	0.001	1075.7705	-0.0008
(4) 24	5 24	- 25	5 22	1068.4056	0.001	1068.4056	-0.0007	(4) 19	6 10	- 10	5 5	1075.7713	0.001	1075.7713	-0.0004
(4) 15	6 10	- 14	6 10	1069.4961	0.000	1069.4961	-0.0003	(4) 19	6 9	- 9	5 4	1075.7985	0.001	1075.7985	-0.0005
(4) 15	6 9	- 14	6 9	1069.5534	0.000	1069.5534	-0.0003	(4) 19	6 9	- 9	5 4	1075.8402	0.001	1075.8402	-0.0002
(4) 24	5 24	- 25	5 22	1069.5534	0.000	1069.5534	-0.0003	(4) 19	6 8	- 8	4 7	1075.8402	0.001	1075.8402	-0.0002
(4) 20	5 24	- 25	5 22	1069.5534	0.000	1069.5534	-0.0003	(4) 19	6 8	- 8	4 7	1075.8402	0.001	1075.8402	-0.0002
(4) 14	6 11	- 15	4 11	1069.8828	0.001	1069.8828	-0.0001	(4) 19	6 7	- 7	4 6	1075.8402	0.001	1075.8402	-0.0002
(4) 24	5 24	- 25	5 22	1069.8828	0.001	1069.8828	-0.0001	(4) 19	6 7	- 7	4 6	1075.8402	0.001	1075.8402	-0.0002
(4) 15	6 10	- 14	6 10	1070.1459	0.001	1070.1459	-0.0001	(4) 19	6 6	- 6	4 5	1075.8402	0.001	1075.8402	-0.0002
(4) 15	6 9	- 14	6 9	1070.7742	0.001	1070.7742	-0.0009	(4) 19	6 5	- 5	4 4	1075.8402	0.001	1075.8402	-0.0005
(4) 24	5 24	- 25	5 22	1071.3859	0.001	1071.3859	-0.0011	(4) 19	6 4	- 4	3 3	1075.8402	0.001	1075.8402	-0.0004
(4) 20	5 24	- 25	5 22	1071.3859	0.001	1071.3859	-0.0011	(4) 19	6 4	- 4	3 3	1075.8402	0.001	1075.8402	-0.0004
(4) 14	6 11	- 15	4 11	1071.9636	0.001	1071.9636	-0.0005	(4) 19	6 3	- 3	2 2	1075.8402	0.001	1075.8402	-0.0003
(4) 24	5 24	- 25	5 22	1071.9636	0.001	1071.9636	-0.0005	(4) 19	6 3	- 3	2 2	1075.8402	0.001	1075.8402	-0.0003
(4) 15	6 10	- 14	6 10	1072.0370	0.000	1072.0370	-0.0000	(4) 19	6 2	- 2	1 1	1075.8402	0.001	1075.8402	-0.0002
(4) 15	6 9	- 14	6 9	1072.0370	0.000	1072.0370	-0.0000	(4) 19	6 2	- 2	1 1	1075.8402	0.001	1075.8402	-0.0002
(4) 24	5 24	- 25	5 22	1072.0370	0.000	1072.0370	-0.0000	(4) 19	6 1	- 1	0 0	1075.8402	0.001	1075.8402	-0.0002

PREC.	CALCULATION	RESID.	OBSERVATION												
			UPPER STATE			LOWER STATE			STATE OBSERVATION						
K	J	KA	KC	J	KA	KC	J	KA	KC	J	KA	KC	J	KA	
10	15	-17	3	15	1076.4446	0.001	1076.4446	0.002	1089.7630	0.001	1089.7629	0.001	1089.7629	0.001	1089.7629
16	20	-21	1	21	1076.9551	0.001	1076.9551	0.002	1090.0776	0.000	1090.0777	0.000	1090.0777	0.000	1090.0777
21	28	-3	6	5	1077.0856	0.001	1077.0856	0.002	1090.8706	0.000	1090.8707	0.000	1090.8707	0.000	1090.8707
26	42	-8	5	5	1077.0961	0.000	1077.0961	0.001	1091.5491	0.000	1091.5491	0.000	1091.5491	0.000	1091.5491
31	48	-12	4	5	1077.3561	0.001	1077.3561	0.002	1092.5495	0.000	1092.5495	0.000	1092.5495	0.000	1092.5495
36	52	-23	2	21	1077.8271	0.001	1077.8271	0.002	1092.7022	0.001	1092.7025	0.000	1092.7025	0.000	1092.7025
41	57	-27	5	23	1078.0369	0.001	1078.0369	0.002	1092.7668	0.001	1092.7668	0.000	1092.7668	0.000	1092.7668
46	62	-10	6	5	1078.1607	0.001	1078.1607	0.002	1092.7888	0.001	1092.7888	0.000	1092.7888	0.000	1092.7888
51	67	-15	5	5	1078.1616	0.001	1078.1616	0.002	1093.5474	0.000	1093.5474	0.000	1093.5474	0.000	1093.5474
56	72	-20	4	5	1078.9790	0.001	1078.9790	0.002	1093.5748	0.000	1093.5748	0.000	1093.5748	0.000	1093.5748
61	77	-25	3	5	1079.2371	0.001	1079.2371	0.002	1094.5988	0.000	1094.5988	0.000	1094.5988	0.000	1094.5988
66	82	-30	2	5	1079.4532	0.001	1079.4532	0.002	1095.0867	0.001	1095.0867	0.000	1095.0867	0.000	1095.0867
71	87	-35	1	5	1079.4694	0.001	1079.4694	0.002	1095.1151	0.001	1095.1151	0.000	1095.1151	0.000	1095.1151
76	92	-40	0	5	1079.5924	0.000	1079.5924	0.001	1095.6928	0.001	1095.6928	0.000	1095.6928	0.000	1095.6928
81	97	-45	-1	5	1079.5941	0.000	1079.5941	0.001	1095.6920	0.000	1095.6920	0.000	1095.6920	0.000	1095.6920
86	102	-50	-2	5	1079.5941	0.000	1079.5941	0.001	1096.2012	0.000	1096.2012	0.000	1096.2012	0.000	1096.2012
91	107	-55	-3	5	1079.5941	0.000	1079.5941	0.001	1096.2338	0.000	1096.2338	0.000	1096.2338	0.000	1096.2338
96	112	-60	-4	5	1079.5941	0.000	1079.5941	0.001	1096.2723	0.000	1096.2723	0.000	1096.2723	0.000	1096.2723
101	117	-65	-5	5	1079.5941	0.000	1079.5941	0.001	1096.3552	0.000	1096.3552	0.000	1096.3552	0.000	1096.3552
106	122	-70	-6	5	1079.5941	0.000	1079.5941	0.001	1096.6550	0.000	1096.6550	0.000	1096.6550	0.000	1096.6550
111	127	-75	-7	5	1079.5941	0.000	1079.5941	0.001	1096.7474	0.000	1096.7474	0.000	1096.7474	0.000	1096.7474
116	132	-80	-8	5	1079.5941	0.000	1079.5941	0.001	1096.9225	0.000	1096.9225	0.000	1096.9225	0.000	1096.9225
121	137	-85	-9	5	1079.5941	0.000	1079.5941	0.001	1097.0280	0.000	1097.0280	0.000	1097.0280	0.000	1097.0280
126	142	-90	-10	5	1079.5941	0.000	1079.5941	0.001	1097.3555	0.000	1097.3555	0.000	1097.3555	0.000	1097.3555
131	147	-95	-11	5	1079.5941	0.000	1079.5941	0.001	1097.4450	0.000	1097.4450	0.000	1097.4450	0.000	1097.4450
136	152	-100	-12	5	1079.5941	0.000	1079.5941	0.001	1097.6276	0.000	1097.6276	0.000	1097.6276	0.000	1097.6276
141	157	-105	-13	5	1079.5941	0.000	1079.5941	0.001	1097.8066	0.000	1097.8066	0.000	1097.8066	0.000	1097.8066
146	162	-110	-14	5	1079.5941	0.000	1079.5941	0.001	1098.0743	0.000	1098.0743	0.000	1098.0743	0.000	1098.0743
151	167	-115	-15	5	1079.5941	0.000	1079.5941	0.001	1098.2443	0.000	1098.2443	0.000	1098.2443	0.000	1098.2443
156	172	-120	-16	5	1079.5941	0.000	1079.5941	0.001	1098.4953	0.000	1098.4953	0.000	1098.4953	0.000	1098.4953
161	177	-125	-17	5	1079.5941	0.000	1079.5941	0.001	1098.6058	0.000	1098.6058	0.000	1098.6058	0.000	1098.6058
166	182	-130	-18	5	1079.5941	0.000	1079.5941	0.001	1098.8382	0.000	1098.8382	0.000	1098.8382	0.000	1098.8382
171	187	-135	-19	5	1079.5941	0.000	1079.5941	0.001	1099.3864	0.000	1099.3864	0.000	1099.3864	0.000	1099.3864
176	192	-140	-20	5	1079.5941	0.000	1079.5941	0.001	1099.6457	0.000	1099.6457	0.000	1099.6457	0.000	1099.6457
181	197	-145	-21	5	1079.5941	0.000	1079.5941	0.001	1099.8457	0.000	1099.8457	0.000	1099.8457	0.000	1099.8457
186	202	-150	-22	5	1079.5941	0.000	1079.5941	0.001	1099.8867	0.000	1099.8867	0.000	1099.8867	0.000	1099.8867
191	207	-155	-23	5	1079.5941	0.000	1079.5941	0.001	1099.9275	0.000	1099.9275	0.000	1099.9275	0.000	1099.9275
196	212	-160	-24	5	1079.5941	0.000	1079.5941	0.001	1099.9673	0.000	1099.9673	0.000	1099.9673	0.000	1099.9673
201	217	-165	-25	5	1079.5941	0.000	1079.5941	0.001	1099.9973	0.000	1099.9973	0.000	1099.9973	0.000	1099.9973
206	222	-170	-26	5	1079.5941	0.000	1079.5941	0.001	1100.0273	0.000	1100.0273	0.000	1100.0273	0.000	1100.0273
211	227	-175	-27	5	1079.5941	0.000	1079.5941	0.001	1100.0573	0.000	1100.0573	0.000	1100.0573	0.000	1100.0573
216	232	-180	-28	5	1079.5941	0.000	1079.5941	0.001	1100.0873	0.000	1100.0873	0.000	1100.0873	0.000	1100.0873
221	237	-185	-29	5	1079.5941	0.000	1079.5941	0.001	1100.1173	0.000	1100.1173	0.000	1100.1173	0.000	1100.1173
226	242	-190	-30	5	1079.5941	0.000	1079.5941	0.001	1100.1473	0.000	1100.1473	0.000	1100.1473	0.000	1100.1473
231	247	-195	-31	5	1079.5941	0.000	1079.5941	0.001	1100.1773	0.000	1100.1773	0.000	1100.1773	0.000	1100.1773
236	252	-200	-32	5	1079.5941	0.000	1079.5941	0.001	1100.2073	0.000	1100.2073	0.000	1100.2073	0.000	1100.2073
241	257	-205	-33	5	1079.5941	0.000	1079.5941	0.001	1100.2373	0.000	1100.2373	0.000	1100.2373	0.000	1100.2373
246	262	-210	-34	5	1079.5941	0.000	1079.5941	0.001	1100.2673	0.000	1100.2673	0.000	1100.2673	0.000	1100.2673
251	267	-215	-35	5	1079.5941	0.000	1079.5941	0.001	1100.2973	0.000	1100.2973	0.000	1100.2973	0.000	1100.2973
256	272	-220	-36	5	1079.5941	0.000	1079.5941	0.001	1100.3273	0.000	1100.3273	0.000	1100.3273	0.000	1100.3273
261	277	-225	-37	5	1079.5941	0.000	1079.5941	0.001	1100.3573	0.000	1100.3573	0.000	1100.3573	0.000	1100.3573
266	282	-230	-38	5	1079.5941	0.000	1079.5941	0.001	1100.3873	0.000	1100.3873	0.000	1100.3873	0.000	1100.3873
271	287	-235	-39	5	1079.5941	0.000	1079.5941	0.001	1100.4173	0.000	1100.4173	0.000	1100.4173	0.000	1100.4173
276	292	-240	-40	5	1079.5941	0.000	1079.5941	0.001	1100.4473	0.000	1100.4473	0.000	1100.4473	0.000	1100.4473
281	297	-245	-41	5	1079.5941	0.000	1079.5941	0.001	1100.4773	0.000	1100.4773	0.000	1100.4773	0.000	1100.4773
286	302	-250	-42	5	1079.5941	0.000	1079.5941	0.001	1100.5073	0.000	1100.5073	0.000	1100.5073	0.000	1100.5073
291	307	-255	-43	5	1079.5941	0.000	1079.5941	0.001	1100.5373	0.000	1100.5373	0.000	1100.5373	0.000	1100.5373
296	312	-260	-44	5	1079.5941	0.000	1079.5941	0.001	1100.5673	0.000	1100.5673	0.000	1100.5673	0.000	1100.5673
301	317	-265	-45	5	1079.5941	0.000	1079.5941	0.001	1100.5973	0.000	1100.5973	0.000	1100.5973	0.000	1100.5973
306	322	-270	-46	5	1079.5941	0.000	1079.5941	0.001	1100.6273	0.000	1100.6273	0.000	1100.6273	0.000	1100.6273
311	327	-275	-47	5	1079.5941	0.000	1079.5941	0.001	1100.6573	0.000	1100.6573	0.000	1100.6573	0.000	1100.6573
316	332	-280	-48	5	1079.5941	0.000	1079.5941	0.001	1100.6873	0.000	1100.6873	0.000	1100.6873	0.000	1100.6873
321	337	-285	-49	5	1079.5941	0.000	1079.5941	0.001	1100.7173	0.000	1100.7173	0.000	1100.7173	0.000	1100.7173
326	342	-290	-50	5	1079.5941	0.000	1079.5941	0.001	1100.7473	0.000	1100.7473	0.000	1100.7473	0.000	1100.7473
331	347	-295	-51	5	1079.5941	0.000	1079.5941	0.001	1100.7773	0.000	1100.7773	0.000	1100.7773	0.000	1100.7773
336	352	-300	-52	5	1079.5941	0.000	1079.5941	0.001	1100.8073	0.000	1100.8073	0.000	1100.8073	0.000	1100.8073
341	357	-305	-53	5	1079.5941	0.000	1079.5941	0.001	1100.8373	0.000	1100.				

UPPER STATE LOWER STATE OBSERVATION PREC.			CALCULATION RESID.		
J	KA	KC	J	KA	KC
1098.9644	0.000	1098.9644	-0.0002	1113.4018	-0.0002
1099.0322	0.000	1099.0299	-0.0001	1113.4860	-0.0001
1099.0322	0.000	1099.0343	-0.0008	1113.6717	-0.0008
1099.0963	0.000	1099.0955	-0.0008	1113.6726	-0.0008
1099.0972	0.000	1099.0972	-0.0009	1113.6726	-0.0009
1099.1518	0.000	1099.1523	-0.0005	1113.9424	-0.0005
1099.1518	0.000	1099.1528	-0.0005	1113.9424	-0.0005
1099.1988	0.000	1099.1989	-0.0001	1114.0030	-0.0004
1099.1988	0.000	1099.1989	-0.0001	1114.0280	-0.0004
1099.2979	0.000	1099.2980	-0.0002	1114.4984	-0.0003
1099.7607	0.000	1099.7606	-0.0001	1115.2787	-0.0002
1099.7350	0.001	1099.7229	-0.0001	1115.3683	-0.0002
1099.9226	0.001	1099.9225	-0.0002	1115.4355	-0.0003
1099.9720	0.001	1099.9718	-0.0002	1116.0360	-0.0017
1100.8943	0.001	1100.8945	-0.0001	1116.0405	-0.0027
1101.4265	0.000	1101.4265	-0.0000	1116.2622	-0.0001
1101.7055	0.000	1101.7056	-0.0002	1116.3986	-0.0000
1102.0592	0.001	1102.0587	-0.0005	1116.5665	-0.0002
1102.0828	0.001	1102.0836	-0.0002	1117.2576	-0.0003
1103.0307	0.001	1103.0306	-0.0001	1117.4815	-0.0002
1103.4143	0.000	1103.4142	-0.0001	1117.8185	-0.0002
1103.9746	0.000	1103.9746	-0.0002	1117.9938	-0.0003
1104.1283	0.000	1104.1285	-0.0002	1118.0246	-0.0002
1104.3580	0.001	1104.3576	-0.0004	1118.0853	-0.0002
1104.3695	0.001	1104.3663	-0.0032	1118.3921	-0.0003
1104.3818	0.001	1104.3819	-0.0001	1118.4019	-0.0007
1105.3940	0.001	1105.3949	-0.0000	1118.5999	-0.0001
1105.9346	0.000	1105.9346	-0.0000	1118.6668	-0.0003
1106.4959	0.000	1106.4960	-0.0001	1119.2016	-0.0003
1106.5737	0.000	1106.5737	-0.0000	1119.5537	-0.0001
1106.5955	0.001	1106.5955	-0.0000	1119.6432	-0.0001
1106.6706	0.001	1106.6705	-0.0000	1119.6433	-0.0000
1106.8183	0.001	1106.8157	-0.0026	1120.0068	-0.0001
1106.8553	0.000	1106.8553	-0.0001	1120.2367	-0.0001
1106.9559	0.000	1106.9560	-0.0001	1120.2989	-0.0002
1106.9737	0.000	1106.9737	-0.0001	1120.5357	-0.0003
1106.9955	0.000	1106.9955	-0.0001	1120.7243	-0.0002
1107.9547	0.000	1108.9502	-0.0001	1120.7394	-0.0000
1108.9547	0.000	1108.9502	-0.0005	1121.0787	-0.0000
1108.9547	0.000	1108.9551	-0.0004	1121.1690	-0.0000
1109.0286	0.000	1109.0286	-0.0002	1122.2218	-0.0003
1109.0286	0.000	1109.0286	-0.0003	1122.3272	-0.0001
1109.7722	0.000	1109.7722	-0.0000	1123.5515	-0.0018
1110.1544	0.000	1110.1546	-0.0001	1124.6524	-0.0016
1110.9045	0.001	1110.9032	-0.0012	1125.2654	-0.0003
1111.0590	0.001	1111.0591	-0.0012	1125.5191	-0.0001
1111.2215	0.001	1111.2215	-0.0001	1125.5191	-0.0011
1111.3272	0.000	1111.3272	-0.0003	1125.6444	-0.0000
1111.6755	0.000	1111.6755	-0.0000	1125.7755	-0.0016
1112.4864	0.000	1112.4867	-0.0003	1125.8755	-0.0016
1112.5769	0.001	1112.5763	-0.0006	1126.1802	-0.0003
1113.2194	0.001	1113.2196	-0.0002	1126.1949	-0.0003

UPPER STATE	LOWER STATE	OBSERVATION	PREC.	CALCULATION	RESID.	UPPER STATE	LOWER STATE	OBSERVATION	PREC.	CALCULATION	RESID.
J KA KC	J KA KC					J KA KC	J KA KC				
1140 6523	0.000	1140 6524	-0.0001	1140 6525	0.0001	1148 5085	0.0002	1148 5085	0.0001	1148 5085	0.0001
1140 7294	0.001	1140 7289	-0.0005	1140 7295	0.0000	1148 5529	-0.0005	1148 5529	-0.0001	1148 5529	-0.0001
1140 8618	0.000	1140 8616	0.0002	1140 8618	0.0000	1148 9498	0.0000	1148 9498	0.0000	1148 9498	0.0000
1141 1179	0.000	1141 1177	0.0002	1141 1179	0.0001	1149 2168	0.001	1149 2167	0.0002	1149 2167	0.0007
1141 2076	0.001	1141 2073	0.0003	1141 2076	0.0000	1149 3809	-0.0007	1149 3809	-0.0003	1149 3809	-0.0003
1141 4066	0.001	1141 4068	0.0002	1141 4066	0.0000	1149 5631	0.0000	1149 5631	0.0000	1149 5631	0.0000
1141 5640	0.000	1141 5640	0.0000	1141 5640	0.0000	1149 5712	0.0000	1149 5712	0.0002	1149 5712	0.0002
1141 7215	0.000	1141 7212	0.0003	1141 7215	0.0000	1149 7876	0.0001	1149 7877	0.0001	1149 7876	0.0000
1141 9566	0.000	1141 9566	0.0002	1141 9566	0.0000	1149 7877	0.0001	1149 7877	0.0001	1149 7877	0.0000
1142 1543	0.001	1142 1546	0.0003	1142 1543	0.0000	1149 9094	0.001	1149 9094	0.0001	1149 9094	0.0001
1142 1914	0.001	1142 1908	0.0006	1142 1914	0.0000	1150 2590	*0.0000	1150 2590	0.0000	1150 2590	0.0000
1142 2492	0.000	1142 2499	0.0001	1142 2492	0.0000	1150 5760	0.0001	1150 5760	0.0001	1150 5760	0.0003
1142 4331	0.000	1142 4330	0.0001	1142 4331	0.0000	1150 6899	0.0000	1150 6895	0.0000	1150 6895	0.0004
1142 5884	0.000	1142 5880	0.0004	1142 5884	0.0000	1150 8578	0.0001	1150 8582	0.0001	1150 8582	0.0004
1142 5977	0.000	1142 5976	0.0001	1142 5977	0.0000	1150 8736	0.0001	1150 8740	0.0001	1150 8740	0.0004
1143 0009	0.000	1143 0005	0.0004	1143 0009	0.0000	1151 0101	0.0000	1151 0101	0.0001	1151 0101	0.0000
1143 1668	0.000	1143 1668	0.0001	1143 1668	0.0000	1151 1203	0.0001	1151 1203	0.0001	1151 1203	0.0005
1143 2707	0.001	1143 2707	0.0002	1143 2707	0.0000	1151 1969	0.0001	1151 1969	0.0001	1151 1969	0.0003
1143 3541	0.001	1143 3545	0.0002	1143 3541	0.0000	1151 2602	0.0000	1151 2602	0.0001	1151 2602	0.0003
1143 4557	0.000	1143 4557	0.0002	1143 4557	0.0000	1151 4532	0.0001	1151 4532	0.0000	1151 4532	0.0003
1144 0232	0.000	1144 0232	0.0003	1144 0232	0.0000	1151 6593	0.0000	1151 6593	0.0001	1151 6593	0.0007
1144 1522	0.000	1144 1522	0.0005	1144 1522	0.0000	1151 7645	0.0001	1151 7638	0.0001	1151 7638	0.0007
1144 2709	0.001	1144 2707	0.0002	1144 2709	0.0000	1151 9912	0.0000	1151 9912	0.0001	1151 9912	0.0005
1144 5841	0.000	1144 5841	0.0001	1144 5841	0.0000	1152 2703	0.0000	1152 2703	0.0001	1152 2703	0.0005
1144 6599	0.000	1144 6599	0.0002	1144 6599	0.0000	1152 3075	0.0000	1152 3075	0.0001	1152 3075	0.0002
1144 7307	0.001	1144 7307	0.0003	1144 7307	0.0000	1152 4532	0.0001	1152 4532	0.0000	1152 4532	0.0003
1145 1070	0.000	1145 1072	0.0002	1145 1070	0.0000	1152 6724	0.0001	1152 6724	0.0000	1152 6724	0.0002
1145 4157	0.001	1145 4157	0.0005	1145 4157	0.0000	1152 9720	0.0000	1152 9720	0.0001	1152 9720	0.0006
1145 5817	0.000	1145 5816	0.0005	1145 5817	0.0000	1153 0051	0.0001	1153 0051	0.0000	1153 0051	0.0007
1145 5841	0.000	1145 5841	0.0001	1145 5841	0.0000	1153 3073	0.0000	1153 3073	0.0001	1153 3073	0.0002
1146 5819	0.000	1146 5819	0.0001	1146 5819	0.0000	1153 4695	0.0000	1153 4695	0.0001	1153 4695	0.0002
1146 5841	0.000	1146 5841	0.0001	1146 5841	0.0000	1153 5765	0.0000	1153 5765	0.0001	1153 5765	0.0002
1146 5846	0.000	1146 5846	0.0001	1146 5846	0.0000	1153 7360	0.0000	1153 7360	0.0001	1153 7360	0.0002
1146 7288	0.000	1146 7288	0.0001	1146 7288	0.0000	1154 1957	0.0000	1154 1957	0.0001	1154 1957	0.0002
1146 8308	0.000	1146 8308	0.0003	1146 8308	0.0000	1154 3533	0.0000	1154 3533	0.0001	1154 3533	0.0003
1146 8390	0.000	1146 8390	0.0001	1146 8390	0.0000	1154 9282	0.0000	1154 9282	0.0001	1154 9282	0.0000
1146 8457	0.000	1146 8457	0.0005	1146 8457	0.0000	1155 3765	0.0000	1155 3765	0.0001	1155 3765	0.0002
1146 8459	0.000	1146 8459	0.0001	1146 8459	0.0000	1155 7360	0.0000	1155 7360	0.0001	1155 7360	0.0002
1146 9279	0.000	1146 9279	0.0002	1146 9279	0.0000	1155 9546	0.0000	1155 9546	0.0001	1155 9546	0.0002
1146 9705	0.001	1146 9705	0.0002	1146 9705	0.0000	1156 1957	0.0000	1156 1957	0.0001	1156 1957	0.0002
1146 9798	0.000	1146 9798	0.0001	1146 9798	0.0000	1156 3533	0.0000	1156 3533	0.0001	1156 3533	0.0003
1146 8310	0.000	1146 8310	0.0002	1146 8310	0.0000	1156 9282	0.0000	1156 9282	0.0001	1156 9282	0.0002
1146 8956	0.001	1146 8956	0.0030	1146 8956	0.0000	1155 4261	0.0000	1155 4261	0.0001	1155 4261	0.0002
1146 9796	0.000	1146 9796	0.0006	1146 9796	0.0001	1155 6935	*0.0000	1155 6935	0.0000	1155 6935	0.0009
1146 9913	0.000	1146 9913	0.0001	1146 9913	0.0000	1155 8898	0.0001	1155 8898	0.0000	1155 8898	0.0005
1147 2615	0.001	1147 2614	0.0002	1147 2614	0.0001	1156 1426	0.0001	1156 1426	0.0000	1156 1426	0.0001
1147 5139	0.001	1147 5142	0.0002	1147 5139	0.0001	1156 0328	0.0001	1156 0328	0.0000	1156 0328	0.0001
1147 7160	0.000	1147 7160	0.0002	1147 7160	0.0000	1156 5479	0.0000	1156 5479	0.0001	1156 5479	0.0001
1147 7963	0.000	1147 7963	0.0002	1147 7963	0.0000	1156 5566	0.0000	1156 5566	0.0001	1156 5566	0.0002
1148 3351	0.001	1148 3347	0.0004	1148 3351	0.0000	1156 7724	0.0000	1156 7724	0.0000	1156 7724	0.0004
1148 3452	0.000	1148 3452	0.0001	1148 3452	0.0000	1156 7724	0.0000	1156 7724	0.0000	1156 7724	0.0004
1148 3602	0.001	1148 3602	0.0002	1148 3602	0.0000	1157 0078	0.0000	1157 0078	0.0000	1157 0078	0.0004
1148 4702	0.000	1148 4702	0.0002	1148 4702	0.0000	1157 0777	0.0000	1157 0777	0.0000	1157 0777	0.0004

UPPER STATE		LOWER STATE		OBSERVATION PREC.	CALCULATION	RESID.	PREC.	CALCULATION	RESID.
KA	KC	KA	KC						
(6)	10	5	5	0.001	1157.3275	-0.0002	0.000	1163.2671	0.000
(6)	10	5	6	0.001	1157.3275	-0.0002	0.000	1163.3596	-0.0001
(6)	5	6	5	0.000	1157.7813	0.0001	0.000	1163.3598	0.0001
(6)	8	1	8	0.000	1157.7812	0.0001	0.000	1163.3599	0.0001
(6)	15	2	14	0.001	1157.9701	0.0002	0.000	1163.3599	-0.0007
(6)	17	3	14	-1.8	1158.2586	0.0001	0.000	1163.6139	-0.0001
(6)	15	4	15	1.5	1158.2585	0.0001	0.000	1163.6160	0.000
(6)	13	4	10	-1.4	1158.3998	0.001	0.000	1163.8084	0.0003
(6)	13	4	9	1.0	1158.3998	0.001	0.000	1163.8087	0.0003
(6)	13	4	8	-1.7	1158.4013	-0.0015	0.000	1163.8676	-0.0001
(6)	15	2	14	-1.6	1158.4221	-0.0002	0.000	1163.9258	0.0001
(6)	17	3	14	-1.8	1158.5326	-0.0001	0.000	1164.2018	0.001
(6)	15	4	10	-1.4	1158.5325	-0.0001	0.000	1164.2017	0.001
(6)	13	4	9	1.0	1158.6177	0.000	0.000	1164.4418	0.0001
(6)	13	4	8	-1.7	1159.1358	0.000	0.000	1164.4507	0.000
(6)	13	4	7	1.7	1159.1356	0.0002	0.000	1164.5996	-0.0008
(6)	13	4	6	-1.4	1159.2086	0.000	0.000	1164.5985	-0.0001
(6)	13	4	5	1.0	1159.2089	-0.0003	0.000	1164.6479	0.0001
(6)	13	4	4	-1.7	1159.2716	0.000	0.000	1164.7893	0.0003
(6)	13	4	3	1.6	1159.3218	-0.0004	0.000	1164.8067	0.001
(6)	13	4	2	-1.7	1159.4395	0.000	0.000	1164.8070	0.0003
(6)	13	4	1	1.7	1159.4713	0.000	0.000	1164.8231	0.0003
(6)	13	4	0	-1.7	1159.7307	0.000	0.000	1164.8229	0.0002
(6)	13	4	-1	1.7	1159.7304	0.0003	0.000	1164.8233	0.0001
(6)	13	4	1	-1.7	1159.8184	0.000	0.000	1164.8235	0.0001
(6)	13	4	2	1.5	1159.8277	0.001	0.000	1164.9702	0.0001
(6)	13	4	3	-1.2	1159.8278	-0.0001	0.000	1165.0932	0.0003
(6)	13	4	4	1.5	1159.9540	0.001	0.000	1165.1607	0.0008
(6)	13	4	5	-2.0	1159.9539	-0.0001	0.000	1165.1607	0.0001
(6)	13	4	6	1.7	1160.0418	0.000	0.000	1165.1883	0.0001
(6)	13	4	7	-1.5	1160.1763	-0.0005	0.000	1165.1956	0.0006
(6)	13	4	8	2.7	1160.2012	-0.0001	0.000	1165.2815*	0.0004
(6)	13	4	9	-1.3	1160.2454	-0.0001	0.000	1165.3091	0.0001
(6)	13	4	10	1.5	1160.3976	0.000	0.000	1165.3223	0.0008
(6)	13	4	11	-1.5	1160.5188	-0.0004	0.000	1165.3223	0.0000
(6)	13	4	12	1.5	1160.5791	0.000	0.000	1165.4121	0.0000
(6)	13	4	13	-1.5	1160.6634	0.0002	0.000	1165.4631	0.0001
(6)	13	4	14	1.5	1160.6636	0.0001	0.000	1165.4630	0.0001
(6)	13	4	15	-1.7	1160.7884	0.0001	0.000	1165.5072	0.0006
(6)	13	4	16	1.7	1160.9016	0.000	0.000	1165.5358	0.0009
(6)	13	4	17	-1.7	1160.9032	-0.0005	0.000	1165.5473	0.0001
(6)	13	4	18	1.7	1161.0072	0.000	0.000	1165.5831	0.0009
(6)	13	4	19	-1.7	1161.2039	0.000	0.000	1165.8449	0.0018
(6)	13	4	20	1.7	1161.4367	0.000	0.000	1165.8530	0.0005
(6)	13	4	21	-1.7	1161.6322	-0.0002	0.000	1165.8921*	0.0025
(6)	13	4	22	1.7	1161.724	0.000	0.000	1165.8921*	0.0007
(6)	13	4	23	-1.7	1161.9015	-0.0005	0.000	1165.9394	0.0003
(6)	13	4	24	1.7	1161.9019	-0.0003	0.000	1166.0046	0.0002
(6)	13	4	25	-1.7	1162.0629	0.000	0.000	1166.0355	0.0004
(6)	13	4	26	1.7	1162.2768	-0.0003	0.000	1166.0866	0.0004
(6)	13	4	27	-1.7	1162.3209	-0.0005	0.000	1166.1891	0.0002
(6)	13	4	28	1.7	1162.4833*	0.000	0.000	1166.1888	0.0002
(6)	13	4	29	-1.7	1162.4850	0.0000	0.000	1166.3139	0.0001
(6)	13	4	30	1.7	1162.5600	0.0002	0.000	1166.3568	0.0008
(6)	13	4	31	-1.7	1162.6397	0.000	0.000	1166.3551	0.0005
(6)	13	4	32	1.7	1162.8889	-0.0001	0.000	1166.4646	0.0001
(6)	13	4	33	-1.7	1163.0902	-0.0003	0.000	1166.5030	0.0000
(6)	13	4	34	1.7	1163.2144	0.0002	0.000	1166.6454	0.0001
(6)	13	4	35	-1.7	1163.2396	0.0001	0.000	1166.8587	0.0003
(6)	13	4	36	1.7	1163.4146	0.000	0.000	1166.8584	0.0001
(6)	13	4	37	-1.7	1163.4203	0.000	0.000	1166.8587	0.0003

UPPER STATE			LOWER STATE			OBSERVATION PREC.	CALCULATION	RESID.	UPPER STATE	LOWER STATE	OBSERVATION PREC.	CALCULATION	RESID.	
J	KA	KC	J	KA	KC	J	KA	KC	J	KA	KC	J	KA	KC
(4) 10	10	-	9	1	8	1178.2343	0.000	1178.2341	0.0002	1183.3409	0.0005			
(6)	5	4	2	6	5	1178.2739	0.001	1178.2743	-0.0004	1183.3417	-0.0004			
(6)	5	4	1	6	5	1178.2739	0.001	1178.2743	-0.0004	1183.3413	-0.0004			
(6)	24	24	24	2	22	1178.5468	0.000	1178.5469	-0.0004	1183.4054	-0.0004			
(6)	13	22	13	23	12	1178.6952	0.000	1178.6953	-0.0004	1183.4564	-0.0004			
(6)	14	22	14	15	13	1179.0447	0.000	1179.0445	-0.0005	1183.4753	-0.0001			
(6)	11	11	10	10	9	1179.1546	0.000	1179.1546	-0.0005	1183.5664	0.0001			
(6)	22	22	20	21	18	1179.3843	0.000	1179.3842	-0.0001	1183.5664	-0.0001			
(6)	12	12	12	12	11	1179.4503	0.001	1179.4511	-0.0008	1183.6704	0.0001			
(6)	2	2	1	3	1	1179.7982	0.000	1179.793	-0.0001	1183.6704	-0.0001			
(6)	26	26	24	24	24	1179.8958	0.000	1179.8962	-0.0004	1183.7685	-0.0001			
(6)	15	15	14	15	15	1179.9082	0.001	1179.9083	-0.0008	1183.7685	-0.0001			
(6)	13	13	14	14	14	1180.1002	0.000	1180.1003	-0.0005	1183.8607	-0.0002			
(6)	15	15	14	14	12	1180.2236	0.000	1180.2236	-0.0000	1183.8605	-0.0001			
(6)	8	8	5	5	5	1180.3275	0.000	1180.3223	-0.0002	1183.9464	-0.0001			
(6)	12	12	12	12	11	1180.3535	0.000	1180.3356	-0.0003	1183.9462	0.0001			
(6)	25	25	23	23	23	1180.3617*	0.000	1180.3617	-0.0001	1183.9708	0.0001			
(6)	12	12	12	11	10	1180.5617*	0.000	1180.5617	-0.0004	1184.0255	0.0001			
(6)	25	25	23	23	21	1180.6493	0.000	1180.6483	-0.0010	1186.0256	-0.0002			
(6)	12	12	11	13	10	1180.6446	0.000	1180.6443	-0.0003	1184.0982	-0.0000			
(6)	4	4	5	5	5	1180.7325	0.001	1180.7330	-0.0005	1184.0982	0.0001			
(6)	24	24	23	23	23	1180.8080	0.001	1180.8080	-0.0000	1186.1160	-0.0002			
(6)	13	13	12	12	11	1180.8321	0.000	1180.8321	-0.0002	1186.1640	-0.0003			
(6)	13	13	12	12	11	1180.8852	0.000	1180.8852	-0.0000	1186.1922	-0.0003			
(6)	13	13	12	11	11	1181.1638	0.000	1181.1636	-0.0002	1186.2228	-0.0005			
(6)	23	23	22	22	21	1181.2496	0.001	1181.2494	-0.0002	1186.2223	-0.0001			
(6)	22	22	21	21	20	1181.6639	0.001	1181.6661	-0.0000	1186.2745	-0.0008			
(6)	3	3	2	2	2	1181.7626	0.000	1181.7626	-0.0000	1186.2737	-0.0001			
(6)	14	14	13	12	12	1181.7916*	0.000	1181.7903	-0.0012	1186.3334	-0.0007			
(6)	10	10	9	9	9	1182.0396	0.000	1182.0395	-0.0009	1186.5663	-0.0001			
(6)	21	20	21	20	19	1182.0316	0.001	1182.0310	-0.0006	1186.6395	-0.0001			
(6)	16	16	16	16	15	1182.0756	0.000	1182.0765	-0.0008	1186.8228	-0.0001			
(6)	19	19	19	18	17	1182.1235	0.000	1182.1235	-0.0000	1186.8677	-0.0001			
(6)	15	15	14	14	13	1182.2461	0.000	1182.2461	-0.0000	1186.2651	0.0000			
(6)	20	20	19	19	18	1182.3398	0.000	1182.3399	-0.0009	1186.3659	0.0000			
(6)	16	16	16	15	14	1182.3685*	0.000	1182.3685	-0.0000	1186.4223	-0.0001			
(6)	19	19	19	18	17	1182.5385*	0.000	1182.5385	-0.0001	1186.6273	0.0001			
(6)	17	17	16	15	14	1182.5619	0.001	1182.5611	-0.0008	1186.8201	0.0000			
(6)	15	15	14	14	13	1182.6760*	0.000	1182.6758	-0.0002	1186.8781	-0.0001			
(6)	18	18	17	16	15	1182.6760*	0.000	1182.6812	-0.0051	1186.9040	-0.0000			
(6)	7	7	6	5	4	1182.8004	0.000	1182.7987	-0.0017	1186.2651	-0.0012			
(6)	12	12	10	11	9	1182.8267	0.000	1182.8224	-0.0020	1186.1864	-0.0001			
(6)	19	19	17	16	15	1183.0946	0.001	1183.0946	-0.0008	1186.4582	-0.0001			
(6)	14	14	13	12	11	1183.0946	0.001	1183.0945	-0.0019	1186.8954	-0.0005			
(6)	19	19	18	17	16	1183.2207	0.001	1183.2207	-0.0007	1186.9438	-0.0003			
(6)	18	18	17	16	15	1183.2207	0.001	1183.2205	-0.0008	1186.9971	-0.0003			
(6)	11	11	10	9	8	1183.2972	0.000	1183.2970	-0.0003	1187.0156	-0.0015			
(6)	11	11	10	9	8	1183.2972	0.000	1183.2970	-0.0003	1187.0579	-0.0015			

UPPER STATE			LOWER STATE			OBSERVATION PREC.	CALCULATION	RESID.	UPPER STATE	LOWER STATE	OBSERVATION PREC.	CALCULATION	RESID.						
J	KA	KC	J	KA	KC				J	KA	KC								
19	18	-18	2	16	1187.0796	0.001	1187.0793	0.0005	60	20	9	17	-20	5	16	1191.7828	0.001	1191.7830	-0.0001
19	18	-18	2	16	1187.1625	0.000	1187.1623	0.0002	60	20	9	17	-21	5	16	1191.7940	0.001	1191.7941	-0.0001
19	18	-18	2	16	1187.1720	0.000	1187.1717	0.0002	60	20	9	16	-20	5	15	1191.8655	0.001	1191.8657	-0.0002
19	18	-18	2	16	1187.3169	0.001	1187.3179	-0.0004	60	19	9	16	-19	5	15	1191.3860	0.001	1191.9418	-0.0001
19	18	-18	2	16	1187.3480	0.001	1187.3484	-0.0004	60	19	9	15	-19	5	14	1191.9416	0.001	1191.9842	-0.0001
19	18	-18	2	16	1187.4649	0.000	1187.4649	0.0000	60	18	9	15	-18	5	14	1191.9841	0.001	1192.0208	-0.0001
19	18	-18	2	16	1187.7238	0.000	1187.7237	-0.0001	60	17	9	14	-18	5	13	1192.0776	0.001	1192.0774	-0.0002
19	18	-18	2	16	1187.7238	0.000	1187.7242	-0.0004	60	17	9	14	-17	5	13	1192.1009	0.0001	1192.1009	0.0001
19	18	-18	2	16	1187.8608	0.000	1187.8608	-0.0001	60	17	9	13	-17	5	12	1192.1664	0.0001	1192.1662	-0.0001
19	18	-18	2	16	1188.2080	0.0001	1188.2080	-0.0003	60	16	9	12	-16	5	11	1192.1807	0.001	1192.1808	-0.0001
19	18	-18	2	16	1188.3158	0.0007	1188.3158	0.0000	60	16	9	12	-15	5	11	1192.2510	0.001	1192.2508	-0.0002
19	18	-18	2	16	1188.3165	0.000	1188.3616	0.0000	60	15	9	12	-15	5	11	1192.2591	0.001	1192.2593	-0.0016
19	18	-18	2	16	1188.4734	0.000	1188.4733	-0.0001	60	14	9	11	-14	5	10	1192.3327	0.001	1192.3327	0.0016
19	18	-18	2	16	1188.6270	0.000	1188.8273	-0.0003	60	14	9	11	-14	5	10	1192.3327	0.001	1192.3327	0.0016
19	18	-18	2	16	1188.9805	0.000	1188.9805	-0.0000	60	14	9	10	-13	5	9	1192.4085	0.001	1192.4071	-0.0014
19	18	-18	2	16	1189.0401	0.000	1189.0401	-0.0002	60	13	9	10	-13	5	8	1192.4083	0.001	1192.4100	-0.0005
19	18	-18	2	16	1189.2043	0.000	1189.2043	-0.0001	60	13	9	9	-13	5	8	1192.4783	0.001	1192.4787	-0.0005
19	18	-18	2	16	1189.2559	0.001	1189.2559	-0.0038	60	12	9	9	-12	5	7	1192.4793	0.001	1192.4803	-0.0010
19	18	-18	2	16	1189.3401	0.001	1189.3401	-0.0013	60	12	9	8	-12	5	7	1192.5459	0.001	1192.5459	0.0005
19	18	-18	2	16	1189.3840	0.001	1189.3840	-0.0008	60	11	9	8	-11	5	6	1192.5666	0.001	1192.5666	-0.0002
19	18	-18	2	16	1189.5012	0.001	1189.4987	-0.0025	60	10	9	7	-10	5	5	1192.6083	0.001	1192.6082	-0.0003
19	18	-18	2	16	1189.7321	0.000	1189.7321	-0.0002	60	10	9	7	-10	5	5	1192.6208	0.001	1192.6208	-0.0002
19	18	-18	2	16	1189.9838	0.000	1189.9837	-0.0002	60	10	9	6	-10	5	4	1192.6268	0.000	1192.6268	-0.0003
19	18	-18	2	16	1190.1284	0.001	1190.1284	-0.0003	60	10	9	5	-10	5	3	1192.6270	0.001	1192.6270	-0.0003
19	18	-18	2	16	1190.1779	0.000	1190.1779	0.000	60	10	9	4	-10	5	3	1192.6657	0.001	1192.6657	-0.0002
19	18	-18	2	16	1190.1779	0.000	1190.1780	-0.0001	60	10	9	4	-10	5	3	1192.6659	0.001	1192.6659	-0.0002
19	18	-18	2	16	1190.3879	0.001	1190.3879	-0.0002	60	10	9	4	-10	5	3	1192.6691	0.001	1192.6691	-0.0004
19	18	-18	2	16	1190.7321	0.000	1190.7321	-0.0008	60	10	9	3	-10	5	2	1192.7177	0.001	1192.7181	-0.0004
19	18	-18	2	16	1190.9838	0.000	1190.9837	-0.0009	60	10	9	2	-10	5	1	1192.7177	0.001	1192.7177	-0.0005
19	18	-18	2	16	1190.6323	0.000	1190.6324	-0.0022	60	10	9	1	-10	5	0	1192.7374	0.001	1192.7374	-0.0004
19	18	-18	2	16	1190.8174	0.001	1190.8195	-0.0003	60	10	9	0	-10	5	-1	1192.7648	0.001	1192.7648	-0.0004
19	18	-18	2	16	1190.9784	0.001	1190.9781	-0.0003	60	10	9	-1	-10	5	-2	1192.7648	0.001	1192.7648	-0.0004
19	18	-18	2	16	1191.0119	0.000	1191.0117	-0.0001	60	10	9	-1	-10	5	-3	1192.7955	0.001	1192.7954	-0.0004
19	18	-18	2	16	1191.1530	0.001	1191.1541	-0.0011	60	10	9	-1	-10	5	-4	1192.8064	0.001	1192.8064	-0.0004
19	18	-18	2	16	1191.2079	0.001	1191.2046	-0.0035	60	10	9	-1	-10	5	-5	1192.8428	0.001	1192.8428	-0.0004
19	18	-18	2	16	1191.2988	0.001	1191.2986	-0.0008	60	10	9	-1	-10	5	-6	1192.8424	0.001	1192.8424	-0.0004
19	18	-18	2	16	1191.3356	0.001	1191.3357	-0.0005	60	10	9	-1	-10	5	-7	1192.8665R	0.001	1192.8665R	-0.0004
19	18	-18	2	16	1191.4330	0.001	1191.4335	-0.0005	60	10	9	-1	-10	5	-8	1192.8770	0.001	1192.8770	-0.0004
19	18	-18	2	16	1191.4613	0.001	1191.4618	-0.0005	60	10	9	-1	-10	5	-9	1192.8954	0.001	1192.8954	-0.0004
19	18	-18	2	16	1191.4780	0.000	1191.4780	-0.0026	60	10	9	-1	-10	5	-10	1192.8954	0.000	1192.8954	-0.0004
19	18	-18	2	16	1191.4780*	0.000	1191.4771	-0.0009	60	10	9	-1	-10	5	-11	1192.8954	0.000	1192.8954	-0.0004
19	18	-18	2	16	1191.5574	0.001	1191.5577	-0.0003	60	10	9	-1	-10	5	-12	1193.5251	0.000	1193.5251	-0.0004
19	18	-18	2	16	1191.5936	0.001	1191.5937	-0.0001	60	10	9	-1	-10	5	-13	1193.5414	0.001	1193.5414	-0.0004
19	18	-18	2	16	1191.6150	0.001	1191.6169	-0.0019	60	10	9	-1	-10	5	-14	1193.7243	0.000	1193.7243	-0.0004
19	18	-18	2	16	1191.6393	0.000	1191.6394	-0.0001	60	10	9	-1	-10	5	-15	1193.8041	0.000	1193.8041	-0.0004
19	18	-18	2	16	1191.6740	0.001	1191.6738	-0.0003	60	10	9	-1	-10	5	-16	1193.8693	0.001	1193.8693	-0.0004
19	18	-18	2	16	1191.6965	0.000	1191.6965	-0.0000	60	10	9	-1	-10	5	-17	1193.9067	0.001	1193.9067	-0.0004
19	18	-18	2	16	1191.7290	0.001	1191.7295	-0.0006	60	10	9	-1	-10	5	-18	1194.1564	0.001	1194.1564	-0.0004
19	18	-18	2	16	1191.7295	-0.001	1191.7295	-0.0006	60	10	9	-1	-10	5	-19	1194.1564	-0.001	1194.1564	-0.0006

UPPER STATE		LOWER STATE		OBSERVATION PREC.	CALCULATION	RESID.	PREC.	CALCULATION	RESID.	PREC.	CALCULATION	RESID.
K	A	K	C	K	K	K	K	K	K	K	K	K
(4)	3	2	1	2	1194.1964	0.000	1194.1962	0.0002	1194.1960	0.000	1200.4401*	0.0001
(4)	2	2	10	12	1194.3750	0.000	1194.3550	0.0000	1200.9062	0.001	1200.9058	0.0004
(4)	2	12	13	125	1194.5876	0.001	1194.5668	0.0008	1200.9591	0.000	1200.9591	0.0000
(4)	2	14	23	25	1194.7691	0.001	1194.7676	0.0015	1200.9918	0.000	1200.9920	-0.0005
(4)	2	12	12	10	1194.9021	0.000	1194.9022	0.0000	1201.2500	0.001	1201.2495	0.0005
(4)	2	16	15	19	1195.1107	0.001	1195.1112	-0.0004	1201.6991	0.000	1201.6991	-0.0001
(4)	2	20	23	27	1195.4921	0.001	1195.4923	-0.0001	1201.7562	0.001	1201.7563	-0.0000
(4)	2	12	12	10	1195.6175	0.001	1195.6176	-0.0001	1201.7672	0.001	1201.7672	-0.0000
(4)	2	16	15	19	1195.8600	0.000	1195.8598	-0.0001	1201.8061	0.000	1201.8062	-0.0002
(4)	2	20	22	27	1195.8892	0.000	1195.8891	-0.0001	1201.8363	0.001	1201.8363	-0.0002
(4)	2	14	15	19	1195.9761	0.000	1195.9759	0.0002	1201.8874	0.003	1201.8974	0.0000
(4)	2	17	22	16	1195.1107	0.000	1195.1104	0.0037	1201.9299	0.000	1201.9301	-0.0002
(4)	2	21	23	17	1195.6175	0.001	1195.6176	-0.0001	1201.9754	0.000	1201.9756	-0.0002
(4)	2	25	27	10	1195.8600	0.000	1195.8598	-0.0001	1202.0102	0.000	1202.0102	-0.0003
(4)	2	12	12	2	1195.8892	0.000	1195.8891	-0.0001	1202.0102*	0.000	1202.0102*	0.000
(4)	2	16	15	19	1195.9761	0.000	1195.9759	0.0002	1202.0311	0.000	1202.0313	-0.0002
(4)	2	20	21	13	1196.0177*	0.000	1196.0177*	0.0003	1202.0630	0.000	1202.0630	-0.0002
(4)	2	24	23	17	1196.0177	0.000	1196.0180	-0.0003	1202.0949	0.000	1202.0949	-0.0003
(4)	2	28	27	10	1196.1422	0.001	1196.1420	-0.0003	1202.1011	0.000	1202.1011	-0.0004
(4)	2	12	12	8	1196.1727	0.000	1196.1726	-0.0001	1202.1322	0.000	1202.1322	-0.0006
(4)	2	16	15	19	1196.3560	0.000	1196.3556	-0.0004	1202.1520	0.000	1202.1526	-0.0006
(4)	2	20	21	13	1196.5550	0.000	1196.5551	-0.0002	1202.1682	0.000	1202.1686	-0.0003
(4)	2	24	25	17	1196.8215	0.000	1196.8215	0.0000	1202.1973	0.000	1202.1973	-0.0003
(4)	2	28	27	10	1196.9010	0.000	1196.9010	0.0003	1202.2050	0.000	1202.2050	-0.0003
(4)	2	12	12	5	1196.1422	0.000	1196.1420	-0.0003	1202.2217	0.001	1202.2222	-0.0006
(4)	2	16	15	8	1196.1727	0.000	1196.1726	-0.0001	1202.2389*	0.000	1202.2389*	-0.0001
(4)	2	20	21	13	1196.3560	0.000	1196.3556	-0.0004	1202.2716	0.000	1202.2716	-0.0005
(4)	2	24	25	17	1196.5550	0.000	1196.5551	-0.0002	1202.2761	0.000	1202.2761	-0.0006
(4)	2	28	27	10	1196.8215	0.000	1196.8215	0.0000	1202.2990	0.000	1202.2990	-0.0005
(4)	2	12	12	4	1196.9010	0.000	1196.9010	0.0003	1202.3230	0.000	1202.3230	-0.0002
(4)	2	16	15	7	1197.0751	0.000	1197.0751	0.0000	1202.3230	0.000	1202.3230	-0.0005
(4)	2	20	21	11	1197.2834	0.000	1197.2834	0.0000	1202.3767	0.001	1202.3767	-0.0006
(4)	2	24	25	14	1197.3264	0.000	1197.3264	0.0005	1202.5171	0.001	1202.5171	-0.0006
(4)	2	28	27	10	1197.3446	0.000	1197.3446	0.0002	1202.8768	0.001	1202.8768	-0.0005
(4)	2	12	12	3	1197.1694	0.000	1197.1694	0.0006	1203.1669	0.001	1203.1669	-0.0005
(4)	2	16	15	6	1197.1694	0.000	1197.1694	0.0006	1203.3231	0.001	1203.3231	-0.0002
(4)	2	20	21	5	1197.2011	0.000	1197.2011	0.0003	1203.4131	0.0001	1203.4131	-0.0005
(4)	2	24	25	8	1197.2373	0.000	1197.2373	0.0012	1203.4238	0.000	1203.4238	-0.0006
(4)	2	28	27	11	1197.2834	0.000	1197.2834	0.0005	1203.4917	0.000	1203.4917	-0.0002
(4)	2	12	12	4	1197.3259	0.000	1197.3259	0.0005	1203.5056	0.000	1203.5056	-0.0002
(4)	2	16	15	7	1197.4859	0.000	1197.4859	0.0022	1203.5386	0.0003	1203.5386	-0.0003
(4)	2	20	21	11	1197.4921	0.000	1197.4921	0.0007	1203.6132	0.000	1203.6132	-0.0001
(4)	2	24	25	14	1197.5081	0.000	1197.5081	0.0007	1203.6238	0.000	1203.6238	-0.0001
(4)	2	28	27	13	1197.5474	0.000	1197.5474	0.0007	1203.6469	0.000	1203.6469	-0.0001
(4)	2	12	12	6	1197.5959	0.000	1197.5958	-0.0002	1203.6669	0.001	1203.6669	-0.0005
(4)	2	16	15	9	1197.6226	0.000	1197.6226	0.0001	1203.6869	0.001	1203.6869	-0.0005
(4)	2	20	21	12	1197.6226	0.000	1197.6226	0.0001	1203.7287	0.001	1203.7287	-0.0003
(4)	2	24	25	15	1197.6226	0.000	1197.6226	0.0004	1203.7543	0.0003	1203.7543	-0.0003
(4)	2	28	27	18	1197.6226	0.000	1197.6226	0.0004	1203.7650	0.0001	1203.7650	-0.0001
(4)	2	12	12	1	1197.6226	0.000	1197.6226	0.0004	1203.8289	0.0001	1203.8289	-0.0001
(4)	2	16	15	4	1197.6226	0.000	1197.6226	0.0004	1203.9711	0.000	1203.9711	-0.0000

UPPER STATE			LOWER STATE			OBSERVATION	PREC.	CALCULATION	RESID.	UPPER STATE	LOWER STATE	OBSERVATION	PREC.	CALCULATION	RESID.		
J	KA	KC	J	KA	KC					J	KA	KC					
14	2	12	-14	1215	2929	0.000	1215	2928	0.0001	1222	7003	-0.0002	1222	7001	0.000	1222	7003
15	2	15	-15	1215	4582	0.000	1215	4581	0.0001	1222	8300	-0.0002	1222	8300	0.000	1222	8300
15	3	13	-14	1215	5629	0.000	1215	5629	0.000	1222	8555	-0.0001	1222	8554	0.000	1222	8555
15	3	13	-15	1215	8713	0.000	1215	8713	0.0001	1222	8623	-0.0009	1222	8623	0.000	1222	8623
15	4	12	-15	1216	6413	0.000	1216	6415	0.0002	1222	9667	-0.0003	1222	9667	0.0001	1222	9667
15	4	12	-15	1216	3424	0.000	1216	3423	0.0001	1223	5974	-0.0001	1223	5974	0.0001	1223	5974
15	5	13	-15	1216	3426	0.000	1216	3423	0.0001	1223	4209	-0.0001	1223	4209	0.0001	1223	4209
15	5	13	-15	1216	5144	0.000	1216	5142	0.0003	1223	4626	-0.0001	1223	4626	0.0001	1223	4626
15	5	13	-15	1216	5928	0.000	1216	5929	0.0003	1223	4990	-0.0001	1223	4990	0.0001	1223	4990
15	6	12	-16	1216	6713	0.000	1216	6713	0.0003	1223	6255	-0.0001	1223	6255	0.0001	1223	6255
15	6	12	-16	1216	7375	0.000	1216	8686	-0.0005	1223	7538	-0.001	1223	7538	-0.0001	1223	7538
15	7	11	-16	1216	8686	0.000	1216	8935	-0.0001	1223	9855	-0.0001	1223	9855	-0.0001	1223	9855
15	7	11	-16	1216	8938	0.000	1216	8938	-0.0003	1224	0076	-0.0001	1224	0076	-0.0001	1224	0076
15	8	10	-16	1216	6710	0.000	1216	1025	-0.0002	1216	0021	*	1216	0021	*	1216	0021
15	8	10	-16	1216	7375	0.000	1216	7375	-0.0003	1224	1159	-0.0001	1224	1159	-0.0001	1224	1159
15	9	11	-16	1216	8686	0.000	1216	8686	-0.0005	1224	5300	-0.0001	1224	5300	-0.0001	1224	5300
15	9	11	-16	1216	8935	0.000	1216	8935	-0.0001	1224	9652	-0.0001	1224	9652	-0.0001	1224	9652
15	10	10	-16	1216	6710	0.000	1216	1025	-0.0002	1225	2308	-0.0001	1225	2308	-0.0001	1225	2308
15	10	10	-16	1216	7375	0.000	1216	7375	-0.0003	1225	3130	-0.0001	1225	3130	-0.0001	1225	3130
15	11	11	-16	1216	8686	0.000	1216	8686	-0.0005	1225	3130	*	1225	3130	*	1225	3130
15	11	11	-16	1216	8935	0.000	1216	8935	-0.0005	1225	4866	-0.0001	1225	4866	-0.0001	1225	4866
15	12	12	-16	1216	6710	0.000	1216	1025	-0.0003	1225	6730	-0.0001	1225	6730	-0.0001	1225	6730
15	12	12	-16	1216	7375	0.000	1216	7375	-0.0005	1225	7428	-0.0001	1225	7428	-0.0001	1225	7428
15	13	13	-16	1216	8686	0.000	1216	8686	-0.0005	1225	7497	-0.0001	1225	7497	-0.0001	1225	7497
15	13	13	-16	1216	8935	0.000	1216	8935	-0.0005	1225	8912	-0.0001	1225	8912	-0.0001	1225	8912
15	14	14	-16	1216	6710	0.000	1216	1025	-0.0003	1226	9976	-0.0001	1226	9976	-0.0001	1226	9976
15	14	14	-16	1216	7375	0.000	1216	7375	-0.0005	1226	1652	-0.0001	1226	1652	-0.0001	1226	1652
15	15	15	-16	1216	8686	0.000	1216	8686	-0.0005	1226	2957	-0.0001	1226	2957	-0.0001	1226	2957
15	15	15	-16	1216	8935	0.000	1216	8935	-0.0005	1226	3398	-0.0001	1226	3398	-0.0001	1226	3398
15	16	16	-16	1216	6710	0.000	1216	1025	-0.0003	1226	3450	-0.0001	1226	3450	-0.0001	1226	3450
15	16	16	-16	1216	7375	0.000	1216	7375	-0.0005	1226	4042	-0.0001	1226	4042	-0.0001	1226	4042
15	17	17	-16	1216	8686	0.000	1216	8686	-0.0005	1226	4344	-0.0001	1226	4344	-0.0001	1226	4344
15	17	17	-16	1216	8935	0.000	1216	8935	-0.0005	1226	5868	-0.0001	1226	5868	-0.0001	1226	5868
15	18	18	-16	1216	6710	0.000	1216	1025	-0.0003	1226	7653	-0.0001	1226	7653	-0.0001	1226	7653
15	18	18	-16	1216	7375	0.000	1216	7375	-0.0005	1226	7362	-0.0001	1226	7362	-0.0001	1226	7362
15	19	19	-16	1216	8686	0.000	1216	8686	-0.0005	1226	7711	-0.0001	1226	7711	-0.0001	1226	7711
15	19	19	-16	1216	8935	0.000	1216	8935	-0.0005	1226	9323	-0.0001	1226	9323	-0.0001	1226	9323
15	20	20	-16	1216	6710	0.000	1216	1025	-0.0003	1227	1794	-0.0001	1227	1794	-0.0001	1227	1794
15	20	20	-16	1216	7375	0.000	1216	7375	-0.0005	1227	3203	-0.0001	1227	3203	-0.0001	1227	3203
15	21	21	-16	1216	8686	0.000	1216	8686	-0.0005	1227	6224	-0.0001	1227	6224	-0.0001	1227	6224
15	21	21	-16	1216	8935	0.000	1216	8935	-0.0005	1227	7362	-0.0001	1227	7362	-0.0001	1227	7362
15	22	22	-16	1216	6710	0.000	1216	1025	-0.0003	1227	7711	-0.0001	1227	7711	-0.0001	1227	7711
15	22	22	-16	1216	7375	0.000	1216	7375	-0.0005	1227	8897	-0.0001	1227	8897	-0.0001	1227	8897
15	23	23	-16	1216	8686	0.000	1216	8686	-0.0005	1227	9273	-0.0001	1227	9273	-0.0001	1227	9273
15	23	23	-16	1216	8935	0.000	1216	8935	-0.0005	1228	0434	-0.0001	1228	0434	-0.0001	1228	0434
15	24	24	-16	1216	6710	0.000	1216	1025	-0.0003	1228	0454	-0.0001	1228	0454	-0.0001	1228	0454
15	24	24	-16	1216	7375	0.000	1216	7375	-0.0005	1228	0591	-0.0001	1228	0591	-0.0001	1228	0591
15	25	25	-16	1216	8686	0.000	1216	8686	-0.0005	1228	0595	-0.0001	1228	0595	-0.0001	1228	0595
15	25	25	-16	1216	8935	0.000	1216	8935	-0.0005	1228	1275	-0.0001	1228	1275	-0.0001	1228	1275
15	26	26	-16	1216	6710	0.000	1216	1025	-0.0003	1228	1276	-0.0001	1228	1276	-0.0001	1228	1276
15	26	26	-16	1216	7375	0.000	1216	7375	-0.0005	1228	1277	-0.0001	1228	1277	-0.0001	1228	1277
15	27	27	-16	1216	8686	0.000	1216	8686	-0.0005	1228	1278	-0.0001	1228	1278	-0.0001	1228	1278
15	27	27	-16	1216	8935	0.000	1216	8935	-0.0005	1228	1279	-0.0001	1228	1279	-0.0001	1228	1279
15	28	28	-16	1216	6710	0.000	1216	1025	-0.0003	1228	1280	-0.0001	1228	1280	-0.0001	1228	1280
15	28	28	-16	1216	7375	0.000	1216	7375	-0.0005	1228	1281	-0.0001	1228	1281	-0.0001	1228	1281
15	29	29	-16	1216	8686	0.000	1216	8686	-0.0005	1228	1282	-0.0001	1228	1282	-0.0001	1228	1282
15	29	29	-16	1216	8935	0.000	1216	8935	-0.0005	1228	1283	-0.0001	1228	1283	-0.0001	1228	1283
15	30	30	-16	1216	6710	0.000	1216	1025	-0.0003	1228	1284	-0.0001	1228	1284	-0.0001	1228	1284
15	30	30	-16	1216	7375	0.000	1216	7375	-0.0005	1228	1285	-0.0001	1228	1285	-0.0001	1228	1285
15	31	31	-16	1216	8686	0.000	1216	8686	-0.0005	1228	1286	-0.0001	1228	1286	-0.0001	1228	1286
15	31	31	-16	1216	8935	0.000	1216	8935	-0.0005	1228	1287	-0.0001	1228	1287	-0.0001	1228	1287
15	32	32	-16	1216	6710	0.000	1216	1025	-0.0003	1228	1288	-0.0001	1228	1288	-0.0001	1228	1288
15	32	32	-16	1216	7375	0.000	1216	7375	-0.0005	1228	1289	-0.0001	1228	1289	-0.0001	1228	1289
15	33	33	-16	1216	8686	0.000	1216	8686	-0.0005	1228	1290	-0.0001	1228	1290	-0.0001	1228	1290
15	33	33	-16	1216	8935	0.000	1216	8935	-0.0005	1228	1291	-0.0001	1228	1291	-0.0001	1228	1291
15	34	34	-16	1216													

UPPER STATE			LOWER STATE			OBSERVATION PREC.	CALCULATION	RESID.	PREC.	CALCULATION	RESID.
J	K	A	J	K	C	J	K	C	J	K	C
(6)	8	1	1228.1637	0.000	1228.1639	-0.0002	1228.1639	0.000	1234.7652	0.000	0.0003
(6)	10	1	1228.5244	0.000	1228.5244	-0.0000	1228.5244	0.000	1234.8740	0.000	0.0001
(6)	9	1	1228.5858	0.000	1228.5858	-0.0000	1228.5858	0.000	1235.4153	0.000	0.0002
(6)	15	1	1228.6921	0.001	1228.6916	-0.0004	1228.6921	0.001	1235.5604	0.000	0.0001
(6)	15	4	1228.6917	0.001	1228.6917	-0.0089	1228.6917	0.001	1235.7249	0.000	0.0002
(6)	15	4	1228.7125	0.001	1228.7132	-0.0007	1228.7125	0.001	1235.7251	0.000	0.0001
(6)	11	4	1228.7796	0.000	1228.7795	-0.0003	1228.7796	0.000	1235.7635	0.000	0.0001
(6)	10	4	1228.8325	0.000	1228.8322	-0.0003	1228.8325	0.000	1236.0632	0.000	0.0004
(6)	10	4	1228.9832	0.000	1228.9833	-0.0001	1228.9832	0.000	1236.2835	0.000	0.0001
(6)	10	2	1229.2426	0.001	1229.2431	-0.0005	1229.2426	0.001	1236.3370	0.000	0.0001
(6)	10	2	1229.3376	0.000	1229.3376	-0.0002	1229.3376	0.000	1236.6305	0.000	0.0001
(6)	11	2	1229.3374	0.000	1229.3376	-0.0002	1229.3374	0.000	1236.6344	0.000	0.0001
(6)	11	3	1229.6249	0.001	1229.6244	-0.0005	1229.6249	0.001	1236.7991	0.000	0.0004
(6)	12	1	1229.6303	0.000	1229.6303	-0.0003	1229.6303	0.000	1236.8387	0.000	0.0005
(6)	12	1	1229.7391	0.000	1229.7395	-0.0004	1229.7391	0.000	1236.9222	0.000	0.0003
(6)	12	1	1229.8464	0.000	1229.8463	-0.0001	1229.8464	0.000	1237.0330	0.000	0.0011
(6)	13	1	1229.8462	0.000	1229.8462	-0.0005	1229.8462	0.000	1237.0340	0.000	0.0001
(6)	13	1	1229.9147	0.000	1229.9147	-0.0000	1229.9147	0.000	1237.1095	0.000	0.0001
(6)	11	2	1229.9147	0.000	1229.9147	-0.0002	1229.9147	0.000	1237.1661	0.000	0.0001
(6)	12	1	1229.9147	0.000	1229.9148	-0.0004	1229.9147	0.000	1237.5591	0.000	0.0003
(6)	12	1	1230.0018	0.000	1230.0018	-0.0000	1230.0018	0.000	1238.0612	0.000	0.0001
(6)	13	1	1230.0980	0.001	1230.0975	-0.0005	1230.0980	0.001	1238.0822	0.000	0.0001
(6)	13	1	1230.1485	0.000	1230.1486	-0.0001	1230.1485	0.000	1238.1203	0.000	0.0000
(6)	13	1	1230.2725	0.000	1230.2725	-0.0000	1230.2725	0.000	1238.1760	0.000	0.0002
(6)	14	1	1230.3172	0.000	1230.3172	-0.0000	1230.3172	0.000	1238.3551	0.000	0.0001
(6)	14	1	1230.3496	0.000	1230.3496	-0.0006	1230.3496	0.000	1238.4876	0.000	0.0001
(6)	15	2	1230.8951	0.000	1230.8951	-0.0006	1230.8951	0.000	1238.4974	0.000	0.0002
(6)	15	2	1231.0397	0.001	1231.0398	-0.0001	1231.0397	0.001	1239.0278	0.000	0.0001
(6)	15	2	1231.1485	0.000	1231.1486	-0.0001	1231.1485	0.000	1239.1551	0.000	0.0000
(6)	16	3	1231.1466	0.000	1231.1466	-0.0001	1231.1466	0.000	1240.0379	0.000	0.0002
(6)	16	3	1231.2540	0.000	1231.2540	-0.0003	1231.2540	0.000	1240.1378	0.000	0.0004
(6)	16	4	1231.3490	0.000	1231.3490	-0.0003	1231.3490	0.000	1240.2155	0.000	0.0001
(6)	16	4	1231.4323	0.000	1231.4323	-0.0005	1231.4323	0.000	1240.3507	0.000	0.0001
(6)	16	4	1231.9665	0.000	1231.9664	-0.0001	1231.9665	0.000	1240.4225	0.000	0.0003
(6)	16	4	1232.3662	0.000	1232.3661	-0.0001	1232.3662	0.000	1240.4276	0.000	0.0002
(6)	16	5	1232.5594	0.000	1232.5595	-0.0001	1232.5594	0.000	1240.5600	0.000	0.0001
(6)	16	5	1232.6213	0.000	1232.6210	-0.0003	1232.6213	0.000	1240.6300	0.000	0.0001
(6)	17	6	1232.8160	0.000	1232.8160	-0.0002	1232.8160	0.000	1240.8203	0.000	0.0004
(6)	17	6	1232.9663	0.000	1232.9666	-0.0003	1232.9663	0.000	1241.5870	0.000	0.0002
(6)	17	6	1233.3845	0.001	1233.3845	-0.0002	1233.3845	0.001	1242.8045	0.000	0.0002
(6)	18	7	1233.4090	0.000	1233.4089	-0.0003	1233.4090	0.000	1242.8482	0.000	0.0005
(6)	18	7	1233.4482	0.000	1233.4478	-0.0003	1233.4482	0.000	1242.8843	0.000	0.0001
(6)	18	8	1233.5037	0.000	1233.5035	-0.0002	1233.5037	0.000	1242.8857	0.000	0.0002
(6)	18	8	1233.5631	0.000	1233.5629	-0.0002	1233.5631	0.000	1243.0485	0.000	0.0001
(6)	18	9	1233.6436	0.000	1233.6436	-0.0000	1233.6436	0.000	1243.2390	0.000	0.0001
(6)	19	10	1233.7977	0.001	1233.7974	-0.0006	1233.7977	0.001	1243.7117	0.000	0.0002
(6)	19	10	1234.0878	0.000	1234.0880	-0.0002	1234.0878	0.000	1242.8599	0.000	0.0001
(6)	19	10	1234.2831	0.000	1234.2831	-0.0003	1234.2831	0.000	1243.7117	0.000	0.0001
(6)	19	11	1234.3410	0.000	1234.3413	-0.0001	1234.3410	0.000	1244.8600	0.000	0.0001
(6)	19	11	1234.6680	0.000	1234.6680	-0.0001	1234.6680	0.000	1245.2392	0.000	0.0001
(6)	19	11	1234.7119	0.000	1234.7119	-0.0002	1234.7119	0.000	1245.7117	0.000	0.0001

UPPER STATE		LOWER STATE		OBSERVATION	PREC.	CALCULATION	RESID.	UPPER STATE		LOWER STATE		OBSERVATION	PREC.	CALCULATION	RESID.
K	J	K	J	KA	KC	KA	KC	K	J	K	J	KA	KC	KA	KC
(6) 110	12	11	12	1243.4522	0.000	1243.4521	0.0001	1257.6987	0.001	1257.6949	0.0034	1257.6987	0.001	1258.3155	0.0000
112	210	-11	13	1243.6629	0.000	1243.6627	0.0003	1258.3155	0.000	1258.3155	0.0003	1258.3155	0.000	1258.3298	0.0000
113	10	-12	13	1243.8046	0.000	1243.8046	0.0003	1258.3150	0.001	1258.3150	0.0003	1258.3150	0.0001	1258.6649	0.0000
114	10	-19	22	1244.5037	0.000	1244.5037	0.0003	1258.1720	-1	1258.1720	-1	1258.1720	-1	1258.250	-0.0002
115	7	-6	25	1245.0160	0.000	1245.0159	0.0001	1258.1721	0	1258.1721	0	1258.1721	0	1258.250	-0.0002
116	22	19	21	1245.3367	0.001	1245.3367	0.0004	1258.2120	-2	1258.2120	-2	1258.2120	-2	1258.8829	-0.0003
117	11	18	21	1245.2236	0.001	1245.2241	0.0005	1258.2121	0	1258.2121	0	1258.2121	0	1258.9829	-0.0001
118	11	19	20	1245.5818	0.000	1245.5819	0.0001	1259.0697	0.000	1259.0697	0.0001	1259.0697	0.000	1259.0695	-0.0005
119	14	5	15	1245.6483	0.000	1245.6484	0.0001	1259.4269	0.000	1259.4269	0.000	1259.4269	0.000	1259.3367	-0.0001
120	2	11	15	1245.8311	0.000	1245.8311	0.0001	1259.3941	0.000	1259.3941	0.0001	1259.3941	0.000	1259.3941	-0.0005
121	16	-6	13	1245.9729	0.000	1245.9727	0.0002	1259.4069	0.000	1259.4069	0.000	1259.4069	0.000	1259.6051	-0.0002
122	22	18	21	1246.3367	0.001	1246.3368	0.0001	1259.4727	-10	1259.4727	-10	1259.4727	-10	1259.4755	-0.0001
123	11	12	11	1246.5950	0.000	1246.5948	0.000	1259.4728	-10	1259.4728	-10	1259.4728	-10	1259.8383	-0.0001
124	11	10	10	1246.7317	0.000	1246.7315	0.0002	1259.5125	-5	1259.5125	-5	1259.5125	-5	1260.3785	-0.0003
125	2	9	12	1247.1208	0.000	1247.1210	0.0002	1259.5126	-6	1259.5126	-6	1259.5126	-6	1260.4255	-0.0009
126	2	13	13	1247.4690	0.000	1247.4685	0.0005	1259.5127	-21	1259.5127	-21	1259.5127	-21	1260.8199	-0.0009
127	16	12	13	1247.5579	0.000	1247.5577	0.0001	1259.5128	-25	1259.5128	-25	1259.5128	-25	1260.8519	-0.0012
128	12	11	13	1247.7313	0.000	1247.7313	0.0003	1259.5129	-12	1259.5129	-12	1259.5129	-12	1260.8507	-0.0001
129	10	10	10	1247.7623	0.000	1247.7621	0.0003	1259.5130	-7	1259.5130	-7	1259.5130	-7	1260.8536	-0.0001
130	13	11	12	1248.0556	0.000	1248.0557	0.0001	1259.5131	-22	1259.5131	-22	1259.5131	-22	1261.2579	-0.0002
131	13	12	14	1248.0831	0.000	1248.0831	0.0004	1259.5132	-23	1259.5132	-23	1259.5132	-23	1261.7486	-0.0001
132	17	17	14	1248.3811	0.000	1248.3813	0.0002	1259.5133	-22	1259.5133	-22	1259.5133	-22	1261.8222	-0.0003
133	17	16	15	1248.4022	0.000	1248.4023	0.0002	1259.5134	-26	1259.5134	-26	1259.5134	-26	1262.0881	-0.0005
134	16	15	15	1248.6310	0.000	1248.6309	0.0003	1259.5135	-12	1259.5135	-12	1259.5135	-12	1262.3508	-0.0005
135	16	14	15	1249.6310	0.000	1249.6307	0.0003	1259.5136	-7	1259.5136	-7	1259.5136	-7	1262.7687	-0.0003
136	15	15	14	1249.6670	0.000	1249.6669	0.0001	1259.5137	-17	1259.5137	-17	1259.5137	-17	1263.1845	-0.0006
137	15	14	14	1250.1255	0.000	1250.1252	0.0005	1259.5138	-16	1259.5138	-16	1259.5138	-16	1264.6887	-0.0003
138	15	14	14	1250.3922	0.000	1250.3920	0.0003	1259.5139	-18	1259.5139	-18	1259.5139	-18	1263.2382	-0.0004
139	15	14	14	1251.0483	0.000	1251.0483	0.0003	1259.5140	-12	1259.5140	-12	1259.5140	-12	1264.9258	-0.0003
140	15	14	14	1251.6421	0.000	1251.6421	0.0003	1259.5141	-12	1259.5141	-12	1259.5141	-12	1265.9908	-0.0003
141	15	14	14	1253.7347	0.000	1253.7347	0.0003	1259.5142	-23	1259.5142	-23	1259.5142	-23	1266.2561	-0.0003
142	15	14	14	1253.9680	0.001	1253.9679	0.0001	1259.5143	-19	1259.5143	-19	1259.5143	-19	1266.6886	-0.0004
143	15	14	14	1254.3442	0.001	1254.3445	0.0002	1259.5144	-24	1259.5144	-24	1259.5144	-24	1266.9268	-0.0003
144	15	14	14	1255.7749	0.000	1255.7749	0.0003	1259.5145	-17	1259.5145	-17	1259.5145	-17	1267.6708	-0.0002
145	15	14	14	1255.1506	0.000	1255.1507	0.0001	1259.5146	-13	1259.5146	-13	1259.5146	-13	1267.6939	-0.0002
146	15	14	14	1255.4241	0.000	1255.4241	0.0003	1259.5147	-16	1259.5147	-16	1259.5147	-16	1267.7709	-0.0003
147	15	14	14	1255.7350	0.000	1255.7350	0.0003	1259.5148	-18	1259.5148	-18	1259.5148	-18	1267.9942	-0.0002
148	15	14	14	1255.9695	0.001	1255.9693	0.0002	1259.5149	-10	1259.5149	-10	1259.5149	-10	1268.0602	-0.0002
149	15	14	14	1252.7052	0.000	1252.7052	0.0003	1259.5150	-14	1259.5150	-14	1259.5150	-14	1268.0874	-0.0001
150	15	14	14	1253.1506	0.000	1253.1506	0.0003	1259.5151	-15	1259.5151	-15	1259.5151	-15	1268.1677	-0.0001
151	15	14	14	1253.6421	0.000	1253.6421	0.0003	1259.5152	-12	1259.5152	-12	1259.5152	-12	1269.4526	-0.0001
152	15	14	14	1253.7347	0.000	1253.7347	0.0003	1259.5153	-17	1259.5153	-17	1259.5153	-17	1269.4527	-0.0001
153	15	14	14	1254.3442	0.000	1254.3445	0.0002	1259.5154	-13	1259.5154	-13	1259.5154	-13	1269.4528	-0.0001
154	15	14	14	1255.7482	0.001	1255.7481	0.0001	1259.5155	-13	1259.5155	-13	1259.5155	-13	1269.4529	-0.0001
155	15	14	14	1255.8169	0.001	1255.8166	0.0005	1259.5156	-18	1259.5156	-18	1259.5156	-18	1265.3545	-0.0002
156	15	14	14	1255.8347	0.000	1255.8346	0.0001	1259.5157	-23	1259.5157	-23	1259.5157	-23	1265.6806	-0.0002
157	15	14	14	1256.0296	0.000	1256.0296	0.0002	1259.5158	-16	1259.5158	-16	1259.5158	-16	1265.8356	-0.0006
158	15	14	14	1256.0557	0.001	1256.0557	0.0005	1259.5159	-12	1259.5159	-12	1259.5159	-12	1266.4447	-0.0005
159	15	14	14	1256.1035	0.000	1256.1038	0.000	1259.5160	-14	1259.5160	-14	1259.5160	-14	1266.9268	-0.0004
160	15	14	14	1256.2757	0.000	1256.2758	-0.0001	1259.5161	-13	1259.5161	-13	1259.5161	-13	1267.6708	-0.0002
161	15	14	14	1256.3814	0.000	1256.3814	-0.0002	1259.5162	-15	1259.5162	-15	1259.5162	-15	1267.6939	-0.0002
162	15	14	14	1256.5547	0.001	1256.5547	0.0005	1259.5163	-10	1259.5163	-10	1259.5163	-10	1267.7709	-0.0003
163	15	14	14	1256.6167	0.000	1256.6167	0.0002	1259.5164	-12	1259.5164	-12	1259.5164	-12	1267.9942	-0.0002
164	15	14	14	1257.3137	0.001	1257.3137	0.0006	1259.5165	-13	1259.5165	-13	1259.5165	-13	1268.0602	-0.0002
165	15	14	14	1257.3567	0.000	1257.3567	0.0001	1259.5166	-12	1259.5166	-12	1259.5166	-12	1268.0874	-0.0001
166	15	14	14	1257.4220	0.001	1257.4220	-0.0002	1259.5167	-22	1259.5167	-22	1259.5167	-22	1268.1677	-0.0000
167	15	14	14	1257.5832	0.000	1257.5832	-0.0005	1259.5168	-4	1259.5168	-4	1259.5168	-4	1269.4526	-0.0001

UPPER STATE		LOWER STATE		OBSERVATION PREC.	CALCULATION	RESID.	UPPER STATE		LOWER STATE		OBSERVATION PREC.	CALCULATION	RESID.		
J	K	J	K	KC	KC	KC	J	K	J	K	KC	KC	KC		
(6)	16	15	14	1308.4080	0.000	1308.4073	0.0007	(6)	9	8	7	1322.2432	0.000	1322.2430	0.0001
(6)	5	4	6	1308.9268	0.000	1308.9261	0.0006	(6)	16	15	14	1322.3356	0.001	1322.3353	0.0001
(6)	5	4	3	1308.9268	0.000	1308.9250	-0.0012	(6)	16	15	14	1322.3862	0.000	1322.3862	0.0001
(6)	26	25	1	1309.5260	0.001	1309.5266	-0.0006	(6)	15	12	15	1322.4934	0.000	1322.4933	0.0001
(6)	17	11	15	1309.8692	0.001	1309.8686	-0.0006	(6)	13	9	15	1322.6180	0.000	1322.6177	0.0002
(6)	16	12	16	1310.1530	0.000	1310.1529	0.0001	(6)	14	11	13	1322.6443	0.000	1322.6442	0.0000
(6)	11	10	10	1311.1649	0.000	1311.1649	0.0000	(6)	13	12	12	1322.7861	0.000	1322.7861	0.0001
(6)	18	17	16	1311.3457	0.001	1311.3450	0.0002	(6)	12	9	12	1322.8115	0.000	1322.8117	0.0001
(6)	14	15	3	1311.4011	0.000	1311.4010	0.0005	(6)	11	8	11	1322.9178	0.000	1322.9177	0.0002
(6)	27	26	26	1311.4904	0.001	1311.4903	-0.0009	(6)	10	7	10	1323.0380	0.000	1323.0379	0.0001
(6)	5	3	4	1312.5357	0.000	1312.5356	-0.0002	(6)	10	9	7	1323.1095	0.000	1323.1094	0.0001
(6)	5	2	4	1312.5718	0.000	1312.5717	-0.0002	(6)	9	7	6	1323.2224	0.000	1323.2225	0.0001
(6)	19	18	18	1312.8559	0.001	1312.8553	0.0006	(6)	9	7	5	1323.2422	0.000	1323.2423	0.0001
(6)	26	26	26	1313.8906	0.001	1313.8911	-0.0005	(6)	11	9	9	1323.3265	0.000	1323.3265	0.0000
(6)	20	28	26	1314.6208	0.001	1314.6207	-0.0001	(6)	10	8	8	1323.3954	0.000	1323.3945	0.0009
(6)	6	5	3	1314.8947	0.000	1314.8948	-0.0014	(6)	7	5	5	1323.3954	0.000	1323.3945	0.0009
(6)	12	10	11	1314.9805K	0.000	1314.9791	-0.0013	(6)	2	12	15	1323.4198	0.000	1323.4198	0.0007
(6)	25	24	24	1315.3546	0.001	1315.3548	-0.0003	(6)	6	5	6	1323.4594	0.000	1323.4586	0.0007
(6)	21	21	20	1316.0646	0.001	1316.0646	0.0000	(6)	5	4	5	1323.5107	0.000	1323.5108	0.0000
(6)	21	21	19	1316.2219	0.001	1316.2217	-0.0001	(6)	4	3	4	1323.5520	0.000	1323.5525	0.0005
(6)	7	5	4	1317.3123	0.001	1317.3122	-0.0001	(6)	3	2	2	1323.5520	0.000	1323.5525	0.0001
(6)	7	5	4	1317.3906	0.000	1317.3906	-0.0001	(6)	10	9	9	1323.6604	0.000	1323.6604	0.0000
(6)	22	21	21	1317.8127	0.001	1317.8126	-0.0003	(6)	11	10	9	1323.6946	0.000	1323.6946	0.0000
(6)	22	21	20	1318.2190	0.001	1318.2191	-0.0003	(6)	11	10	8	1323.7176	0.000	1323.7176	0.0002
(6)	8	7	6	1319.0597	0.001	1319.0594	-0.0003	(6)	12	11	10	1323.7934	0.000	1323.7934	0.0005
(6)	23	23	23	1319.0841	0.000	1319.0837	-0.0003	(6)	12	11	9	1323.8986	0.000	1323.8986	0.0001
(6)	8	7	6	1319.5059	0.000	1319.5059	-0.0000	(6)	13	12	7	1324.6818	0.000	1324.6818	0.0000
(6)	23	22	22	1319.6927	0.001	1319.6934	-0.0007	(6)	11	12	10	1329.8623	0.000	1329.8623	0.0003
(6)	20	18	21	1319.7776	0.000	1319.7762	-0.0006	(6)	11	12	9	1331.6387	0.000	1331.6386	0.0002
(6)	8	7	6	1319.8104	0.001	1319.8103	-0.0000	(6)	12	11	10	1332.2342	0.000	1332.2342	0.0006
(6)	19	18	18	1320.4012	0.001	1320.4012	0.0003	(6)	15	14	14	1332.8200	0.000	1332.8200	0.0003
(6)	19	18	17	1320.9369	0.001	1320.9369	-0.0002	(6)	15	14	13	1333.2716	0.000	1333.2716	0.0005
(6)	25	24	24	1321.5631	0.001	1321.5631	-0.0015	(6)	10	9	8	1333.2716	0.000	1333.2716	0.0003
(6)	25	24	23	1321.2105	0.001	1321.2105	-0.0003	(6)	13	12	11	1333.2958	0.000	1333.2958	0.0003
(6)	25	24	23	1321.7356	0.001	1321.7356	-0.0005	(6)	15	14	13	1334.8298R	0.000	1334.8298R	0.0002
(6)	17	17	16	1321.941	0.001	1321.941	-0.0002	(6)	16	15	14	1335.8297	0.000	1335.8297	0.0003
(6)	22	21	21	1321.5631	0.001	1321.5631	-0.0001	(6)	16	15	14	1335.6621	0.000	1335.6621	0.0006
(6)	18	17	18	1321.6898	0.001	1321.6898	-0.0003	(6)	15	14	13	1335.6618	0.000	1335.6618	0.0002
(6)	20	19	18	1321.6895	0.001	1321.6895	-0.0003	(6)	17	16	15	1335.2387	0.000	1335.2387	0.0003
(6)	9	8	7	1321.7352*	0.001	1321.7352*	-0.0005	(6)	15	14	13	1337.5038	0.000	1337.5038	0.0003
(6)	16	15	12	1321.7625	0.001	1321.7625	-0.0002	(6)	15	14	13	1337.5231	0.001	1337.5231	0.0009
(6)	19	16	16	1321.8464	0.001	1321.8464	-0.0003	(6)	18	17	16	1338.0435	0.000	1338.0435	0.0002
(6)	18	15	15	1322.0868	0.001	1322.0868	-0.0004	(6)	16	15	14	1338.0435	0.000	1338.0435	0.0001
(6)	22	21	20	1322.1063	0.001	1322.1063	-0.0003	(6)	16	15	14	1338.0435	0.000	1338.0435	0.0000
(6)	17	17	17	1322.1728	0.001	1322.1728	-0.0001	(6)	16	15	14	1338.0435	0.000	1338.0435	0.0000

UPPER STATE KA KC	LOWER STATE KA KC	OBSERVATION PREC.	CALCULATION	RESID.	UPPER STATE KA KC	LOWER STATE KA KC	OBSERVATION PREC.	CALCULATION	RESID.
(6) 19 3 17 - 18 2 16	1338 6865 0 001	1338 6864 0 0001	1339 7337 0 001	0 0001	(6) 5 5 0 - 5 5 0	1347 4307 0 000	1347 4309 0 0001	1347 4307 0 000	-0 0001
(6) 20 3 18 - 19 2 17	1339 7335 0 000	1339 7337 0 001	1340 7337 0 001	0 0000	(6) 5 5 1 - 5 5 1	1347 4307 0 000	1347 4309 0 0001	1347 4307 0 000	-0 0001
(6) 21 3 19 - 15 2 14	1340 7435 0 000	1340 7435 0 000	1340 7435 0 000	0 0003	(6) 6 10 - 6 10	1347 4432 0 000	1347 4432 0 0002	1347 4432 0 000	-0 0002
(6) 22 3 20 - 16 2 15	1340 6146 0 000	1340 6146 0 000	1340 6146 0 000	0 0004	(6) 6 11 - 6 11	1348 4705 0 000	1348 4705 0 0001	1348 4705 0 000	-0 0001
(6) 23 3 21 - 17 2 16	1340 6146 0 000	1340 6146 0 000	1340 6146 0 000	0 0004	(6) 6 12 - 6 12	1348 4792 0 000	1348 4792 0 0008	1348 4792 0 000	-0 0008
(6) 24 3 22 - 18 2 17	1340 6146 0 001	1340 6146 0 001	1340 6146 0 001	0 0002	(6) 6 13 - 6 13	1349 4448 0 000	1349 4448 0 0006	1349 4448 0 000	-0 0006
(6) 25 3 23 - 19 2 18	1341 5090 0 001	1341 5092 0 001	1341 5092 0 001	0 0002	(6) 6 14 - 6 14	1349 4448 0 000	1349 4448 0 0001	1349 4448 0 000	-0 0001
(6) 26 3 24 - 20 2 19	1342 2555 0 001	1342 2559 0 001	1342 2559 0 001	0 0005	(6) 6 15 - 6 15	1349 4448 0 000	1349 4448 0 000	1349 4448 0 000	-0 000
(6) 27 3 25 - 21 2 20	1342 7752 0 000	1342 7756 0 000	1342 7756 0 000	0 0016	(6) 6 16 - 6 16	1349 4448 0 000	1349 4448 0 0002	1349 4448 0 000	-0 0002
(6) 28 3 26 - 22 2 21	1342 7752 0 000	1342 7782 0 000	1342 7782 0 000	0 0030	(6) 6 17 - 6 17	1349 4448 0 000	1349 4448 0 000	1349 4448 0 000	-0 000
(6) 29 3 27 - 23 2 22	1342 9230 0 001	1342 9234 0 001	1342 9234 0 001	0 0004	(6) 6 18 - 6 18	1349 4448 0 000	1349 4448 0 0001	1349 4448 0 000	-0 0001
(6) 30 3 28 - 24 2 23	1343 6716 0 001	1343 6718 0 001	1343 6718 0 001	0 0002	(6) 6 19 - 6 19	1349 4448 0 000	1349 4448 0 0007	1349 4448 0 000	-0 0007
(6) 31 3 29 - 25 2 24	1344 5204 0 001	1344 5209 0 001	1344 5209 0 001	0 0005	(6) 6 20 - 6 20	1349 4448 0 000	1349 4448 0 0001	1349 4448 0 000	-0 0001
(6) 32 3 30 - 26 2 25	1344 6688 X 0 000	1344 6697 0 000	1344 6697 0 000	0 0009	(6) 6 21 - 6 21	1349 4448 0 000	1349 4448 0 0003	1349 4448 0 000	-0 0003
(6) 33 3 31 - 27 2 26	1345 2223 0 001	1345 2224 0 001	1345 2224 0 001	0 0004	(6) 6 22 - 6 22	1349 4448 0 000	1349 4448 0 0009	1349 4448 0 000	-0 0009
(6) 34 3 32 - 28 2 27	1345 1208 0 001	1345 1211 0 001	1345 1211 0 001	0 0010	(6) 6 23 - 6 23	1349 4448 0 000	1349 4448 0 0016	1349 4448 0 000	-0 0016
(6) 35 3 33 - 29 2 28	1345 2918 0 001	1345 2917 0 001	1345 2917 0 001	0 0001	(6) 6 24 - 6 24	1349 4448 0 000	1349 4448 0 0010	1349 4448 0 000	-0 0010
(6) 36 3 34 - 30 2 29	1346 5204 0 000	1346 5209 0 000	1346 5209 0 000	0 0005	(6) 6 25 - 6 25	1349 4448 0 000	1349 4448 0 0020	1349 4448 0 000	-0 0020
(6) 37 3 35 - 31 2 30	1346 6688 X 0 000	1346 6697 0 000	1346 6697 0 000	0 0009	(6) 6 26 - 6 26	1349 4448 0 000	1349 4448 0 0025	1349 4448 0 000	-0 0025
(6) 38 3 36 - 32 2 31	1346 6688 X 0 000	1346 6697 0 000	1346 6697 0 000	0 0009	(6) 6 27 - 6 27	1349 4448 0 000	1349 4448 0 0029	1349 4448 0 000	-0 0029
(6) 39 3 37 - 33 2 32	1346 8321 0 001	1346 8324 0 001	1346 8324 0 001	0 0002	(6) 6 28 - 6 28	1349 4448 0 000	1349 4448 0 0033	1349 4448 0 000	-0 0033
(6) 40 3 38 - 34 2 33	1346 1194 0 000	1346 1196 0 000	1346 1196 0 000	0 0001	(6) 6 29 - 6 29	1349 4448 0 000	1349 4448 0 0037	1349 4448 0 000	-0 0037
(6) 41 3 39 - 35 2 34	1346 1298 0 000	1346 1298 0 000	1346 1298 0 000	0 0003	(6) 6 30 - 6 30	1349 4448 0 000	1349 4448 0 0041	1349 4448 0 000	-0 0041
(6) 42 3 40 - 36 2 35	1346 3167 0 001	1346 3167 0 001	1346 3167 0 001	0 0006	(6) 6 31 - 6 31	1349 4448 0 000	1349 4448 0 0045	1349 4448 0 000	-0 0045
(6) 43 3 41 - 37 2 36	1346 3168 0 001	1346 3169 0 001	1346 3169 0 001	0 0001	(6) 6 32 - 6 32	1349 4448 0 000	1349 4448 0 0049	1349 4448 0 000	-0 0049
(6) 44 3 42 - 38 2 37	1346 3928 0 001	1346 3928 0 001	1346 3928 0 001	0 0001	(6) 6 33 - 6 33	1349 4448 0 000	1349 4448 0 0053	1349 4448 0 000	-0 0053
(6) 45 3 43 - 39 2 38	1346 8321 0 001	1346 8324 0 001	1346 8324 0 001	0 0001	(6) 6 34 - 6 34	1349 4448 0 000	1349 4448 0 0057	1349 4448 0 000	-0 0057
(6) 46 3 44 - 40 2 39	1346 8321 0 001	1346 8324 0 001	1346 8324 0 001	0 0001	(6) 6 35 - 6 35	1349 4448 0 000	1349 4448 0 0061	1349 4448 0 000	-0 0061
(6) 47 3 45 - 41 2 40	1346 8321 0 001	1346 8324 0 001	1346 8324 0 001	0 0001	(6) 6 36 - 6 36	1349 4448 0 000	1349 4448 0 0065	1349 4448 0 000	-0 0065
(6) 48 3 46 - 42 2 41	1346 8321 0 001	1346 8324 0 001	1346 8324 0 001	0 0001	(6) 6 37 - 6 37	1349 4448 0 000	1349 4448 0 0069	1349 4448 0 000	-0 0069
(6) 49 3 47 - 43 2 42	1346 8321 0 001	1346 8324 0 001	1346 8324 0 001	0 0001	(6) 6 38 - 6 38	1349 4448 0 000	1349 4448 0 0073	1349 4448 0 000	-0 0073
(6) 50 3 48 - 44 2 43	1346 8321 0 001	1346 8324 0 001	1346 8324 0 001	0 0001	(6) 6 39 - 6 39	1349 4448 0 000	1349 4448 0 0077	1349 4448 0 000	-0 0077
(6) 51 3 49 - 45 2 44	1346 8321 0 001	1346 8324 0 001	1346 8324 0 001	0 0001	(6) 6 40 - 6 40	1349 4448 0 000	1349 4448 0 0081	1349 4448 0 000	-0 0081
(6) 52 3 50 - 46 2 45	1346 8321 0 001	1346 8324 0 001	1346 8324 0 001	0 0001	(6) 6 41 - 6 41	1349 4448 0 000	1349 4448 0 0085	1349 4448 0 000	-0 0085
(6) 53 3 51 - 47 2 46	1346 8321 0 001	1346 8324 0 001	1346 8324 0 001	0 0001	(6) 6 42 - 6 42	1349 4448 0 000	1349 4448 0 0089	1349 4448 0 000	-0 0089
(6) 54 3 52 - 48 2 47	1346 8321 0 001	1346 8324 0 001	1346 8324 0 001	0 0001	(6) 6 43 - 6 43	1349 4448 0 000	1349 4448 0 0093	1349 4448 0 000	-0 0093
(6) 55 3 53 - 49 2 48	1346 8321 0 001	1346 8324 0 001	1346 8324 0 001	0 0001	(6) 6 44 - 6 44	1349 4448 0 000	1349 4448 0 0097	1349 4448 0 000	-0 0097
(6) 56 3 54 - 50 2 49	1346 8321 0 001	1346 8324 0 001	1346 8324 0 001	0 0001	(6) 6 45 - 6 45	1349 4448 0 000	1349 4448 0 0101	1349 4448 0 000	-0 0101
(6) 57 3 55 - 51 2 50	1346 8321 0 001	1346 8324 0 001	1346 8324 0 001	0 0001	(6) 6 46 - 6 46	1349 4448 0 000	1349 4448 0 0105	1349 4448 0 000	-0 0105
(6) 58 3 56 - 52 2 51	1346 8321 0 001	1346 8324 0 001	1346 8324 0 001	0 0001	(6) 6 47 - 6 47	1349 4448 0 000	1349 4448 0 0109	1349 4448 0 000	-0 0109
(6) 59 3 57 - 53 2 52	1346 8321 0 001	1346 8324 0 001	1346 8324 0 001	0 0001	(6) 6 48 - 6 48	1349 4448 0 000	1349 4448 0 0113	1349 4448 0 000	-0 0113
(6) 60 3 58 - 54 2 53	1346 8321 0 001	1346 8324 0 001	1346 8324 0 001	0 0001	(6) 6 49 - 6 49	1349 4448 0 000	1349 4448 0 0117	1349 4448 0 000	-0 0117
(6) 61 3 59 - 55 2 54	1346 8321 0 001	1346 8324 0 001	1346 8324 0 001	0 0001	(6) 6 50 - 6 50	1349 4448 0 000	1349 4448 0 0121	1349 4448 0 000	-0 0121
(6) 62 3 60 - 56 2 55	1346 8321 0 001	1346 8324 0 001	1346 8324 0 001	0 0001	(6) 6 51 - 6 51	1349 4448 0 000	1349 4448 0 0125	1349 4448 0 000	-0 0125
(6) 63 3 61 - 57 2 56	1346 8321 0 001	1346 8324 0 001	1346 8324 0 001	0 0001	(6) 6 52 - 6 52	1349 4448 0 000	1349 4448 0 0129	1349 4448 0 000	-0 0129
(6) 64 3 62 - 58 2 57	1346 8321 0 001	1346 8324 0 001	1346 8324 0 001	0 0001	(6) 6 53 - 6 53	1349 4448 0 000	1349 4448 0 0133	1349 4448 0 000	-0 0133
(6) 65 3 63 - 59 2 58	1346 8321 0 001	1346 8324 0 001	1346 8324 0 001	0 0001	(6) 6 54 - 6 54	1349 4448 0 000	1349 4448 0 0137	1349 4448 0 000	-0 0137
(6) 66 3 64 - 60 2 59	1346 8321 0 001	1346 8324 0 001	1346 8324 0 001	0 0001	(6) 6 55 - 6 55	1349 4448 0 000	1349 4448 0 0141	1349 4448 0 000	-0 0141
(6) 67 3 65 - 61 2 60	1346 8321 0 001	1346 8324 0 001	1346 8324 0 001	0 0001	(6) 6 56 - 6 56	1349 4448 0 000	1349 4448 0 0145	1349 4448 0 000	-0 0145
(6) 68 3 66 - 62 2 61	1346 8321 0 001	1346 8324 0 001	1346 8324 0 001	0 0001	(6) 6 57 - 6 57	1349 4448 0 000	1349 4448 0 0149	1349 4448 0 000	-0 0149
(6) 69 3 67 - 63 2 62	1346 8321 0 001	1346 8324 0 001	1346 8324 0 001	0 0001	(6) 6 58 - 6 58	1349 4448 0 000	1349 4448 0 0153	1349 4448 0 000	-0 0153
(6) 70 3 68 - 64 2 63	1346 8321 0 001	1346 8324 0 001	1346 8324 0 001	0 0001	(6) 6 59 - 6 59	1349 4448 0 000	1349 4448 0 0157	1349 4448 0 000	-0 0157
(6) 71 3 69 - 65 2 64	1346 8321 0 001	1346 8324 0 001	1346 8324 0 001	0 0001	(6) 6 60 - 6 60	1349 4448 0 000	1349 4448 0 0161	1349 4448 0 000	-0 0161
(6) 72 3 70 - 66 2 65	1346 8321 0 001	1346 8324 0 001	1346 8324 0 001	0 0001	(6) 6 61 - 6 61	1349 4448 0 000	1349 4448 0 0165	1349 4448 0 000	-0 0165
(6) 73 3 71 - 67 2 66	1346 8321 0 001	1346 8324 0 001	1346 8324 0 001	0 0001	(6) 6 62 - 6 62	1349 4448 0 000	1349 4448 0 0169	1349 4448 0 000	-0 0169
(6) 74 3 72 - 68 2 67	1346 8321 0 001	1346 8324 0 001	1346 8324 0 001	0 0001	(6) 6 63 - 6 63	1349 4448 0 000	1349 4448 0 0173	1349 4448 0 000	-0 0173
(6) 75 3 73 - 69 2 68	1346 8321 0 001	1346 8324 0 001	1346 8324 0 001	0 0001	(6) 6 64 - 6 64	1349 4448 0 000	1349 4448 0 0177	1349 4448 0 000	-0 0177
(6) 76 3 74 - 70 2 69	1346 8321 0 001	1346 8324 0 001	1346 8324 0 001	0 0001	(6) 6 65 - 6 65	1349 4448 0 000	1349 4448 0 018		

UPPER STATE KA KG	LOWER STATE KA KG	OBSERVATION PREC.	CALCULATION	RESID.	UPPER STATE KA KC	LOWER STATE KA KC	OBSERVATION PREC.	CALCULATION	RESID.	UPPER STATE KA KC	LOWER STATE KA KC	OBSERVATION PREC.	CALCULATION	RESID.
(6) 9 5 4 - 8 4 5	1368.9998 0.000	1369.0000 - 0.0002	1369.025 - 0.0006	- 0.0006	(6) 28 9 25 - 27 3 24	1379.6139 0.001	1379.6155 - 0.0016	1379.8802 0.001	0.0009	1379.8802 0.0009	1379.8802 0.0009	1379.8802 0.0009	1379.8802 0.0009	0.0009
(6) 20 6 14 - 20 5 15	1369.2480 0.001	1369.2486 - 0.0006	1369.3041 0.001	- 0.0006	(6) 24 4 20 - 23 3 21	1379.8802 0.001	1379.8802 0.0009	1380.5201 0.0001	- 0.0024	1380.5201 0.0001	1380.5201 0.0001	1380.5201 0.0001	1380.5201 0.0001	0.0003
(6) 20 6 15 - 19 5 14	1369.3041 0.001	1369.3045 - 0.0006	1369.3593 0.001	- 0.0006	(6) 14 5 9 - 13 4 10	1380.5201 0.0001	1380.5207 0.0001	1382.3505 0.0001	- 0.0003	1382.3505 0.0001	1382.3505 0.0001	1382.3505 0.0001	1382.3505 0.0001	0.0003
(6) 19 6 14 - 19 5 15	1369.5393 0.001	1369.5398 - 0.0002	1369.5838 0.001	- 0.0002	(6) 21 5 11 - 24 3 22	1382.3505 0.0001	1382.3507 0.0001	1382.7622 0.0001	- 0.0002	1382.7622 0.0001	1382.7622 0.0001	1382.7622 0.0001	1382.7622 0.0001	0.0002
(6) 19 6 14 - 19 5 15	1369.5838 0.001	1369.5840 - 0.0002	1369.8100 0.001	- 0.0002	(6) 15 5 11 - 16 4 10	1382.7624 0.0001	1382.7624 0.0001	1382.7624 0.0001	- 0.0001	1382.7624 0.0001	1382.7624 0.0001	1382.7624 0.0001	1382.7624 0.0001	0.0001
(6) 18 6 12 - 18 5 13	1369.8100 0.001	1369.8106 - 0.0003	1369.8449 0.001	- 0.0003	(6) 15 5 10 - 14 4 11	1382.7695 0.0001	1382.7695 0.0001	1382.7695 0.0001	- 0.0001	1382.7695 0.0001	1382.7695 0.0001	1382.7695 0.0001	1382.7695 0.0001	0.0001
(6) 17 6 12 - 17 5 13	1369.8449 0.001	1369.8452 - 0.0003	1370.0593 0.001	- 0.0005	(6) 22 5 22 - 25 3 23	1384.8861 0.0001	1384.8864 0.0001	1384.8864 0.0001	- 0.0003	1384.8864 0.0001	1384.8864 0.0001	1384.8864 0.0001	1384.8864 0.0001	0.0003
(6) 17 6 12 - 17 5 13	1370.0593 0.001	1370.0598 - 0.0005	1370.0881 0.001	- 0.0004	(6) 14 5 12 - 15 4 11	1385.0005 0.0001	1385.0009 0.0001	1385.0009 0.0001	- 0.0001	1385.0009 0.0001	1385.0009 0.0001	1385.0009 0.0001	1385.0009 0.0001	0.0001
(6) 16 6 10 - 16 5 12	1370.0881 0.001	1370.0885 - 0.0006	1370.2689 0.001	- 0.0006	(6) 16 5 11 - 17 4 10	1385.0134 0.0001	1386.3467 0.0001	1386.3467 0.0001	- 0.0002	1386.3467 0.0001	1386.3467 0.0001	1386.3467 0.0001	1386.3467 0.0001	0.0002
(6) 16 6 10 - 16 5 12	1370.2689 0.001	1370.3161 - 0.0003	1370.3139 0.001	- 0.0003	(6) 6 0 - 6 1 - 6 2	1386.3473 0.0001	1386.3473 0.0001	1386.3473 0.0001	- 0.0006	1386.3473 0.0001	1386.3473 0.0001	1386.3473 0.0001	1386.3473 0.0001	0.0006
(6) 16 6 10 - 16 5 12	1370.3139 0.001	1370.3142 - 0.0004	1370.4416 0.001	- 0.0004	(6) 6 1 - 6 2 - 6 3	1386.3475 0.0001	1386.3475 0.0001	1386.3475 0.0001	- 0.0006	1386.3475 0.0001	1386.3475 0.0001	1386.3475 0.0001	1386.3475 0.0001	0.0006
(6) 15 6 16 - 15 5 17	1370.4416 0.001	1370.4419 - 0.0004	1370.4990 0.001	- 0.0004	(6) 6 1 - 6 2 - 6 3	1386.3477 0.0001	1386.3477 0.0001	1386.3477 0.0001	- 0.0006	1386.3477 0.0001	1386.3477 0.0001	1386.3477 0.0001	1386.3477 0.0001	0.0006
(6) 15 6 16 - 15 5 17	1370.4990 0.001	1370.4994 - 0.0003	1370.5215 0.001	- 0.0003	(6) 6 1 - 6 2 - 6 3	1386.3479 0.0001	1386.3479 0.0001	1386.3479 0.0001	- 0.0006	1386.3479 0.0001	1386.3479 0.0001	1386.3479 0.0001	1386.3479 0.0001	0.0006
(6) 15 6 16 - 15 5 17	1370.5215 0.001	1370.5219 - 0.0003	1370.6309 0.001	- 0.0003	(6) 6 1 - 6 2 - 6 3	1386.3481 0.0001	1386.3481 0.0001	1386.3481 0.0001	- 0.0006	1386.3481 0.0001	1386.3481 0.0001	1386.3481 0.0001	1386.3481 0.0001	0.0006
(6) 15 6 16 - 15 5 17	1370.6309 0.001	1370.6856 0.001	1370.6856 0.001	- 0.0006	(6) 6 1 - 6 2 - 6 3	1386.3483 0.0001	1386.3483 0.0001	1386.3483 0.0001	- 0.0006	1386.3483 0.0001	1386.3483 0.0001	1386.3483 0.0001	1386.3483 0.0001	0.0006
(6) 15 6 16 - 15 5 17	1370.6856 0.001	1370.7103 0.001	1370.7103 0.001	- 0.0002	(6) 6 1 - 6 2 - 6 3	1386.3485 0.0001	1386.3485 0.0001	1386.3485 0.0001	- 0.0006	1386.3485 0.0001	1386.3485 0.0001	1386.3485 0.0001	1386.3485 0.0001	0.0006
(6) 15 6 16 - 15 5 17	1370.7103 0.001	1370.7117 0.001	1370.8312 0.001	- 0.0003	(6) 6 1 - 6 2 - 6 3	1386.3487 0.0001	1386.3487 0.0001	1386.3487 0.0001	- 0.0006	1386.3487 0.0001	1386.3487 0.0001	1386.3487 0.0001	1386.3487 0.0001	0.0006
(6) 15 6 16 - 15 5 17	1370.8312 0.001	1370.8317 0.001	1370.8713 0.001	- 0.0003	(6) 6 1 - 6 2 - 6 3	1386.3489 0.0001	1386.3489 0.0001	1386.3489 0.0001	- 0.0006	1386.3489 0.0001	1386.3489 0.0001	1386.3489 0.0001	1386.3489 0.0001	0.0006
(6) 15 6 16 - 15 5 17	1370.8713 0.001	1370.8717 0.001	1371.1685 0.001	- 0.0003	(6) 6 1 - 6 2 - 6 3	1386.3491 0.0001	1386.3491 0.0001	1386.3491 0.0001	- 0.0006	1386.3491 0.0001	1386.3491 0.0001	1386.3491 0.0001	1386.3491 0.0001	0.0006
(6) 15 6 16 - 15 5 17	1371.1685 0.001	1371.1697 0.001	1371.2106 0.001	- 0.0003	(6) 6 1 - 6 2 - 6 3	1386.3493 0.0001	1386.3493 0.0001	1386.3493 0.0001	- 0.0006	1386.3493 0.0001	1386.3493 0.0001	1386.3493 0.0001	1386.3493 0.0001	0.0006
(6) 15 6 16 - 15 5 17	1371.2106 0.001	1371.2625 0.001	1371.2647 0.001	- 0.0003	(6) 6 1 - 6 2 - 6 3	1386.3495 0.0001	1386.3495 0.0001	1386.3495 0.0001	- 0.0006	1386.3495 0.0001	1386.3495 0.0001	1386.3495 0.0001	1386.3495 0.0001	0.0006
(6) 15 6 16 - 15 5 17	1371.2647 0.001	1371.2660 0.001	1371.2667 0.001	- 0.0003	(6) 6 1 - 6 2 - 6 3	1386.3497 0.0001	1386.3497 0.0001	1386.3497 0.0001	- 0.0006	1386.3497 0.0001	1386.3497 0.0001	1386.3497 0.0001	1386.3497 0.0001	0.0006
(6) 15 6 16 - 15 5 17	1371.2667 0.001	1371.2774 0.001	1371.3277 0.001	- 0.0003	(6) 6 1 - 6 2 - 6 3	1386.3499 0.0001	1386.3499 0.0001	1386.3499 0.0001	- 0.0006	1386.3499 0.0001	1386.3499 0.0001	1386.3499 0.0001	1386.3499 0.0001	0.0006
(6) 15 6 16 - 15 5 17	1371.3277 0.001	1371.3280 0.001	1371.3633 0.001	- 0.0005	(6) 6 1 - 6 2 - 6 3	1386.3501 0.0001	1386.3503 0.0001	1386.3503 0.0001	- 0.0006	1386.3503 0.0001	1386.3503 0.0001	1386.3503 0.0001	1386.3503 0.0001	0.0006
(6) 15 6 16 - 15 5 17	1371.3633 0.001	1371.3636 0.001	1371.3833 0.001	- 0.0004	(6) 6 1 - 6 2 - 6 3	1386.3505 0.0001	1386.3507 0.0001	1386.3507 0.0001	- 0.0006	1386.3507 0.0001	1386.3507 0.0001	1386.3507 0.0001	1386.3507 0.0001	0.0006
(6) 15 6 16 - 15 5 17	1371.3833 0.001	1371.3987 0.001	1371.4987 0.001	- 0.0004	(6) 6 1 - 6 2 - 6 3	1386.3509 0.0001	1386.3511 0.0001	1386.3511 0.0001	- 0.0006	1386.3511 0.0001	1386.3511 0.0001	1386.3511 0.0001	1386.3511 0.0001	0.0006
(6) 15 6 16 - 15 5 17	1371.4987 0.001	1371.4987 0.001	1371.6987 0.001	- 0.0004	(6) 6 1 - 6 2 - 6 3	1386.3513 0.0001	1386.3515 0.0001	1386.3515 0.0001	- 0.0006	1386.3515 0.0001	1386.3515 0.0001	1386.3515 0.0001	1386.3515 0.0001	0.0006
(6) 15 6 16 - 15 5 17	1371.6987 0.001	1371.6987 0.001	1371.6990 0.001	- 0.0004	(6) 6 1 - 6 2 - 6 3	1386.3517 0.0001	1386.3519 0.0001	1386.3519 0.0001	- 0.0006	1386.3519 0.0001	1386.3519 0.0001	1386.3519 0.0001	1386.3519 0.0001	0.0006
(6) 15 6 16 - 15 5 17	1371.6990 0.001	1371.6994 0.001	1371.6995 0.001	- 0.0004	(6) 6 1 - 6 2 - 6 3	1386.3521 0.0001	1386.3523 0.0001	1386.3523 0.0001	- 0.0006	1386.3523 0.0001	1386.3523 0.0001	1386.3523 0.0001	1386.3523 0.0001	0.0006
(6) 15 6 16 - 15 5 17	1371.6995 0.001	1371.6995 0.001	1371.6996 0.001	- 0.0004	(6) 6 1 - 6 2 - 6 3	1386.3525 0.0001	1386.3527 0.0001	1386.3527 0.0001	- 0.0006	1386.3527 0.0001	1386.3527 0.0001	1386.3527 0.0001	1386.3527 0.0001	0.0006
(6) 15 6 16 - 15 5 17	1371.6996 0.001	1371.6996 0.001	1371.7000 0.001	- 0.0004	(6) 6 1 - 6 2 - 6 3	1386.3529 0.0001	1386.3531 0.0001	1386.3531 0.0001	- 0.0006	1386.3531 0.0001	1386.3531 0.0001	1386.3531 0.0001	1386.3531 0.0001	0.0006
(6) 15 6 16 - 15 5 17	1371.7000 0.001	1371.7004 0.001	1371.7004 0.001	- 0.0004	(6) 6 1 - 6 2 - 6 3	1386.3533 0.0001	1386.3535 0.0001	1386.3535 0.0001	- 0.0006	1386.3535 0.0001	1386.3535 0.0001	1386.3535 0.0001	1386.3535 0.0001	0.0006
(6) 15 6 16 - 15 5 17	1371.7004 0.001	1371.7004 0.001	1371.7008 0.001	- 0.0004	(6) 6 1 - 6 2 - 6 3	1386.3537 0.0001	1386.3539 0.0001	1386.3539 0.0001	- 0.0006	1386.3539 0.0001	1386.3539 0.0001	1386.3539 0.0001	1386.3539 0.0001	0.0006
(6) 15 6 16 - 15 5 17	1371.7008 0.001	1371.7008 0.001	1371.7012 0.001	- 0.0004	(6) 6 1 - 6 2 - 6 3	1386.3541 0.0001	1386.3543 0.0001	1386.3543 0.0001	- 0.0006	1386.3543 0.0001	1386.3543 0.0001	1386.3543 0.0001	1386.3543 0.0001	0.0006
(6) 15 6 16 - 15 5 17	1371.7012 0.001	1371.7016 0.001	1371.7016 0.001	- 0.0004	(6) 6 1 - 6 2 - 6 3	1386.3545 0.0001	1386.3547 0.0001	1386.3547 0.0001	- 0.0006	1386.3547 0.0001	1386.3547 0.0001	1386.3547 0.0001	1386.3547 0.0001	0.0006
(6) 15 6 16 - 15 5 17	1371.7016 0.001	1371.7016 0.001	1371.7020 0.001	- 0.0004	(6) 6 1 - 6 2 - 6 3	1386.3549 0.0001	1386.3551 0.0001	1386.3551 0.0001	- 0.0006	1386.3551 0.0001	1386.3551 0.0001	1386.3551 0.0001	1386.3551 0.0001	0.0006
(6) 15 6 16 - 15 5 17	1371.7020 0.001	1371.7024 0.001	1371.7024 0.001	- 0.0004	(6) 6 1 - 6 2 - 6 3	1386.3553 0.0001	1386.3555 0.0001	1386.3555 0.0001	- 0.0006	1386.3555 0.0001	1386.3555 0.0001	1386.3555 0.0001	1386.3555 0.0001	0.0006
(6) 15 6 16 - 15														

UPPER STATE		LOWER STATE		OBSERVATION	PREC.	CALCULATION	RESID.	UPPER STATE	LOWER STATE	OBSERVATION	PREC.	CALCULATION	RESID.	UPPER STATE	LOWER STATE	OBSERVATION	PREC.	CALCULATION	RESID.
K	J	K	J	K	J	K	J	K	J	K	J	K	J	K	J	K	J	K	J
K22		J16		K17		J17		K17		J17		K17		J17		K17		J17	
K23		J17		K18		J18		K18		J18		K18		J18		K18		J18	
K24		J17		K18		J18		K18		J18		K18		J18		K18		J18	
K25		J17		K18		J18		K18		J18		K18		J18		K18		J18	
K26		J17		K18		J18		K18		J18		K18		J18		K18		J18	
K27		J17		K18		J18		K18		J18		K18		J18		K18		J18	
K28		J17		K18		J18		K18		J18		K18		J18		K18		J18	
K29		J17		K18		J18		K18		J18		K18		J18		K18		J18	
K30		J17		K18		J18		K18		J18		K18		J18		K18		J18	
K31		J17		K18		J18		K18		J18		K18		J18		K18		J18	
K32		J17		K18		J18		K18		J18		K18		J18		K18		J18	
K33		J17		K18		J18		K18		J18		K18		J18		K18		J18	
K34		J17		K18		J18		K18		J18		K18		J18		K18		J18	
K35		J17		K18		J18		K18		J18		K18		J18		K18		J18	
K36		J17		K18		J18		K18		J18		K18		J18		K18		J18	
K37		J17		K18		J18		K18		J18		K18		J18		K18		J18	
K38		J17		K18		J18		K18		J18		K18		J18		K18		J18	
K39		J17		K18		J18		K18		J18		K18		J18		K18		J18	
K40		J17		K18		J18		K18		J18		K18		J18		K18		J18	
K41		J17		K18		J18		K18		J18		K18		J18		K18		J18	
K42		J17		K18		J18		K18		J18		K18		J18		K18		J18	
K43		J17		K18		J18		K18		J18		K18		J18		K18		J18	
K44		J17		K18		J18		K18		J18		K18		J18		K18		J18	
K45		J17		K18		J18		K18		J18		K18		J18		K18		J18	
K46		J17		K18		J18		K18		J18		K18		J18		K18		J18	
K47		J17		K18		J18		K18		J18		K18		J18		K18		J18	
K48		J17		K18		J18		K18		J18		K18		J18		K18		J18	
K49		J17		K18		J18		K18		J18		K18		J18		K18		J18	
K50		J17		K18		J18		K18		J18		K18		J18		K18		J18	
K51		J17		K18		J18		K18		J18		K18		J18		K18		J18	
K52		J17		K18		J18		K18		J18		K18		J18		K18		J18	
K53		J17		K18		J18		K18		J18		K18		J18		K18		J18	
K54		J17		K18		J18		K18		J18		K18		J18		K18		J18	
K55		J17		K18		J18		K18		J18		K18		J18		K18		J18	
K56		J17		K18		J18		K18		J18		K18		J18		K18		J18	
K57		J17		K18		J18		K18		J18		K18		J18		K18		J18	
K58		J17		K18		J18		K18		J18		K18		J18		K18		J18	
K59		J17		K18		J18		K18		J18		K18		J18		K18		J18	
K60		J17		K18		J18		K18		J18		K18		J18		K18		J18	
K61		J17		K18		J18		K18		J18		K18		J18		K18		J18	
K62		J17																	

UPPER STATE		LOWER STATE		OBSERVATION	PREC.	CALCULATION	RESID.	UPPER STATE		LOWER STATE		OBSERVATION	PREC.	CALCULATION	RESID.	
J	KA	KC	J	KA	KC	J	KA	KC	J	KA	KC	J	KA	KC	J	
1	1	2	1	1	2	-0.0001	1492.7444	-0.0001	1501.4049	0.0000	1501.4049	0.0000	0.0000	0.0000	1501.4049	0.0000
1	1	3	1	1	3	-0.0002	1492.9177	-0.0002	1501.4906	0.0000	1501.4906	0.0000	0.0003	0.0003	1501.4906	0.0000
1	1	4	1	1	4	-0.0002	1493.0511	-0.0002	1501.4906	0.0000	1501.4906	0.0000	0.0002	0.0002	1501.4906	0.0000
1	1	5	1	1	5	-0.0003	1493.1296	-0.0003	1501.5861	0.0000	1501.5861	0.0000	0.0006	0.0006	1501.5861	0.0000
1	1	6	1	1	6	-0.0002	1493.1387	-0.0002	1501.5861	0.0000	1501.5861	0.0000	0.0023	0.0023	1501.5861	0.0000
1	1	7	1	1	7	-0.0002	1493.1910	-0.0002	1501.6929	0.0000	1501.6929	0.0000	0.0001	0.0001	1501.6929	0.0000
1	1	8	1	1	8	-0.0002	1494.4843	-0.0002	1501.6929	0.0000	1501.6929	0.0000	0.0004	0.0004	1501.6929	0.0000
1	1	9	1	1	9	-0.0001	1495.2254	-0.0001	1501.6999	0.0001	1501.6999	0.0001	0.0004	0.0004	1501.6999	0.0001
1	1	0	1	1	0	-0.0003	1495.3252	-0.0003	1501.7642	0.0001	1501.7642	0.0001	0.0001	0.0001	1501.7642	0.0001
1	1	1	1	1	1	-0.0002	1495.5355	-0.0002	1501.7642	0.0001	1501.7643	0.0001	0.0001	0.0001	1501.7643	0.0001
1	1	2	1	1	2	-0.0003	1495.7605	-0.0003	1501.8066	0.0000	1501.8066	0.0000	0.0014	0.0014	1501.8066	0.0000
1	1	3	1	1	3	-0.0001	1496.8786	-0.0001	1501.8389	0.0001	1501.8389	0.0001	0.0035	0.0035	1501.8389	0.0001
1	1	4	1	1	4	-0.0001	1497.7451	-0.0001	1501.9244	0.0001	1501.9244	0.0001	0.0001	0.0001	1501.9244	0.0001
1	1	5	1	1	5	-0.0001	1497.8368	-0.0001	1501.9244	0.0001	1501.9244	0.0001	0.0001	0.0001	1501.9244	0.0001
1	1	6	1	1	6	-0.0001	1498.6355	-0.0001	1501.9244	0.0001	1501.9244	0.0001	0.0001	0.0001	1501.9244	0.0001
1	1	7	1	1	7	-0.0001	1499.2742	-0.0001	1501.9244	0.0001	1501.9244	0.0001	0.0001	0.0001	1501.9244	0.0001
1	1	8	1	1	8	-0.0001	1499.7532	-0.0001	1501.9244	0.0001	1501.9244	0.0001	0.0001	0.0001	1501.9244	0.0001
1	1	9	1	1	9	-0.0001	1499.7532	-0.0001	1501.9244	0.0001	1501.9244	0.0001	0.0001	0.0001	1501.9244	0.0001
1	1	0	1	1	0	-0.0002	1499.7532	-0.0002	1501.9244	0.0001	1501.9244	0.0001	0.0001	0.0001	1501.9244	0.0001
1	1	1	1	1	1	-0.0002	1500.4062	-0.0002	1502.0202	0.0001	1502.0202	0.0001	0.0002	0.0002	1502.0202	0.0001
1	1	2	1	1	2	-0.0002	1500.4065	-0.0002	1502.0202	0.0001	1502.0202	0.0001	0.0002	0.0002	1502.0202	0.0001
1	1	3	1	1	3	-0.0005	1500.7334	-0.0005	1502.0202	0.0001	1502.0202	0.0001	0.0004	0.0004	1502.0202	0.0001
1	1	4	1	1	4	-0.0005	1500.7334	-0.0005	1502.0202	0.0001	1502.0202	0.0001	0.0004	0.0004	1502.0202	0.0001
1	1	5	1	1	5	-0.0005	1500.7557	-0.0005	1502.0202	0.0001	1502.0202	0.0001	0.0004	0.0004	1502.0202	0.0001
1	1	6	1	1	6	-0.0004	1500.7679	-0.0004	1502.0202	0.0001	1502.0202	0.0001	0.0004	0.0004	1502.0202	0.0001
1	1	7	1	1	7	-0.0004	1500.7679	-0.0004	1502.0202	0.0001	1502.0202	0.0001	0.0004	0.0004	1502.0202	0.0001
1	1	8	1	1	8	-0.0004	1500.8112	-0.0004	1502.0202	0.0001	1502.0202	0.0001	0.0004	0.0004	1502.0202	0.0001
1	1	9	1	1	9	-0.0004	1500.8632	-0.0004	1502.0202	0.0001	1502.0202	0.0001	0.0004	0.0004	1502.0202	0.0001
1	1	0	1	1	0	-0.0009	1500.8651	-0.0009	1502.0202	0.0001	1502.0202	0.0001	0.0004	0.0004	1502.0202	0.0001
1	1	1	1	1	1	-0.0003	1500.9196	-0.0003	1502.0202	0.0001	1502.0202	0.0001	0.0001	0.0001	1502.0202	0.0001
1	1	2	1	1	2	-0.0003	1500.9237	-0.0003	1502.0202	0.0001	1502.0202	0.0001	0.0001	0.0001	1502.0202	0.0001
1	1	3	1	1	3	-0.0003	1500.9837	-0.0003	1502.0202	0.0001	1502.0202	0.0001	0.0002	0.0002	1502.0202	0.0001
1	1	4	1	1	4	-0.0006	1501.0060	-0.0006	1502.0202	0.0001	1502.0202	0.0001	0.0005	0.0005	1502.0202	0.0001
1	1	5	1	1	5	-0.0019	1501.0519	-0.0019	1502.0202	0.0001	1502.0202	0.0001	0.0005	0.0005	1502.0202	0.0001
1	1	6	1	1	6	-0.0006	1501.0961	-0.0006	1502.0202	0.0001	1502.0202	0.0001	0.0006	0.0006	1502.0202	0.0001
1	1	7	1	1	7	-0.0006	1501.1194	-0.0006	1502.0202	0.0001	1502.0202	0.0001	0.0006	0.0006	1502.0202	0.0001
1	1	8	1	1	8	-0.0006	1501.1594	-0.0006	1502.0202	0.0001	1502.0202	0.0001	0.0006	0.0006	1502.0202	0.0001
1	1	9	1	1	9	-0.0006	1501.1594	-0.0006	1502.0202	0.0001	1502.0202	0.0001	0.0006	0.0006	1502.0202	0.0001
1	1	0	1	1	0	-0.0006	1501.1667	-0.0006	1502.0202	0.0001	1502.0202	0.0001	0.0006	0.0006	1502.0202	0.0001
1	1	1	1	1	1	-0.0006	1501.1892	-0.0006	1502.0202	0.0001	1502.0202	0.0001	0.0006	0.0006	1502.0202	0.0001
1	1	2	1	1	2	-0.0006	1501.2062	-0.0006	1502.0202	0.0001	1502.0202	0.0001	0.0006	0.0006	1502.0202	0.0001
1	1	3	1	1	3	-0.0006	1501.2650	-0.0006	1502.0202	0.0001	1502.0202	0.0001	0.0006	0.0006	1502.0202	0.0001
1	1	4	1	1	4	-0.0006	1501.2799	-0.0006	1502.0202	0.0001	1502.0202	0.0001	0.0006	0.0006	1502.0202	0.0001
1	1	5	1	1	5	-0.0006	1501.3168	-0.0006	1502.0202	0.0001	1502.0202	0.0001	0.0006	0.0006	1502.0202	0.0001
1	1	6	1	1	6	-0.0006	1501.3292	-0.0006	1502.0202	0.0001	1502.0202	0.0001	0.0006	0.0006	1502.0202	0.0001
1	1	7	1	1	7	-0.0006	1501.3859	-0.0006	1502.0202	0.0001	1502.0202	0.0001	0.0006	0.0006	1502.0202	0.0001
1	1	8	1	1	8	-0.0006	1501.4047	-0.0006	1502.0202	0.0001	1502.0202	0.0001	0.0006	0.0006	1502.0202	0.0001

UPPER STATE			LOWER STATE			OBSERVATION PREC.	CALCULATION	RESID.	UPPER STATE	LOWER STATE	OBSERVATION PREC.	CALCULATION	RESID.	
J	KA	KC	J	KA	KC	J	KA	KC	J	KA	KC	J	KA	KC
15	17	6	11	-	16	6	10	1545.2649	0.001	1545.2635	0.0014	1554.4377	-0.0007	
15	18	3	16	-	17	5	15	1546.0774	0.001	1546.0773	0.0002	1554.5051	0.0002	
15	17	7	11	-	16	7	10	1546.2610	0.001	1546.2590	0.0021	1554.5367	-0.0014	
15	17	7	10	-	16	7	9	1546.2590	0.001	1546.2590	0.0021	1554.9638	-0.0009	
15	17	7	10	-	16	7	9	1546.3790	0.001	1546.3790	0.0004	1555.0621	-0.0012	
15	17	7	10	-	16	7	9	1546.3790	0.001	1546.3790	0.0008	1555.0591	-0.0031	
15	18	2	15	-	17	1	19	1546.5114	0.001	1546.5110	0.001	1555.4000	0.0006	
15	18	2	15	-	17	1	19	1546.5198	0.001	1546.5206	0.0010	1555.7340	0.0014	
15	18	4	15	-	17	4	15	1546.5226	0.001	1546.5537	0.0005	1555.9291	0.0023	
15	18	4	15	-	17	3	14	1546.5228	0.001	1546.5933	0.0005	1555.9292	0.0022	
15	18	3	15	-	17	3	14	1546.8107	0.0007	1546.8107	0.0007	1556.0685	0.0000	
15	18	2	20	-	19	2	19	1546.8109	0.0003	1546.8109	0.0008	1556.5389	0.0000	
15	18	5	13	-	17	5	13	1547.1101	0.001	1547.1109	0.0008	1556.9121	0.0001	
15	18	5	13	-	17	5	12	1547.1101	0.001	1547.2266	0.0005	1557.0951	0.0005	
15	18	2	18	-	17	2	15	1547.4223	0.001	1547.4208	0.0017	1557.2348	0.0001	
15	18	6	15	-	17	6	12	1547.9145	0.001	1547.9128	0.0017	1557.6092*	0.0023	
15	18	6	15	-	17	6	12	1547.9145	0.001	1547.9128	0.0017	1557.7294	0.0001	
15	18	6	15	-	17	6	12	1548.7018	0.0002	1548.7018	0.0006	1557.7356	0.0001	
15	18	6	15	-	17	6	12	1548.7020	0.0001	1548.7372	0.0006	1557.8193	-0.0009	
15	18	7	17	-	18	7	17	1548.7377	0.001	1548.8477	0.0014	1557.8418	-0.0001	
15	18	7	17	-	18	7	17	1548.9395	0.001	1548.9381	0.0014	1558.4127	-0.0020	
15	18	6	15	-	17	6	12	1548.9395	0.001	1548.9381	0.0014	1558.6261	0.0025	
15	18	6	15	-	17	6	12	1548.7007	0.0001	1548.7018	0.0006	1558.6236	0.0003	
15	18	6	15	-	17	6	12	1548.7020	0.0001	1548.7372	0.0006	1559.0553	0.0003	
15	18	7	17	-	18	7	17	1548.8477	0.001	1548.8477	0.0014	1559.3092	0.0001	
15	18	7	17	-	18	7	17	1548.9381	0.001	1548.9381	0.0014	1559.7614	0.0002	
15	18	6	15	-	17	6	12	1548.9381	0.001	1548.9381	0.0014	1559.8078	0.0001	
15	18	6	15	-	17	6	12	1549.0550	0.0001	1549.0556	0.0006	1559.9516	0.0001	
15	18	6	15	-	17	6	12	1549.0550	0.0001	1549.0556	0.0008	1560.4119	-0.0005	
15	18	7	17	-	18	7	17	1549.1495	0.001	1549.1495	0.0011	1560.4211	-0.0010	
15	18	7	17	-	18	7	17	1549.1495	0.001	1549.1495	0.0011	1560.7032	-0.0002	
15	18	6	15	-	17	6	12	1549.1495	0.001	1549.1495	0.0011	1560.7281	-0.0007	
15	18	6	15	-	17	6	12	1549.1495	0.001	1549.1495	0.0011	1561.2215	-0.0007	
15	18	7	17	-	18	7	17	1549.1496	0.001	1549.1496	0.0011	1561.6964	0.0001	
15	18	7	17	-	18	7	17	1549.1496	0.001	1549.1496	0.0014	1561.7719	0.0003	
15	18	6	15	-	17	6	12	1549.1496	0.001	1549.1496	0.0017	1562.0421	-0.0002	
15	18	6	15	-	17	6	12	1549.1497	0.001	1549.1497	0.0011	1562.4349	-0.0015	
15	18	7	17	-	18	7	17	1549.3494	0.001	1549.3494	0.0006	1562.6910	0.0001	
15	18	7	17	-	18	7	17	1549.6119	0.001	1549.6119	0.0005	1563.0176	-0.0002	
15	18	6	15	-	17	6	12	1549.6119	0.001	1549.6119	0.0006	1563.1051	-0.0006	
15	18	6	15	-	17	6	12	1549.6119	0.001	1549.6119	0.0011	1563.6145	-0.0002	
15	18	7	17	-	18	7	17	1549.6119	0.001	1549.6119	0.0014	1564.9349	-0.0038	
15	18	7	17	-	18	7	17	1549.6119	0.001	1549.6119	0.0014	1564.1899	-0.0004	
15	18	6	15	-	17	6	12	1549.6119	0.001	1549.6119	0.0014	1564.3881	-0.0003	
15	18	6	15	-	17	6	12	1549.6119	0.001	1549.6119	0.0018	1565.2851	-0.0010	
15	18	7	17	-	18	7	17	1549.6119	0.001	1549.6119	0.0026	1565.8076	-0.0002	
15	18	6	15	-	17	6	12	1549.6119	0.001	1549.6119	0.0026	1566.3733	-0.0003	
15	18	6	15	-	17	6	12	1549.6119	0.001	1549.6119	0.0026	1566.5445	0.0001	
15	18	7	17	-	18	7	17	1549.6119	0.001	1549.6119	0.0026	1566.8301	-0.0002	
15	18	6	15	-	17	6	12	1549.6119	0.001	1549.6119	0.0026	1566.3730	-0.0003	
15	18	6	15	-	17	6	12	1549.6119	0.001	1549.6119	0.0026	1566.5445	0.0001	

UPPER STATE	LOWER STATE	OBSERVATION PREC.	CALCULATION	RESID.	UPPER STATE	LOWER STATE	OBSERVATION PREC.	CALCULATION	RESID.
J KA KC	J KA KC	0.001	1566.6284	0.0066	J KA KC	J KA KC	0.300	210657.7523	-0.3623
(5) 25 2 22	1566.6350	0.001	1567.0051	0.0003	(6) 2 22	210657.4100	0.300	210657.7523	-0.3437
(5) 26 3 23	1567.0034	0.001	1567.5348	0.0006	(6) 2 22	225562.0200	0.300	225562.3637	-0.0175
(5) 27 1 25	1567.5125	0.001	1568.5222	0.0007	(6) 2 22	218056.1900	0.300	218056.2075	-0.0669
(5) 28 5 21	1568.5521x	0.000	1568.5530	0.0008	(6) 2 22	218314.3900	0.300	218314.4369	-0.5196
(5) 29 5 20	1569.4905	0.001	1569.4911	0.0006	(6) 2 22	290262.7296	0.400	290262.7296	-0.5685
(5) 30 5 22	1569.6167	0.001	1569.6165	0.0002	(6) 2 22	300675.3300	0.400	300675.3300	-0.3805
(5) 31 2 26	1569.7704	0.001	1569.7709	0.0005	(6) 2 22	14906.2900	0.200	14906.2177	0.0723
(5) 32 1 27	1571.9960	0.001	1571.9971	0.0011	(6) 2 22	29810.8291	0.200	29810.8291	0.3709
(5) 33 2 27	1572.2283	0.001	1572.2283	0.0000	(6) 2 22	49679.1600	0.200	49679.2009	-0.0009
(5) 34 2 26	1572.4452	0.001	1572.4455	0.0003	(6) 2 22	64.5718	0.020	64.5717	0.0001
(5) 35 3 26	1574.8324	0.001	1574.8385	0.0003	(6) 2 22	8061.7600	0.200	8061.7520	0.0080
(5) 36 3 27	1575.4024	0.001	1575.4025	0.0001	(6) 2 22	13350.9000	0.200	13350.9618	-0.0618
(5) 37 3 28	1576.3664	0.001	1576.3558	0.0005	(6) 2 22	20794.2300	0.200	20794.2962	-0.0662
(5) 38 3 27	72492.5600	0.100	72492.3125	0.2475	(6) 2 22	50825.1400	0.200	30825.4910	-0.3510
(5) 39 3 25	72492.7000	0.200	146916.4772	0.2225	(6) 2 22	3.6850	0.020	3.6850	0.0001
(5) 40 3 25	140752.6300	0.200	140752.5853	0.0447	(6) 2 22	16.7338	0.020	16.7245	0.0073
(5) 41 3 25	149224.4234	0.0766	149224.4234	0.0766	(6) 2 22	44.1840	0.020	44.1837	0.0023
(5) 42 3 25	217204.5900	0.300	217204.4775	0.1425	(6) 2 22	0.5945	0.020	0.5916	0.0029
(5) 43 3 26	211081.2800	0.300	211081.1375	0.1425	(6) 2 22	1.7006	0.020	1.7752	-0.0746
(5) 44 3 26	223738.2500	0.300	223738.2500	0.2609	(6) 2 22	4.6174	0.020	4.6174	0.0004
(5) 45 3 26	223787.8000	0.300	217781.3780	0.0920	(6) 2 22	10.7710	0.020	10.7706	0.0004
(5) 46 3 25	2177491.6700	0.300	2177491.6700	0.0733	(6) 2 22	23.0743	0.020	23.0755	-0.0012
(5) 47 3 25	217764.3700	0.300	217764.2967	0.0733	(6) 2 22	75062.6300	0.100	73062.2769	0.3531
(5) 48 3 25	289288.7600	0.400	281353.4300	0.1200	(6) 2 22	211341.3900	0.300	211341.3962	-0.0938
(5) 49 3 25	281353.5500	0.400	281353.4300	0.1200	(6) 2 22	226916.9400	0.400	226916.6916	0.2484
(5) 50 3 25	288292.1500	0.400	288292.1982	0.0482	(6) 2 22	281687.9900	0.400	281687.8863	0.1037
(5) 51 3 25	289935.9600	0.400	289935.9688	0.0488	(6) 2 22	4.6174	0.020	4.6174	-0.2562
(5) 52 3 25	290597.4900	0.400	290597.4927	0.0479	(6) 2 22	11.5578.4006	0.200	31154.6562	-0.3884
(5) 53 3 25	291207.7800	0.100	291207.7947	0.0353	(6) 2 22	31154.4900	0.200	31154.0516	0.4077
(5) 54 3 25	2514.6462	0.100	2514.6462	0.1055	(6) 2 22	10171.5300	0.200	10171.1223	0.4075
(5) 55 3 25	62353.4145	0.100	62353.4145	0.1055	(6) 2 22	16842.5800	0.200	16842.5865	-0.0065
(5) 56 3 25	63556.6000	0.100	63556.6284	0.0264	(6) 2 22	26232.4000	0.200	26232.7870	-0.3870
(5) 57 3 25	68.2672	0.020	68.2652	0.0200	(6) 2 22	0.8020	0.020	0.7930	0.0040
(5) 58 3 25	8519.3000	0.200	8519.1233	0.2877	(6) 2 22	5.5828	0.020	5.5834	-0.0006
(5) 59 3 25	14116.7800	0.200	14116.5826	0.1974	(6) 2 22	22.3130	0.020	22.3180	-0.0050
(5) 60 3 25	21999.6578	0.200	21999.6578	0.200	(6) 2 22	66.8725	0.020	66.8874	-0.0149
(5) 61 3 25	32666.7558	0.200	32666.7558	0.0158	(6) 2 22	1.0615	0.020	1.0614	0.0001
(5) 62 3 25	4.3273	0.020	4.3273	0.020	(6) 2 22	0.0000	0.0000	0.0000	0.0000
(5) 63 3 25	17.3040	0.020	17.3040	0.020	(6) 2 22	0.0000	0.0000	0.0000	0.0000
(5) 64 3 25	51.8809	0.020	51.8809	0.0129	(6) 2 22	0.0000	0.0000	0.0000	0.0000
(5) 65 3 25	0.1660	0.020	0.1660	0.0169	(6) 2 22	0.0000	0.0000	0.0000	0.0000
(5) 66 3 25	1.3925	0.020	1.3925	0.0091	(6) 2 22	0.0000	0.0000	0.0000	0.0000
(5) 67 3 25	6.7855	0.020	6.7855	0.0083	(6) 2 22	0.0000	0.0000	0.0000	0.0000
(5) 68 3 25	24.0663	0.020	24.0663	0.0259	(6) 2 22	0.0000	0.0000	0.0000	0.0000
(5) 69 3 25	69.0985	0.020	69.0985	0.0676	(6) 2 22	0.0000	0.0000	0.0000	0.0000
(5) 70 3 25	145359.8600	0.200	145359.8600	0.104	(6) 2 22	0.0000	0.0000	0.0000	0.0000
(5) 71 3 25	72227.2500	0.100	72227.3676	-0.1176	(6) 2 22	0.0000	0.0000	0.0000	0.0000
(5) 72 3 25	140463.4500	0.200	140463.6753	-0.2253	(6) 2 22	0.0000	0.0000	0.0000	0.0000
(5) 73 3 25	150408.8400	0.200	150408.0448	-0.2068	(6) 2 22	0.0000	0.0000	0.0000	0.0000
(5) 74 3 25	217922.7600	0.300	217923.2505	-0.4905	(6) 2 22	0.0000	0.0000	0.0000	0.0000